Doctoral Dissertation

Solid-state bonding by stress migration in Ag thin films

Chulmin Oh

December 2014

Department of Adaptive Machine Systems
Graduate School of Engineering,
Osaka University

Ph. D. Dissertation

Solid-state bonding by stress migration in Ag thin films

Chulmin Oh

Department of Adaptive Machine Systems

Graduate School of Engineering

Osaka University

December 2014

Approved by

Professor Katsuaki Suganuma

Professor Yoritoshi Minamino

Associate Professor Koji Hagihara

Associate Professor Shijo Nagao

Solid-state bonding by stress migration in Ag thin films

Abstract

In recent years, the bonding technology in electronic package has been paid much attention in the electronic industry due to rapidly increasing electronic products. The higher performance in advanced electronics such as smart phones causes the increase of heat generated in integrated circuits (ICs), requiring better thermal performance in bonding technology. The electrode of devices, bonded area in electronic packages, has also increased significantly to meet higher performance. The limited size of electronic packages can be realized by providing thin thickness of ICs, demanding reliable mechanical and environmental performance in bonding technology. In addition, the application of electronic packages is being expanded to the automotive with intelligent performance by adapting to the wide band-gap (WBG) device such as SiC and GaN. The high operating temperature of WBG devices can provide the high efficiencies and electronic insulation performance, improving the performance of the power module in environment friendly vehicles. Therefore, the bonding technology in the electronic package has faced various difficulties along with the development trend of electronic products.

In this dissertation, a pressureless low temperature bonding technology is proposed by using abnormal grain growth on sputtered Ag thin-films to realize extremely high temperature resistance. The bonding by using sputtered Ag thin-films is realized in the form of solid-state bonding under air environment, although another solid-state bonding such as Cu-Cu bonding is performed under vacuum conditions.

To investigate the internal mechanisms of this bonding, three processes are reviewed; sputtering process, bonding process, and substrate materials. The bonding properties of the specimens is measured by a die-shear strength test, as well as by X-ray diffraction measurements of the residual stress in the Ag films to show how the residual stress developments are essential to the bonding technology. In the sputtering process, the experiment results with various deposition temperature of Ag thin films, i.e. initial residual stress, reveal that the bonding process is driven by the thermomechanical stress. Large residual stress change between before and after heat treatment causes larger abnormal grain growth to achieve high bonding strength. In bonding process, the microstructural changes in the Ag films is characterized over various bonding temperatures and times; abnormal grain growth is induced by stress migration at the contact interface, otherwise hillocks grown on the film surface. Perfect bonds with high die strength can only be achieved with abnormal grain growth at the optimum bonding temperature and time. Finally, in the substrate materials, the variation of the substrate material modifies the thermal expansion mismatch between sputtered Ag film and the substrate, thus changing the bonding properties. It confirms that stress-migration and resulting stress relaxation at the bonding temperature plays a key role to control the Ag solid state bonding using sputtered Ag thin-films.

In conclusion, the solid-state bonding method using the Ag material, called Ag stress migration bonding, is successfully achieved by understanding the intrinsic bonding mechanism, realizing it to apply in advanced electronic package such as 3D integration and wide band-gap power device.

Table of contents

Chapter 1

Introduction

1.1 Bonding for electronic packages

1.1.1 Development of Electronic Packages

Over 100 years have passed since the electronic package was developed if it is included optoelectronics and the vacuum tubes [1]. Until the 1960s, semiconductor chips were enclosed in metal or ceramic packages to protect the chip and fragile connecting wire. In those days, the size and performance of the electronic package wasn't a matter of concern since electronic products were operated by combining various simple electrical electronic packages. For example, a transistor with three I/Os used a metal package with three external leads to adapt easily to electronic products, as shown below in Fig. 1.

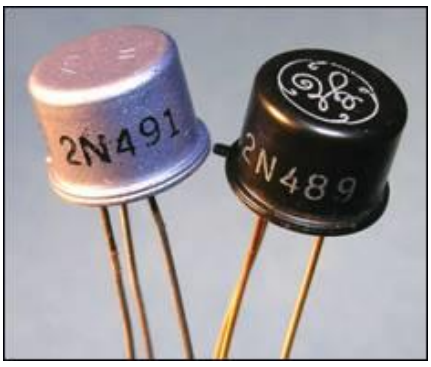

Figure 1. The unijunction transistor developed at GE in the early 1950s [2].

However after 1970, the performance of semiconductor chips increased dramatically by emerging integrated circuits (ICs). The integration of semiconductors, typically driven by Moore's Law, allowed for numerous I/Os to realize higher performance as shown below in Fig. 2 [3].

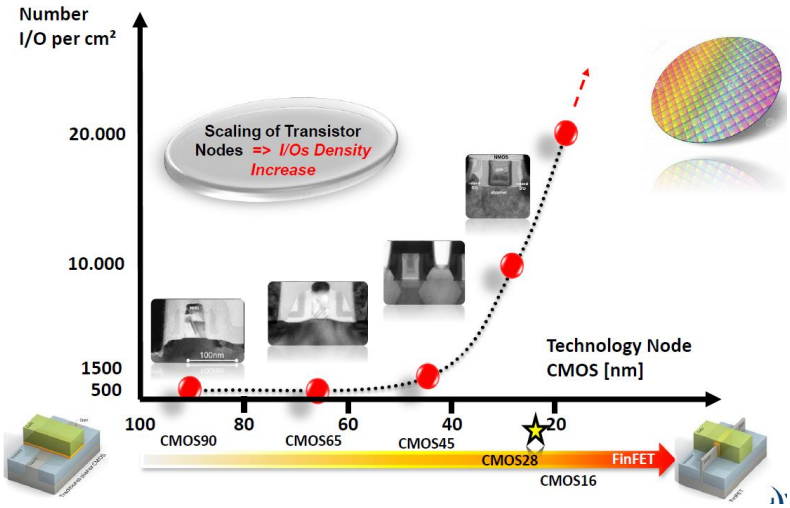

Figure 2. The integration of semiconductors with increasing I/Os [4].

The integration of semiconductors has changed the concept of electronic packages to build more I/Os with a smaller pitch by introducing in Ball Grid Array (BGA) and flip chip packages. As one can see in Fig. 3, the higher the performance of the electronic product, the more I/Os the electronic package needs. In addition, the consumption power increases with increasing the integration of semiconductor, as shown in Fig. 4.

Increased consumption power with I/Os is a considerable factor if we require higher performance in electronic packages. For example, to deal with many I/Os in an electronic package, the substrate materials is changed from metal to polymer material which can laminate the Cu circuit layer with a lot of external solder bumps. However, in view of power consumption, the change of substrate isn't attractive. Therefore, it is important to consider the design of the electronic package including the structure, materials related processes for overcoming the larger consumption power with I/Os.

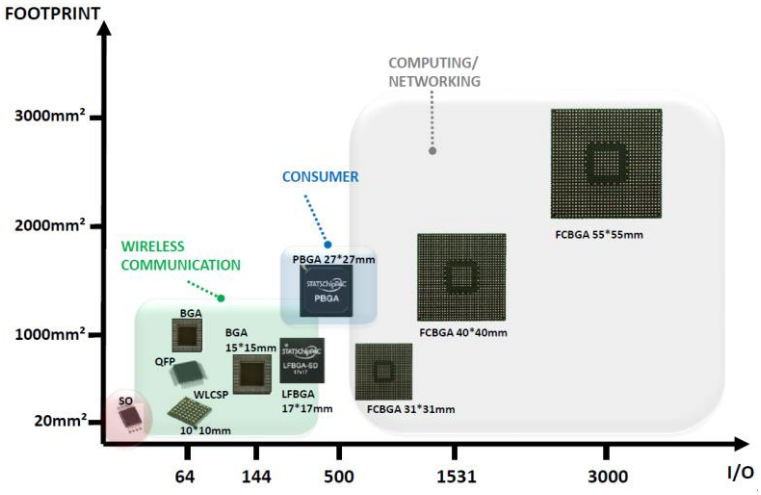

Figure 3. Electronic package development evolutions [4].

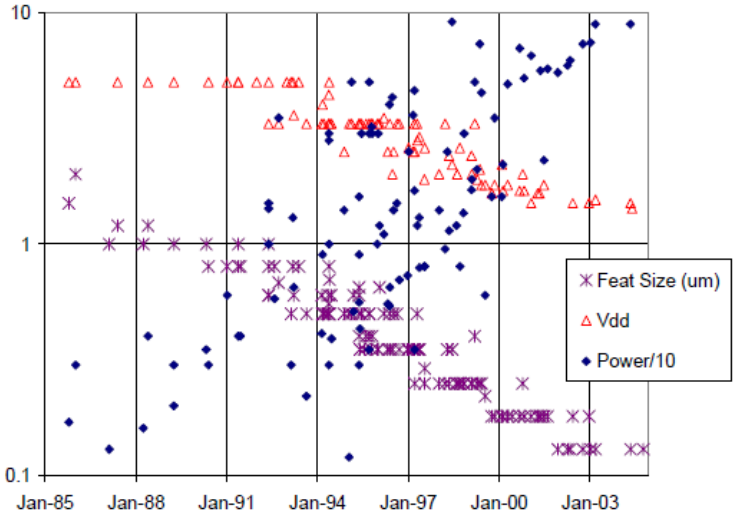

Figure 4. Microprocessor Vdd, Power/10, and feature size according to year [5].

Recently, the size of electronic packages has been limited due to a tremendous development in handheld electronics such as cellular phones. In order to overcome the limited size of electronic packages, stacking method has been utilized with various methods [6-8] and a thinner die is required for smaller package sizes, obtained by back-grinding process.

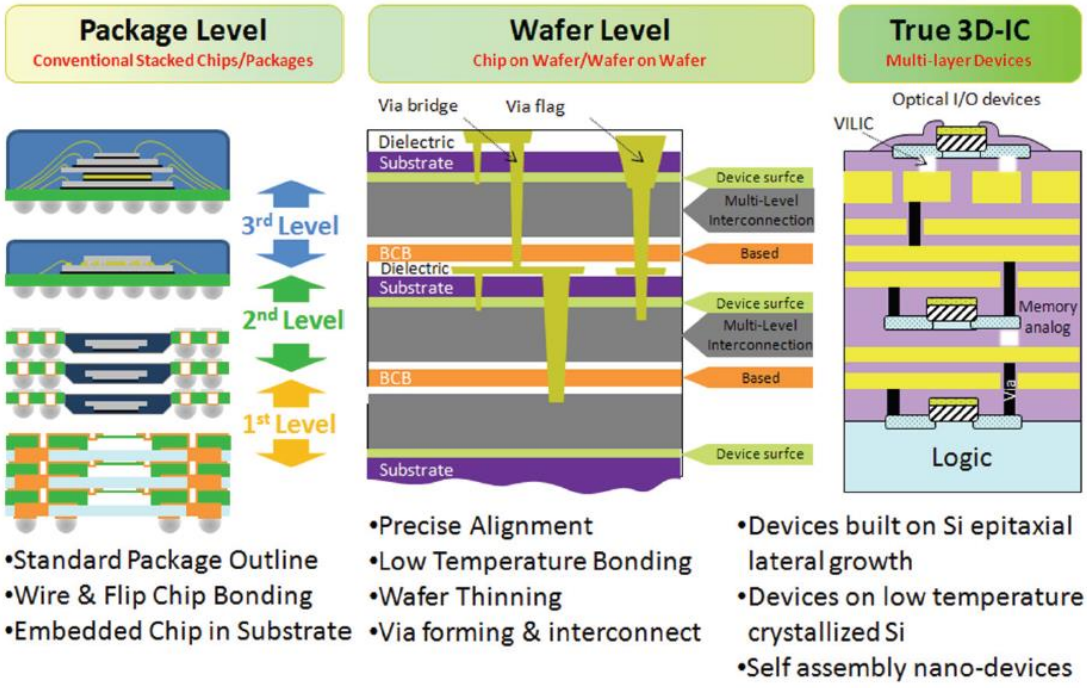

Figure 5. Three stages of 3D package development [6].

Together with higher performance and smaller size, the application of electronic packages has been increasing in the automotive industry. Demand for environmently friendly vehicles brings the power control module to be smart and intelligent, increasing the electrical functionality. If SiC chips are applied in power modules due to high efficiency, the junction temperature will be exceeded over the limit of conventional materials in electronic package. In this case, the materials and design of the electronic package will be reviewed for its thermal performance [9-11]. Therefore, the electronic packages can be applied not only in the electronic field, but also in other fields where electronic devices are involved.

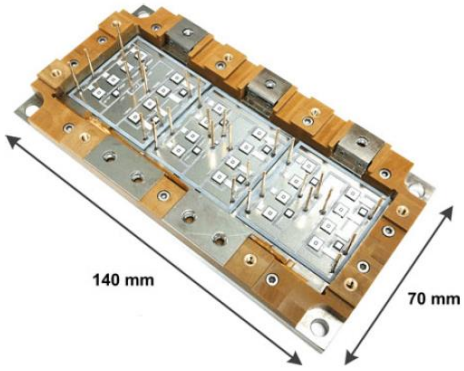

Figure 6. Six-pack SiC JFET-based power module [11].

In summary, the electronic package has been developed toward two ways; the applicative packaging with wide applications and the advanced packaging with higher performance and smaller size as shown in Fig. 7 [12,13].

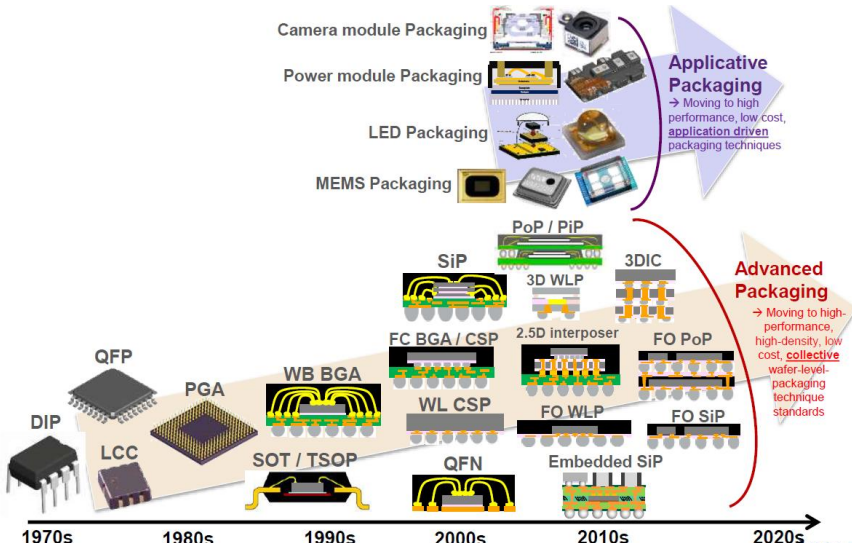

Figure 7. Evolution of electronic package development [12].

1.1.2 Issues Associated with Bonding

Electronic packages in general, consist of bare chip, substrate, wire, and mold compound, playing a role as the interface from bare semiconductor chip to the board. The bare chip, called a die, has millions of transistor circuits that make electrical circuits. As seen in Fig. 8, the die is attached to the substrate mechanically by die bonding process.

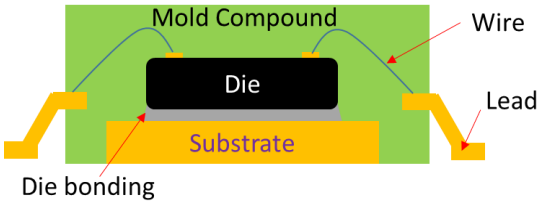

Figure 8. Cross-sectional schematic illustration of semiconductor package.

Selection of a die attached material is important because the die bonding process is dependent on this material. In recent years, the die attached materials have key roles in the developments in electronic package. For instances, the higher performance in electronic package results in an increase in the heat of ICs requiring better thermal performance in bonding materials. In addition, the electrode of devices are increased significantly to satisfy higher performance, making it difficulties to control the bonding uniformity in all the electrodes. The limited size of the electronic package can be realized by providing thin thickness of ICs, demanding the reliable mechanical performance and narrow bonding area in bonding materials.

Finally, the application of electronic package is expanded to the automotive industry with intelligent and high power performance, adapting to wide band-gap (WBG) devices

such as SiC and GaN. The high operating temperature of WBG devices can provide high efficiency and electronic insulation. However, it is necessary to develop the bonding material and process for the high operational temperature. In conclusion, the interconnection technology of electronic packages has faced difficulties along with the development trend of electronic products as shown in Fig. 9.

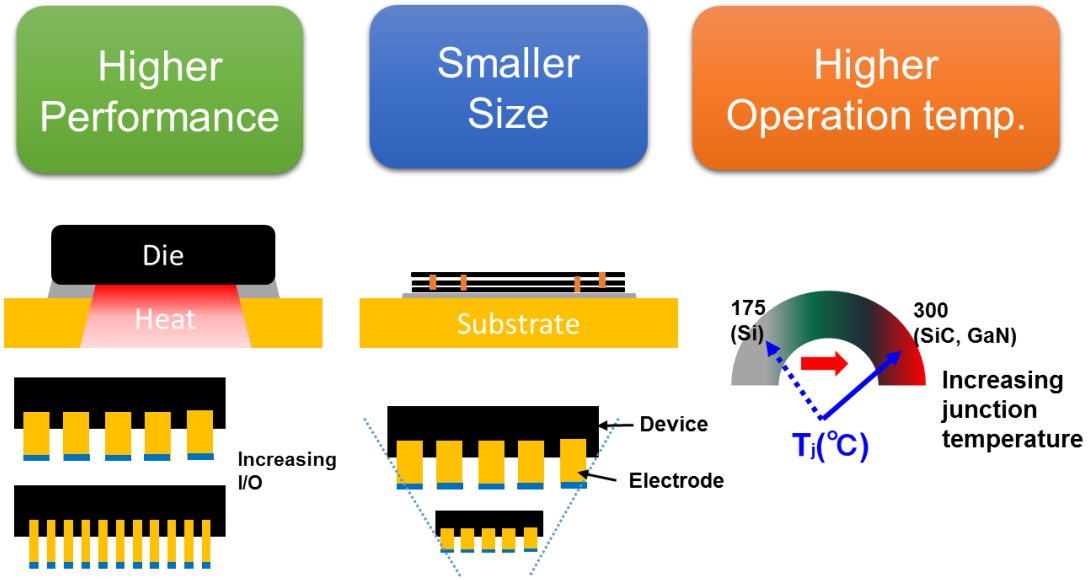

Figure 9. Issues of interconnection technology associated with electronic package development.

1.2. Overview of Bonding Technologies

1.2.1 Soldering

The soldering process is carried out by melting solder materials and stuck between separate materials (see Fig. 10). When it is heated, the solder material melts and spreads over the surfaces of A material and B material. During heating, the molten solder reacts with those materials and form intermetallic compounds (IMC). After the solder is bonded between both surfaces, it is cooled down and the soldering bond is complete. Therefore, the operational temperature cannot exceed the melting temperature of the solder.

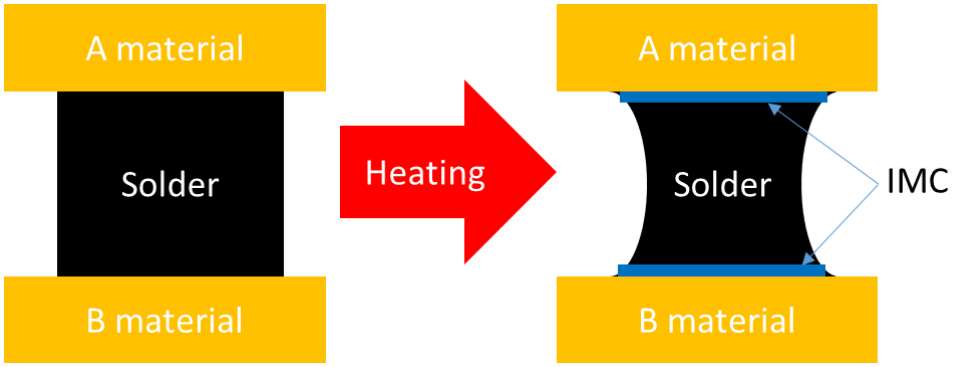

Figure 10. Schematic illustration for soldering process.

Soldering has been widely used in electronic packages as a die attach material. It provides the mechanical and electrical connection between the die and the bonding pad. It also acts as a path for the dissipation of heat generated by the semiconductor chips.

Prior to the 21st century, high-Pb solder was used in the flip chip bonding process as shown in Fig. 11. After the flip chip bonding, eutectic Sn-Pb solder was used in the board-level bonding process because the melting point of eutectic Sn-Pb solder was much lower

than that of high-Pb solder [14]. Since 2006, the usage of Pb in electronics has been prohibited by environmental regulations resulting in the emergence of Pb-free solders such as Sn-Ag, Sn-Bi, Sn-Cu and Sn-Zn [15-16] (see Table 1).

When replacing Sn-Pb solders with Pb-free solders, some reliability issues occurred significantly with development of the semiconductor devices; dissolution, spalling, lift-off, electromigration and whiskers [16-19] as shown in Fig. 12. Soldering temperature rises due to the high melting temperature, which threatens the thermal durability in the electronic package [20, 21]. The various problems caused by using Pb-free solders haven't been solved completely yet although the Pb-free soldering technology is widespread in the electronic industry, from material developments of Pb-free solder to production development of Pb-free electronic assembly. Nevertheless, research of Pb-free solder has improved significantly by considering together the issues of the Pb-free soldering in the stage of development of electronic packages.

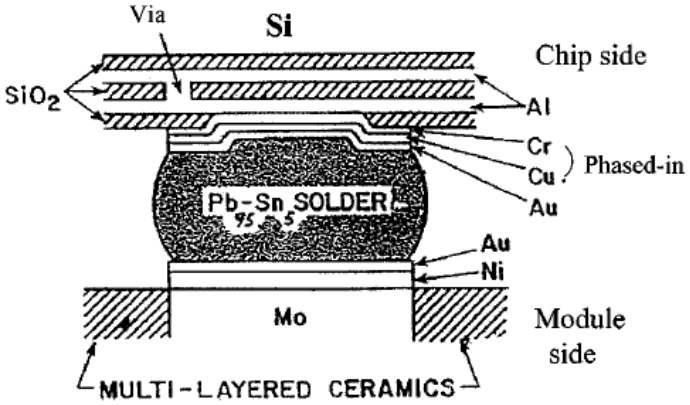

Figure 11. Schematic diagram of a 95Pb5Sn solder bump on a Si chip to a ceramic module [14].

Table 1. Representative Pb-free solders with their properties [15].

Candidates	Temperature(ºC)		Benefits	Drawbacks
	Wave soldering	Reflow soldering		
Sn–(3–3.9)% Ag[–(0.5–0.7)% Cu] or [–(1–3)% Bi]	250–260	235–250	Excellent mechanical properties Soldering temperature can be lowered by Bi	High soldering temperature Lift-off with Bi and Pb Partial melting reaction at 139 ºC with much Bi Poor compatibility with 42 alloys and Sn–Pb plating
Sn–57% Bi [–(0.5–1)% Ag]		180–200	Low soldering temperature	Very brittle but can be improved by Ag addition Poor heat resistance
Sn–(8–9%)Zn [–3% Bi]	~250	220–230	The same soldering temperature as for eutectic Sn–Pb	Severe oxidation but improved by flux Poor heat-resistance of interface with Cu
Sn–0.7% Cu [–Ag, Ni, Au]	250–260		Cheapness	High soldering temperature Lift-off with Pb

*Figures in [ ] are the third alloying elements and their typical compositions.

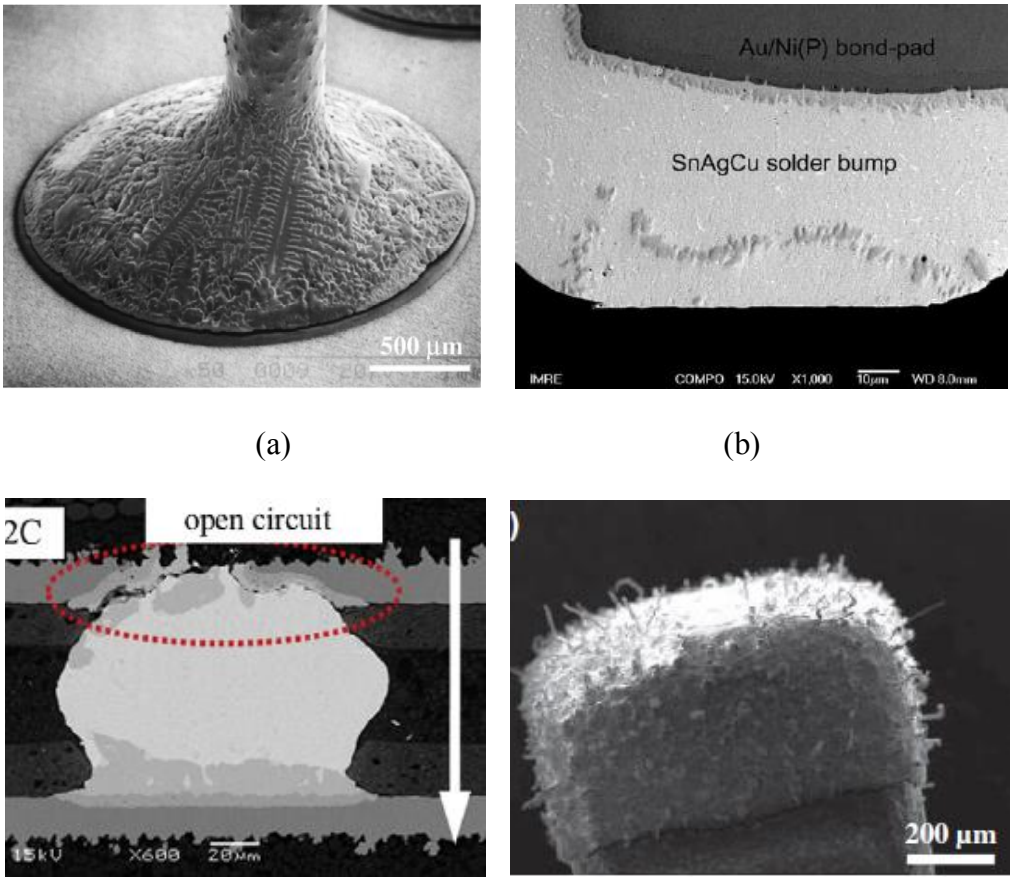

Figure 12. Reliability issues for Pb-free solder; (a) life-off [16], (b) spalling [17], (c) electromigration [18], (b) Sn whisker [19].

High-Pb solder used in die bonding has been exempted in the environmental regulations [22]. Alternative materials for high-Pb solder in die bonding hasn't been approved formally as yet. In order to replace the high-Pb solder with ensured reliability, a lot of solder materials has been studied as shown in Table 2 [24-25]. In addition, application of wide-band gap devices exceeding the melting temperature of high-Pb solder has been attempted in power modules for electronic vehicles, accelerating the

alternative materials development in power electronics.

Until now, soldering has been mostly utilized as a die bonding method in electronic package, especially in power electronic package because of efficient heat conduction, electrical performance, low cost, and high workability such as self-alignment. However, this method comes to its limits by developing advanced electronic packages requiring high operating temperatures with long durability. The exemption of environmental restrictions, allowing to use the high-Pb solder, could be released in the foreseeable future.

Table 2. Typical high temperature solders [23].

Alloys	Composition (wt. %)	Solidus Temperature (ºC)	Liquidus Temperature (ºC)
High-Pb Alloy System			
Pb-Sn	Sn-65Pb	183	248
	Sn-70Pb	183	258
	Sn-80Pb	183	279
	Sn-90Pb	268	301
	Sn-95Pb	300	314
	Sn-98Pb	316	322
Pb-Ag	Pb-2.5Ag	304	304
	Pb-1.5Ag-1Sn	309	309
Sn-Sb Alloy System			
Sn-Sb	Sn-5Sb	235	240
	Sn-25Ag-10Sb (J-alloy)	228	395
Au Alloy System			
Au-Sn	Au-20Sn	280 (eutectic)	
Au-Si	Au-3.15Si	363 (eutectic)	
Au-Ge	Au-12Ge	356 (eutectic)	
Bi Alloy System			
Bi-Ag	Bi-2.5Ag	263 (eutectic)	
	Bi-11Ag	263	360
Cu Alloy System	Sn-(1-4)Cu		
Cu-Sn	Sn-Cu particles composites	227 ~230	~400
Zn Alloy System			
Zn-Al	Zn-(4-6)Al(-Ga, Ge, Mg, Cu)	300~340	
Zn-Sn	Zn-(10-30)Sn	199	360

1.2.2 Sinter joining

Inorganic particles are sintered by solid-state diffusion. Particles can be densified by rearrangement of rotating particles, forming necks among particles. During sintering, the neck among particles forms grain boundary due to a tendency of a net decrease in total energy. The particles densification subjected to the diffusion process is determined by process temperature, time and external applied pressure in the sintering process.

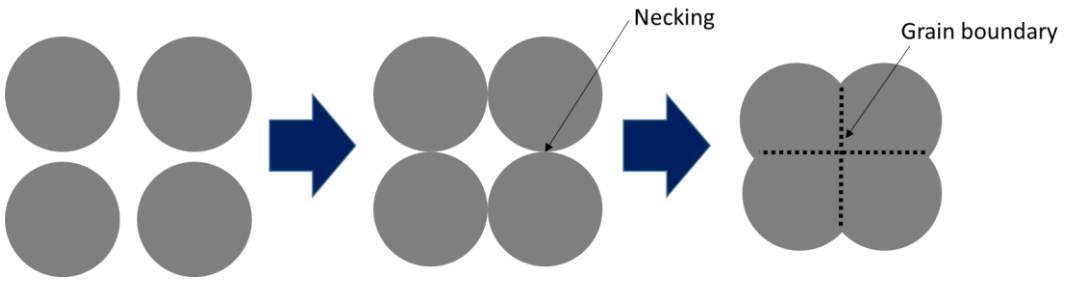

Figure 13. Schematic illustrations for sintering process.

After late 1980s, sintering of Ag particles has been mainly used for interconnection with die in electronic packages [25]. The thermal and electrical performance of Ag particles are better than those of other bonding materials in electronic materials since sintered Ag particles do not melt up to 960 ºC, which allows application to power electronics. By containing the dispersant, binder, and thinner in Ag paste [26], the Ag paste has good workability for screen-printing with particle dispersion, flowability, and adequate viscosity [27].

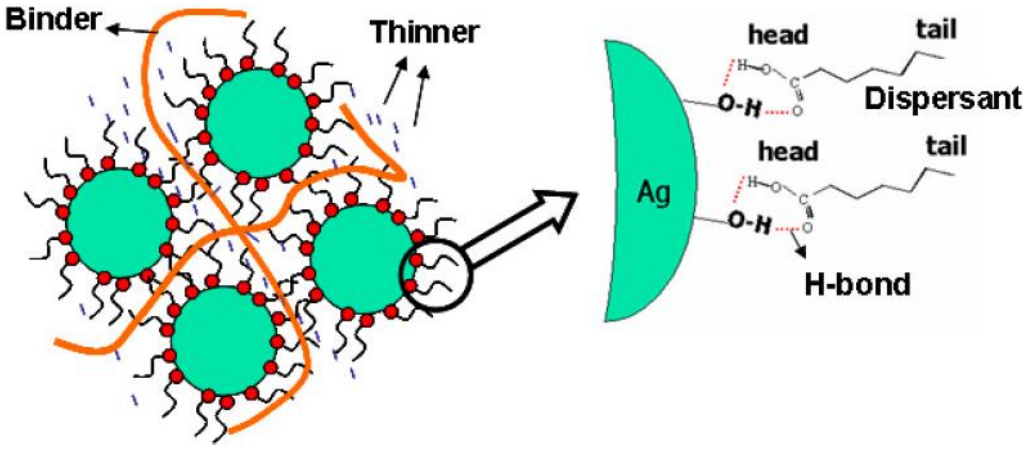

Figure 14. Functions of the dispersant, binder and thinner in the formulation of silver pastes [26].

In the early days, micro-size Ag particles were used to form Ag joints between the die and substrate [28-30]. The micron-scale Ag paste consists of Ag flakes (diameters of ~10 μm) and solvents like cyclohexanol, butanol, terpineol, isoamyl alcohol or an ethylene glycol ether mixture of cyclohexanol–methanol [31, 32]. This type of Ag paste was sintered under a pressure of 9 MPa ranged from 180 ºC to 250 ºC [25]. Alternatively, a higher pressure was used to reduce the sintering temperature and time to control the sintered Ag joint [30]. In addition, in order to achieve the pressure-less bonding, the decomposable silver compounds such as Ag-oxide or Ag-oxalate compounds were used [25]. They provide the bonding medium between adjacent silver particles by reduction pure Ag and oxide above 200 ºC, helping further densification of Ag particles.

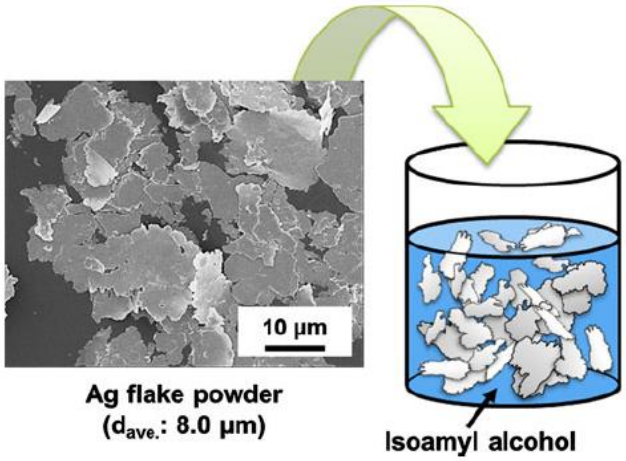

Figure 15. Fabrication process of the Ag micro flake [32].

These days however, nano-size Ag particles have been used in the die bonding process. It is possible to decrease the applied pressure and process temperature in sintering because the surface effectiveness by nano-size particles lead to the diffusion of atoms to neighboring particles during sintering. In case of 26 nm diameter Ag nanoparticles, their surface area is 23 m^2/g [33]. The bonding of Cu wire to Cu pads on polyimide has been achieved at 100 ºC with 5 MPa of external pressure [34]. Low temperature and pressure during sintering not only makes the flexible electronics possible, but also improves the reliability of electronic packages. The pressure-less bonding using Ag nanoparticles have been reported in the literatures [35-37]; they have realized the pressure-less bonding by coating additional polymers on Ag nanoparticles [35,36] or by using the metal-organic silver complex which generates Ag nanoparticles under 200 ºC [37,38].

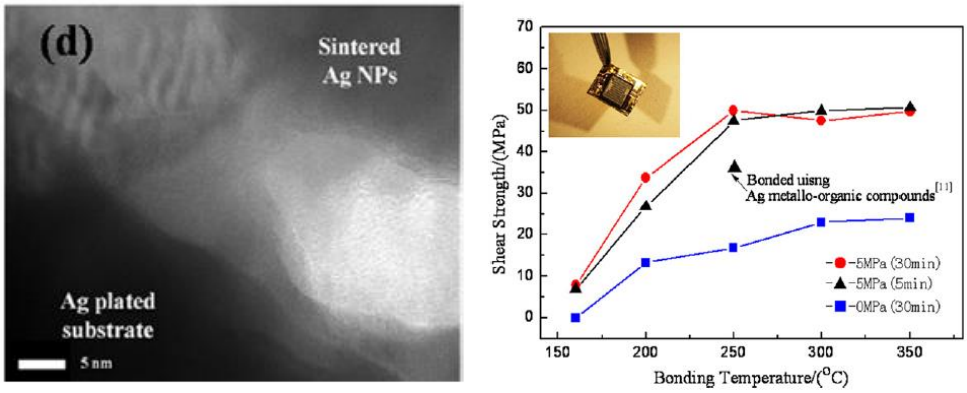

(a) (b)

Figure 16. Pressureless bonding by Ag nanoparticle sintering (a) TEM image of bonding interface, (b) Shear strength with bonding temperature [35].

Recently, the hybrid Ag paste comprising micron-sized Ag particles hybridized with submicron-sized Ag particles has been suggested as the die attach materials with better thermal and electrical performances [28, 39].

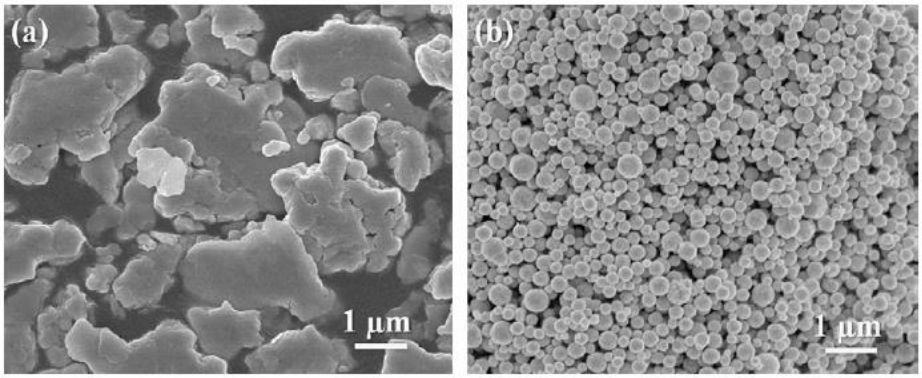

Figure 17. Two Ag particles used for new hybrid pastes: (a) micron-sized particles and (b) submicron-sized particles [28].

The mechanical properties of sintered joint by Ag particles are dependent on the following items [31].

- Particle size, distribution and morphology
- Sintering temperature, heating rate and time
- Bonding pressure during sintering
- Bonding substrate

In high temperature storage tests, the sintered Ag joints did not show any degradation or exhibit a little rise in die-shear strength [25]. And, in thermal fatigue test, Ag nano-size particles was superior to Ag micro-size particles because of higher initial die-shear strength, higher density [25] as shown in Fig. 18. To overcome the thermal-fatigue resistance of Ag micro-size particles, the Ag nano-thick flakes has been utilized for the die bonding of SiC chips [40].

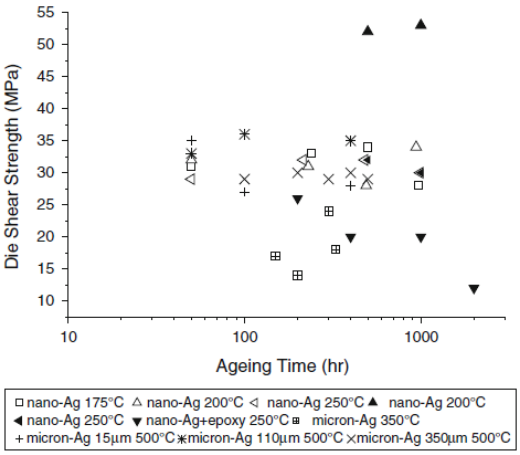

Figure 18. Die-shear strength for various Ag sintered joint [25]

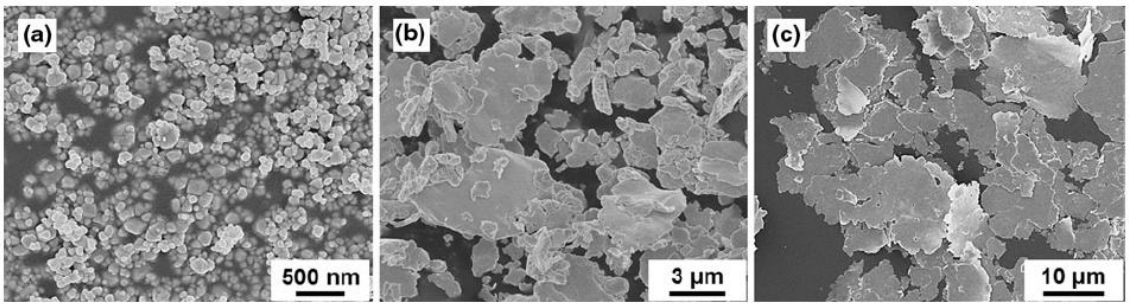

Figure 19. Three different Ag particles; (a) nanoparticles, (b) micro flake, and (c) nano-thick flakes [40].

The sintered Ag has exhibited better thermal and electrical properties, making this method attractive in die bonding [41]. It can be also applied for wide-band gap semiconductor due to its high melting temperature. The sintered Ag joint is the most feasible and has an attractive potential to be employed in industry. However, the bonding process flow from synthesis of Ag particles to bonding process by screen printing is sometimes complex to control every process parameters in each step, making the process window difficult for mass production. In addition, if a large die is bonded, the sintered joint is not covered uniformly in all bonding areas due to insufficient coverage of paste related to releasing the volatile compounds.

1.2.3 Direct Bonding

Besides soldering and sinter joining, the direct bonding method, which is the conventional solid-state bonding, has been paid much attention in the electronics industry. If the same materials which are separated from each other are faced with others under high pressure and high temperature, the homogenous bonding interface is formed by inter-diffusion between same materials as shown in Fig. 20. The bonding reliability is expected to be higher by the removal of additional bonding mediums such as solder or Ag particles.

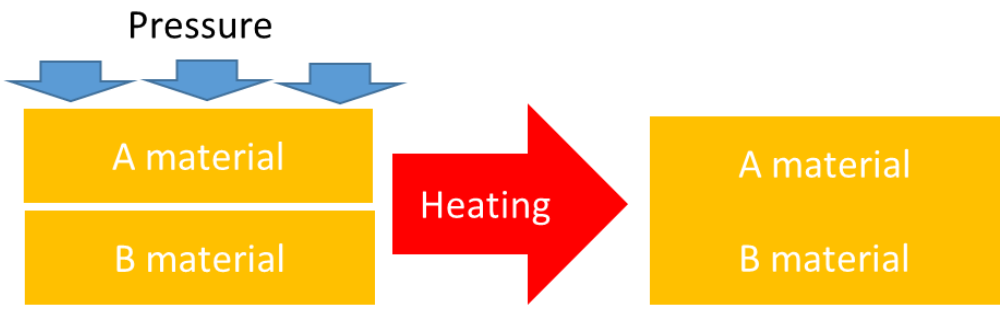

Figure 20. Schematic illustrations for direct bonding.

In direct bonding, Cu material has been used widely for mechanical and electronic interconnections because Cu material is used for electrode of electronic packages with excellent electrical and thermal conductivity.

Cu direct bonding has been developed from the early 2000s to apply in electronic package [42]. By the bonding method, this direct bonding is divided into two classifications; one is ‘thermal compression Cu direct bonding’ and the other, which is minor, is ‘surface activated Cu direct bonding’.

In thermal compression Cu direct bonding, the Cu film on the Si wafer is bonded on

the condition of compressive pressure and high temperature to achieve sufficient bonding results. And then the bonded sample is annealed under 400 ºC or lower to enhance the bonding strength [42-45]. Although the compressive bonding pressure can vary widely from 209 kPa to 1254 kPa with the wide bonding temperatures from 200 ºC to 450 ºC [43], the strong bonded interface is obtained above 300 ºC with 400 kPa and 30 minutes. The vacuum condition of 10^{-4} torr is normally used for good quality bonding [42]. K.N.Chen et al has reported that large Cu grain growth is occurred by disappearing the bonding interface when the sample bonded above 300 ºC is annealed subsequently above 300 ºC for 60 minutes as shown in Fig. 21 [44-45]. In addition, he has provided the morphology and strength map for Cu direct wafer bonding according to different bonding conditions [44].

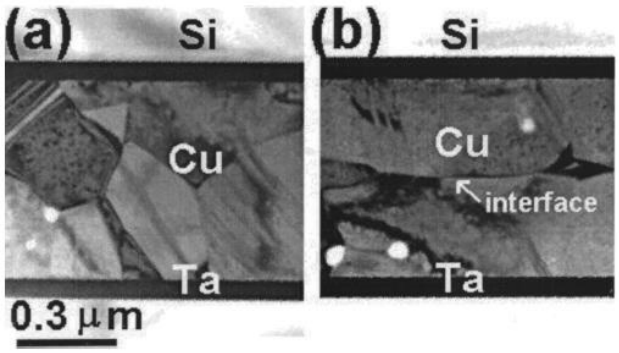

Figure 21. TEM morphologies of (a) grain bonded at 350 °C for 30 min followed by N^2 annealing for 60 min, and (b) interface bonded at 350 °C for 30 min [44].

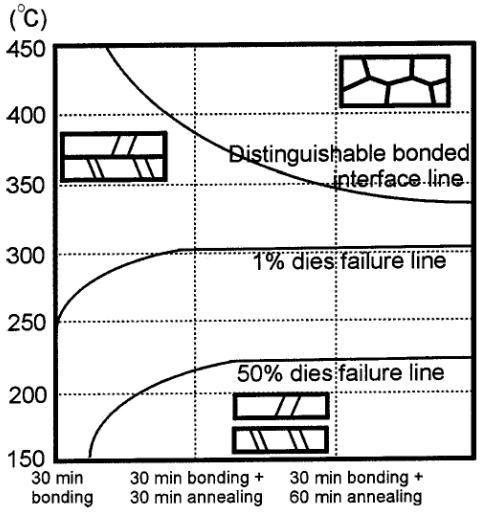

Figure 22. Morphology and strength map for copper wafer bonding under different bonding temperatures and conditions [44].

After the bonding process followed by annealing, abnormal Cu (220) grain growth is observed [46]. The growth of (220) grains is more preferred than that of (111) and (002) grains, because (220) grain has a lower yield stress and the grain growth is generated to minimize the surface or strain energy [46]. Further annealing after bonding can enhance the bond strength and the grain in the bonding interface forms the twin boundary grains as shown in Fig. 23 [47].

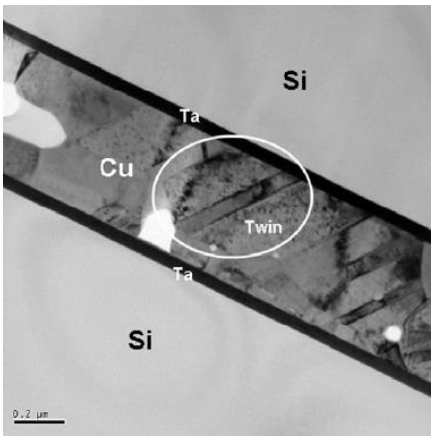

Figure 23. The morphology of Cu bonded layers [46].

In the surface activated Cu direct bonding, otherwise, the bonding process for Cu films is performed at room temperature by using the surface activated bonding equipment as shown in Fig. 24 [48]. The bonding equipment can provide two following items to achieve a desirable bonding strength as follows [48].

- Preparation of the surface cleaning and flattening.

  Cu surfaces were cleaned and activated by accelerated Ar ion beam to remain the adhesive energy on surface achieve a sufficient bonding.

- Ultra high vacuum (UHV) condition

  The surface activated Cu direct bonding can be achieved under an ultra high vacuum chamber (~10^{-8} torr) to prevent foreign contaminants and oxidation process.

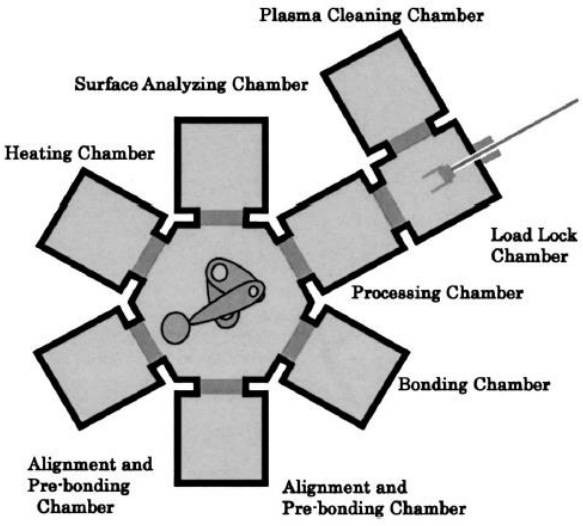

Figure 24. Schematic view of surface activated bonding machine [48].

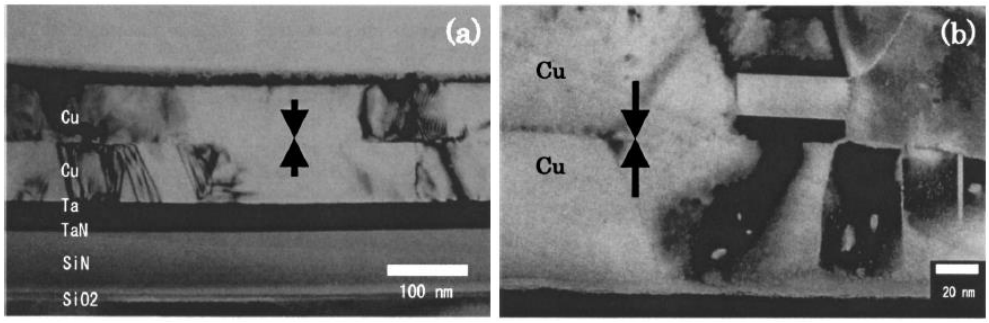

Figure 25. TEM image of the bonded Cu–Cu interface: (a) low magnification TEM image of the bonded sample; (b) high-resolution TEM image [48].

Fig. 25 shows the cross-sectional bonding interface of Cu wafer bonding by surface activated bonding. The bonding interface is formed without voids. The bonding contact is attributed to the plastic deformation of two surfaces by an intermolecular force (van der Waals attraction force) between two Cu surfaces [48]. After tensile test, fracture on the Cu-Cu bonded sample occurs either from the bulk material or from the glue, indicating higher bonded strength at the bonding interface than that at bulk material [48]. R. Tadepalli et al has reported that interface toughness of Cu-Cu surface activation bonding is roughly 3 J/m^2, ideal value for bulk-like bonding by using an atomic force microscope (AFM) pull-off measurements [49]. The activated bonding method can be applied to not only other material such as Al-Al and Al-Si_3N_4 interfaces [50] but also the integration for three dimension (3D) ICs applications [51].

Cu-Cu direct bonding is one of the alternative bonding methods used for advanced devices, providing a sound bonding quality without any bonding medium. However, the complex process for clean surface and high vacuum equipment required for Cu-Cu direct bonding becomes a major concern for mass production. In addition, the bonding pressure required during the bonding process will be a concern for advanced devices using a thin

wafer.

1.2.4 Summary

Many researchers have reviewed the current bonding technologies by their own category to meet the next generation electronic device [15, 23-25, 28, 31, 42, 52]. H. S. Chin et al has suggested a summary of current bonding attach for power devices according to various production methods, properties, and manufacturability as shown in Table 3 [52].

In our case, three kinds of bonding methods which have been developed actively in these days has been reviewed carefully together with the bonding process, duration temperature, and bonding mechanism to understand their advantages and disadvantages as shown in Table 4. In soldering, even if soldering is used widely in general electronics, it is difficult to cope with the high temperature power device due to the lower melting temperature. It is also hard to apply in fine pitch devices because of the solder bridge defecting during bonding. Recently, the sintering method has been rising as an alternative bonding for high temperature power devices due to good bonding performance with a high melting point. However, pressurization is necessary for the bonding process, affecting the advanced integration devices using thin wafers. Moreover, the process flow from fabrication of Ag paste to bonding process is too long to apply in mass production. When a large die is bonded, the uniformity of the bonding area will be a concern because of insufficient coverage of paste related to releasing the volatile compounds. Finally, in direct bonding, the bonding concept is similar to be the ideal bonding theory by bonding each other without any bonding materials. The strong bonding interface is obtained if it is bonded under severe conditions such as surface flatness, cleaning, and vacuum chamber. Due to the severe bonding conditions with a high cost, it is difficult to apply this method in mass production. In case of the surface activated bonding process, for example, cold

rolling with 1000 kgf load is used to contact the wafer pairs, causing serious damage to the device's reliability. Therefore, it is required to choose the optimal bonding method for each device in a short period of time and to develop a new bonding method to cover the advanced device included power device in the long term.

Table 3. Summary of Various Die Attach Materials with Its Methods, Properties, and Manufacturability [52].

Die attach materials	Die attach material product methods	Die attach material properties	Manufacturability
Off-eutectic gold-based die attach material	dissolution	- high-temperature performance - superior corrosion resistance - high electrical and thermal conductivity - fluxless soldering	- suitable only for small die applications because of stiffness property
Bismuth-based high temperature die attach material	dispersing and mixing	- excellent reliability property - higher mechanical strength	- higher processing temperature (773 K) - must fabricate within CTE matched structure to gain desired properties
Liquid-based die attach material	not Reported	- strong adhesion strength - remains stable during temperature cycling - high-temperature storage when the die attach material is molten	- available in solder paste form - performs well in thermal cycling
Silver-indium die attach material	atomic interdiffusion	- higher joint reliability - void free property - thermal stress reduced	- ease of processing with low processing temperature
Silver paste film-sintering	nanosilver purchased commercially	- superior electrical and thermal conductivity - limited fatigue property - good adhesion strength - void-free property - high joint reliability	- complicated manufacturing process - higher processing cost - pressure may physically damage devices
	nanosilver produced by Carey Lea method	- high electrical and thermal conductivity - limited fatigue propert - strong bonding even in smaller die	- ease of manufacturing process, which without application of pressure - lowering processing cost

Table 4. Summary of soldering, sintering, and direct bonding.

	Soldering[15]	Sintering[25]	Direct bonding[42]
Bonding Temp. (ºC)	200-400	200-250	300-400
Bonding pressure. (kPa)	0	400-500	400
Bonding Environment	Air	Air	Vacuum
Melting Temp. (ºC)	200-400	960	1080
Bonding mechanism	Melting	Sintering	Inter-diffusion

1.3 Motivation of Research

1.3.1 Challenges Associated with Bonding

In electronic packages, there are three bonding parts with different bonding positions as shown in Fig. 26.

■ Wire bonding

The wire is bonded on the bonding pad by using friction energy with ultrasonic force. Au ball wire with a diameter of 25.4 μm is used for signal interconnection and Al wedge or ribbon wire is used for power interconnection.

■ Electrode bonding

The solder bonding has been used commercially for bonding between the package electrode and board or between the bumps for chip integration. Cu-Cu direct bonding has been developed to apply in chip integration bonding.

■ Die bonding

Die bonding is realized by bonding the device on the substrate. Soldering has been used for commercial electronic packages, facing the difficulty on advanced device and power devices due to lower melting temperatures. As an alternative bonding method, various bonding methods such as Ag sintering are developed with material development. These days research for the die bonding method has been highlighted in interconnection technology to meet high performance and reliability with high

temperature environments.

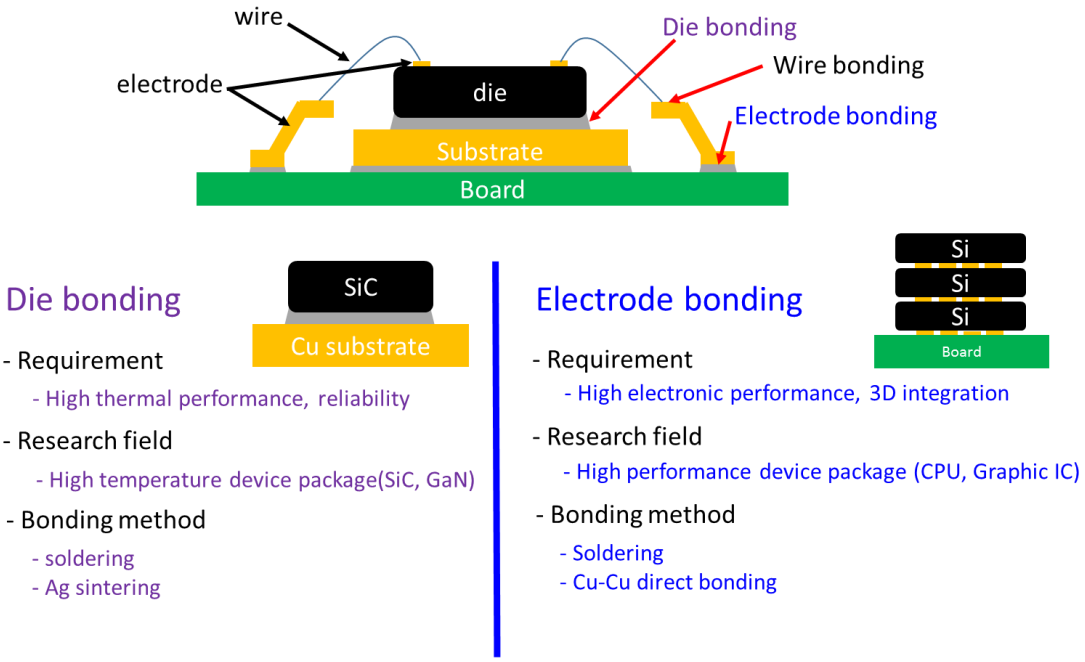

Figure 26. Interconnections in electronic packages.

The die bonding has been researched in various ways to meet a lot of requirements associated with diverse application from smart phones to intelligent environment-friendly automotive. A good『die bonding』, however, is necessary to put the devices under little internal stress during bonding and operation, together with the ability to resist extreme temperatures with mechanical, thermal and electrical contact between the device and substrate.

1.3.2 Bonding Approach Using Stress Migration.

Stress migration (SM) is a physical phenomenon that metallic atoms diffuse by the gradient of hydrostatic stress [53]. Hillock growth caused by stress migration becomes a significant reliability problem in integrated circuits, seeking the preventing method of hillock growth by understanding stress migration [54-56]. In addition, B. Horváth has reported that Sn whisker growth is also caused by stress migration [57].

On the other hand, stress migration can be utilized intentionally to fabricate nanomaterials such as nanowire and nanowhisker as shown in Fig. 27 [58-60].

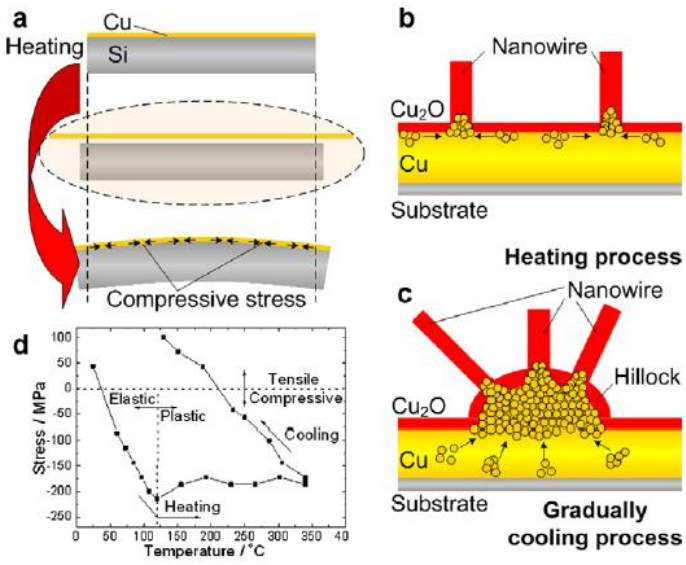

Figure 27. Schematics and supporting data for the growth of nanowires [58].

In the dissertation, hillock growth formed by stress migration is introduced to develop the new bonding method for advanced devices with power devices as shown in Fig. 28. If a lot of hillock growth can be induced by controlling the stress migration, this hillock growth is possible to be utilized as a bonding media between chip and substrate, realizing

the pressure-less bonding without any pressure damage to device. In addition, strong bonding strength is expected because of solid-state bonding between the same materials.

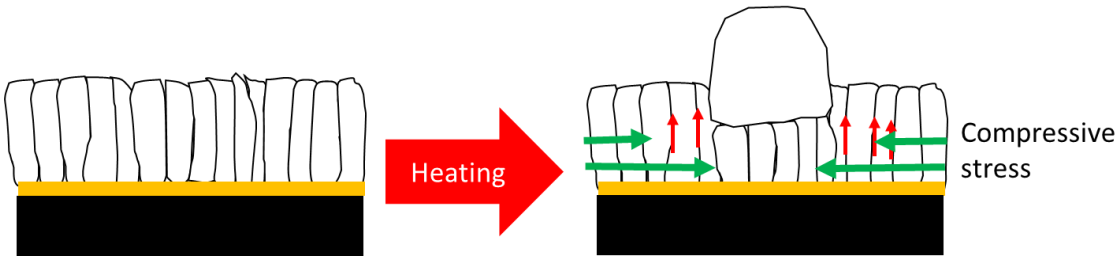

Figure 28. Schematic illustration for hillock growths.

1.4 Organization of the Dissertation

In the previous studies, solid state bonding by using Ag material is successful at lower temperature without pressure [61-62].However, it hasn't been explained clearly how the Ag material can be bonded to each other under lower temperatures without any applied pressure, although the feasibility of Ag solid state bonding is shown. Therefore in this thesis, the solid state bonding method using Ag material, called Ag stress migration bonding, has been developed by understanding the intrinsic bonding mechanism with hillock growth by stress migration, realizing it to apply in advanced electronic package such as 3D integration and wide band gap power device.

Considering the main factor for the Ag stress migration bonding, three processes have been investigated; sputtering, bonding, and substrate material (see Fig. 29). And then the feasibility of flip chip bonding has been reviewd. The results from each effort are organized in the following manner:

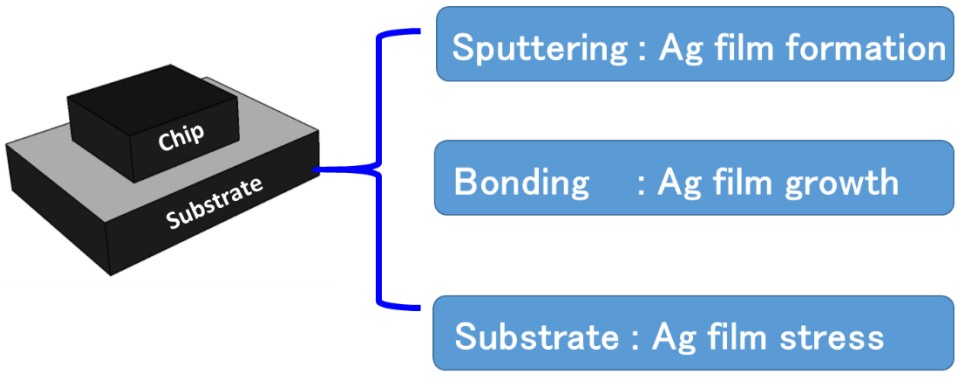

Figure 29. Three processes for Ag stress migration bonding.

Chapter 2 presents the effects of sputtering on Ag stress migration bonding. Ag thin film formed by sputtering is utilized to generate the large stress migration in Ag material. By changing the substrate temperature as a key parameter in the sputtering process, the microstructure formation, hillock growth and bonding properties were investigated. The change of residual stress in Ag thin film was also reviewed to explain the correlation with the bonding strength, determining one of the key factors in Ag stress migration bonding.

Chapter 3 covers the effect of micro-structural evaluation on thin film during the bonding process in Ag stress migration bonding. The change of microstructure with hillock formation on thin film was investigated by scanning electron microscope. The change of residual stress in Ag thin film was measured to confirm the effect of stress relaxation for each condition. The dynamic microstructure growth of Ag thin film under each bonding condition is reviewed, suggesting the optimum bonding condition in Ag stress migration bonding.

Chapter 4 explains the effect of substrate materials in Ag stress migration bonding. Four substrate materials having different thermal expansion coefficients were investigated. At each substrate, the changes in microstructure with hillock formation on thin film were investigated with increasing temperatures. The bonding strength was also measured with increasing temperature. These results demonstrate the effect of stress migration by the thermal stress generated during heating, playing the key role in Ag stress migration bonding.

Chapter 5 opens the feasibility of flip chip bonding using Ag stress migration bonding. After fabricating Cu bumps by sputtering, Ag films were deposited on Cu bumps under optimal conditions. The Cu bump thickness was varied to investigate the effect of Cu bump thickness on hillock growth. The microstructure evolution such as hillock growth on Ag films was observed, as well as the formation of bonding interface with different Cu bump thickness. Based on results, Ag stress migration bonding can be accessible for flip chip bonding.

Chapter 6 includes the conclusion and outlines for future work in Ag stress migration bonding.

References

[1] Ken Gilleo, “Milestones in Packaging”, http://www.et-trends.com/files/Milestones_in_Packaging.pdf

[2] http://semiconductormuseum.com/PhotoGallery/

[3] G. E. Moore, “Cramming More Components onto Integrated Circuits”, Proceedings of the IEEE 86, 82 (1998).

[4] “Converging technologies towards 3D Packaging Solutions”, http://www.i-micronews.com/upload/presentation/

[5] M. Horowitz *et al*, “Scaling, Power, and the Future of CMOS”, Electron Devices Meeting, 2005. IEDM Technical Digest. IEEE International, Washington DC, America, 7 (2005)

[6] Ivan Szendiuch, “Development in Electronic Packaging – Moving to 3D System Configuration”, Radioengineering 20, 214 (2011).

[7] Said F. Al-sarawi *et al*, “A Review of 3-D Packaging Technology”, IEEE Trans. Comp., Packag., Manufact. Technol. 21B, 2 (1998).

[8] Peng Sun *et al*, “Development of a New Package-on-Package (PoP) Structure for Next-Generation Portable Electronics”, 2010 ECTC(Electronic Components and Technology Conference), 1957 (2010).

[9] R.R. Siergiej *et al*, “Advances in SiC materials and devices: an industrial point of view”, Mater. Sci. Eng. B 61-62, 9 (1999).

[10] Hua Lu *et al*, “Design for reliability of power electronics modules”, Microelectron Reliab 49, 1250 (2009).

[11] Fan Xu *et al*, "Development of a SiC JFET-Based Six-Pack Power Module for a Fully Integrated Inverter", IEEE Trans. Power Electron. 28, 1464 (2013).

[12] Rozalia Beica, "3D Packaging Technologies and Industry Trends", http://www.i-micronews.com/upload/presentation/.

[13] Ho-Ming Tong, "Microelectronics packaging: present and future", Mater. Chem. Phys. 40, 147 (1995).

[14] K. N. Tu *et al*, "Physics and materials challenges for lead-free solders", J. Appl. Phys. 93, 1335 (2003).

[15] K. Suganuma, "The Development and Commercialization of Lead-Free Soldering", MRS Bull. 26, 880 (2001).

[16] K. Suganuma, "Advances in lead-free electronics soldering", Curr. Opin. Solid State Mater. Sci. 5, 55 (2001).

[17] K. Zeng, K. N. Tu, "Six cases of reliability study of Pb-free solder joints in electronic packaging technology", Mater. Sci. Eng. R 38, 55 (2002).

[18] K. Lee *et al*, "Influence of crystallographic orientation of Sn–Ag–Cu on electromigration in flip-chip joint", Microelectron Reliab. 51, 2290 (2011).

[19] K. Suganuma *et al*, "Sn whisker growth during thermal cycling", Acta Mater. 59, 7255 (2011).

[20] P. Lall, K. Banerji, "Assembly-level Reliability Characterization of Chip-Scale Packages", 1998 ECTC(Electronic Components and Technology Conference), 482 (1998).

[21] S. R. Vempati *et al*, "Development of 3-D Silicon Die Stacked Package Using Flip Chip Technology with Micro Bump Interconnects", 2009 ECTC(Electronic Components and Technology Conference), 980 (2009).

[22] Directive 2011/65/EU, http://ec.europa.eu/environment/waste/rohs_eee/.

[23] K.Suganuma *et al*, "High-Temperature Lead-Free Solders: Properties and Possibilities", JOM 61, 64 (2009).

[24] Y. Yamada *et al*, "Pb-free High Temperature Solders for Power Device Packaging", Microelectron Reliab. 46, 1932 (2006).

[25] Kim S. Slow, "Are Sintered Silver Joints Ready for Use as Interconnect Material in Microelectronic Packaging?", J. Electron. Mater. 43, 947 (2014).

[26] G. Bai, "Low-temperature Sintering of Nanoscale Silver Paste for Semiconductor Device Interconnection" PhD thesis, Virginia Polytechnic Institute and State University Blacksburg, Virginia, 2005.

[27] M.Kuramoto *et al*, "Die bonding for a nitride light-emitting diode by low-temperature sintering of micrometer size silver particles", IEEE Trans. Compon. Packag. Technol. 33, 801 (2010).

[28] K. Suganuma *et al*, "Low-temperature low-pressure die attach with hybrid silver particle paste", Microelectron Reliab. 52, 375 (2012).

[29] R. Khazaka *et al*, "Review on Joint Shear Strength of Nano-Silver Paste and Its Long-Term High Temperature Reliability", J. Electron. Mater. 43, 2459 (2014).

[30] H. Schwarzbauer *et al*, "Novel large area joining technique for improved power device performance", IEEE Trans. Ind. Appl. 27, 93 (1991).

[31] Kim S. Slow, "Mechanical properties of nano-silver joints as die attach materials", J. Alloys Compd. 514, 6 (2012).

[32] S. Sakamoto *et al*, "Thermal fatigue of Ag flake sintering die-attachment for Si/SiC power devices", J Mater Sci: Mater Electron 24, 2593 (2013).

[33] Z. Wei *et al*, "Particle Size and Pore Structure Characterization of Silver

Nanoparticles Prepared by Confined Arc Plasma", J. Nanomater. 968058, 1 (2009).

[34] A. Hu *et al*, "Low temperature sintering of Ag nanoparticles for flexible electronics packaging", Appl. Phys. Lett. 97, 1531171 (2010).

[35] J. Yan *et al*, "Pressureless bonding process using Ag nanoparticle paste for flexible electronics packaging", Scripta Mater. 66, 582 (2012).

[36] S. Wang *et al*, "Rapid pressureless low-temperature sintering of Ag nanoparticles for high-power density electronic packaging", Scripta Mater. 69, 789 (2013).

[37] A. Oestreicher *et al*, "An innovative method for joining materials at low temperature using silver (nano)particles derived from [$AgO_2C(CH_2OCH_2)_3H$]", Appl. Surf. Sci. 265, 239 (2013).

[38] C.-A. Lu *et al*, "Effects of Silver Oxide Addition on the Electrical Resistivity and Microstructure of Low-Temperature-Curing Metallo-Organic Decomposition Silver Pastes", Jpn. J. Appl. Phys. 46, 4179 (2007).

[39] M.Kuramoto *et al*, "New Silver Paste for Die-Attaching Ceramic Light-Emitting Diode Packages", IEEE Trans. Compon. Packag. Technol. 1, 653 (2011).

[40] S. Sakamoto *et al*, "Microstructural stability of Ag sinter joining in thermal cycling", J Mater Sci: Mater Electron 24, 1332 (2013).

[41] Z.Y. Zhang *et al*, "Pressure-assisted low-temperature sintering of silver paste as an alternative die-attach solution to solder reflow", IEEE Trans. Electron. Packag. Manufact. 23, 279 (2002).

[42] Y.-S. Tang *et al*, "Wafer-level Cu-Cu bonding technology", Microelectron Reliab. 52, 312 (2012).

[43] R. I. Made *et al*, "Experimental characterization and modeling of the mechanical properties of Cu-Cu thermocompression bonds for three-dimensional integrated

circuits", Acta Mater. 60, 578 (2012).

[44] K. N. Chen *et al*, "Morphology and Bond Strength of Copper Wafer Bonding", Electrochem. Solid-State Lett. 7, G14 (2004).

[45] K. N. Chen *et al*, "Temperature and Duration Effects on Microstructure Evolution during Copper Wafer Bonding", J. Electron. Mater. 32, 1371 (2003).

[46] K. N. Chen *et al*, "Microstructure evolution and abnormal grain growth during copper wafer bonding", Appl Phys Lett. 81, 3774 (2002).

[47] K. N. Chen *et al*, "Bonding parameters of blanket copper wafer bonding", J. Electron. Mater. 35, 230 (2006).

[48] T. H. Kim *et al*, "Room temperature Cu–Cu direct bonding using surface activated bonding method", J. Vac. Sci. Technol. A 21, 449 (2003)

[49] R. Tadepalli *et al*, "Formation of Cu–Cu interfaces with ideal adhesive strength via room temperature pressure bonding in ultrahigh vacuum", Appl Phys Lett. 90, 151919 (2007).

[50] T. Suga *et al*, "Structure of Al-Al and Al-Si_3N_4 interfaces bonded at room temperature by means of the surface activation method", Acta Metall. Mater. 40, S113 (1992).

[51] C. S. Tang *et al,* "Wafer-on-wafer stacking by bumpless Cu-Cu bonding and its electrical characteristics", IEEE Electron Device Lett. 32, 943 (2011).

[52] H. S. Chin *et al*, "A Review on Die Attach Materials for SiC-Based High-Temperature Power Devices", Metall. Mater. Trans. B 41B, 824 (2010).

[53] S. Ri *et al*, "Diffusion–fatigue interaction effect on hillock formation in aluminum thin films under thermal cycle testing", Mater. Lett. 79, 139 (2012).

[54] Okabayashi, "Stress-induced void formation in metallization for integrated circuits",

Mater. Sci. Eng. R 11, 191 (1993).

[55] T. C. Wang *et al*, "Stress Migration and Electromigration Improvement for Copper Dual Damascene Interconnection", J. Electrochem Soc 152, G45 (2005).

[56] W. Dauksher *et al*, "A methodology for the calculation of stress migration in die-level interconnects", Microelectron Reliab. 46, 616 (2006).

[57] B. Horváth *et al*, "Whisker growth on annealed and recrystallized tin platings", Thin Solid Films 520, 5733 (2012).

[58] Y. Yue *et al*, "Stress-induced growth of well-aligned Cu_2O nanowire arrays and their photovoltaic effect", Scripta Mater. 66, 81 (2012).

[59] M. Saka *et al*, "Rapid and mass growth of stress-induced nanowhiskers on the surfaces of evaporated polycrystalline Cu films", Scripta Mater. 56, 1031 (2007).

[60] H. Tohmyoh *et al*, "Controlling Ag whisker growth using very thin metallic films", Scripta Mater. 63, 289 (2010).

[61] M. Kuramoto *et al*, "Low-Temperature and Pressureless Ag–Ag Direct Bonding for Light Emitting Diode Die-Attachment", IEEE Trans. Comp. Packag. Technol. 2, 548 (2012).

[62] T. Kunimune *et al*, "Low-Temperature Pressure-Less Silver Direct Bonding", IEEE Trans. Comp. Packag. Technol. 3, 363 (2013).

Chapter 2

Ag Thin Film Formation in Sputtering Process

2.1 Introduction

During deposition process, the microstructure of thin film is classified at least into the three different types with substrate temperature, as shown in Fig. 1 [1, 2]. Refractory metals have structures shown in Fig. 1(a) when deposited at temperatures below 0.3 T_m. At substrate temperature in the range from 0.3 T_m to 0.5 T_m, uniform columnar structure is observed in metallic films as shown in Fig. 1(b). And metallic films have structures shown in Fig. 1(c) when the deposition temperature is above 0.5 T_m [1, 2]. In Fig. 1(a), the grain size of film varies from a few micro-meter at film surface to less than 100 Å at interface of film and substrate. When it is heated, the structures of Fig. 1 (a) and (b) evolve toward the structure of Fig. 1(c) [2].

In addition, the microstructure in thin films with crystallographic orientation can be determined by controlling anther deposition parameters such as the deposition rate and film thickness [3].

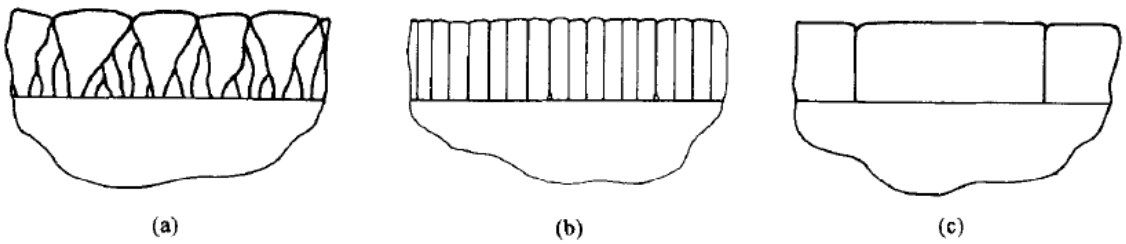

Figure 1 Schematic illustrations of cross-sectional images for microstructures in thin films [2].

The evolution of microstructure in thin films during deposition significantly has an effect on the development of intrinsic stress in thin films [3-5]. Doljack and Hoffman

reported that the tensile stress is occurred at the grain boundary by deforming the distance between adjacent grains when the two surface of individual grains is formed into one grain boundary to reduce surface area [3]. In the contract, compressive stress in thin film is caused by atom peening with sputter deposition energies above the lattice displacement energy, resulting in the compressive stress in thin film during film thickening [5].

Using Ag thin film, the solid-state bonding can be carried out at 250 °C without the application of pressure. An important mechanism in the solid-state bonding is the use of abnormal grain growth, e.g. hillock formation, on sputtered Ag films, commonly recognized as a phenomenon related to stress migration in metal thin films. The stress migration in thin films result from the intrinsic stress in thin films, forming hillock/whisker formation associated with stress relaxation.

In this chapter, the effects of substrate temperatures at deposition are investigated. Hillock growth can be tunable for solid-state bonding by controlling the grain texture in the deposited Ag films, expecting to play the key role in bonding method.

2.2 Experimental procedures

Dummy chips and substrates were prepared using a Si wafer of 0.5 mm in thickness, and they were cut into dimension of 3 mm × 3 mm and 6 mm × 6 mm, respectively. After ultrasonic cleaning for 5 min using acetone, the surface of the chips and the substrates were metalized with a 0.04 μm Ti adhesion layer that was deposited by RF sputtering, and subsequently a 1.0 μm Ag film by DC sputtering. The base pressure of the sputtering vacuum chamber was lower than 5.0×10^{-3} Pa and the Ar flow rate was 10 sccm (standard cubic centimeters per minute). The growth rate of Ti and Ag films was 6 nm/min and 30 nm/min, respectively. The substrate temperature for the deposition process varied from 25 °C to 150 °C to control the microstructure and the residual stress of the sputtered Ag films. A drop of ethylene glycol was spread over a Si substrate before mounting the chip to maintain a certain amount of contact between the Ag metalized surfaces of the chip and the substrate that face each other. The specimens were then bonded by heating at 250 °C for 1 h in an air environment oven without the application of pressure.

The bond strength was evaluated by die-shear tests (Dage 4000) where the shearing rate was set to 50 μm/s and the fly-height of the shearing chip was 1.2 μm from the substrate surface. Five bonded specimens at each substrate temperature upon Ag film deposition were tested. The cross-sectioned microstructure of the bonding interface was observed by scanning electron microscopy (SEM) to reveal the bonding structure at the interface, as well as the surface of the Ag metallized film for any morphological change on the Ag film surface during the bonding process.

In order to evaluate the residual stress on sputtered Ag film by sputtering and heating process, the residual stress of sputtered Ag film was measured by the $\sin^2 \psi$ method of X-

ray diffraction (XRD) at room temperature [6]. For each substrate temperature at film deposition, five samples were measured to determine the residual stress. The diffraction peak at 2θ = 156.87º was selected for the stress measurement with using monochromatic Cu $K\alpha_1$ radiation generated at 40 kV and 30 mA. The diffraction peak is overlapped both (333) and (115). However, because of the strong <111> preferential orientation of sputtered Ag thin films, the diffraction intensity is mainly contributed by (333) rather than (115) for lower ψ angles. In this case, the shift of 2θ diffraction peak position comes from the strained lattice spacing d_{ψ}^{333} due to the films stress, written as a function of ψ as : [7]

$$d_{\psi}^{hkl} = d_0^{hkl}\left(1 + \sigma\left[2\,s_1^{hkl} + \frac{1}{2}s_2^{hkl}\sin^2\psi\right]\right) \tag{1}$$

where d_0^{hkl} denotes unstressed lattice spacing, and s_1^{hkl}, s_2^{hkl} the X-ray elastic constants along <hkl> [7]. Non-linear least square fitting of Eq.(1) is used to determine the film stress σ, where ψ is limited up $\sin^2\psi$ = 0.08. It adopts the bulk Ag cubic lattice constant a = 0.40853 nm for the unstressed bulk spacing d_0^{333} = 0.0786 nm. The X-ray elastic constants are calculated by using Reuss model to s_1^{333} = -2.516 TPa^{-1}, and s_2^{333} = 21.505 TPa^{-1} from the anisotropic elastic constants $\{C_{ij}\}$ of Ag [8]. Note that the determined film stress σ includes the effect of diffraction peak shift at the origin (ψ = 0) through the least square fitting process on Eq.(1).

2.3 Results and discussion

2. 3. 1 The Microstructure of Bonding Interface

The microstructures of the bonded Ag films were observed by SEM on the cross-sectioned Si wafer samples after the bonding process, as shown in Fig. 2. The Ag abnormal grains in the films grew remarkably in both the vertical and horizontal directions, forming an indistinguishable bonding interface between the chip and the substrate. These large grain growths at the Cu-Cu bonding interface were reported under high pressure wafer-bonding conditions of 400 °C for 30 min followed by nitrogen annealing at 400 °C for 30 min [9]. In Ag solid-state bonding case, huge Ag grain growths occur at the bonding interface and at considerably lower temperature without applied pressure compared with those in the Cu-Cu bonding process because of larger thermal expansion [10], faster grain boundary diffusion [11], and less oxidation on the surface [12].

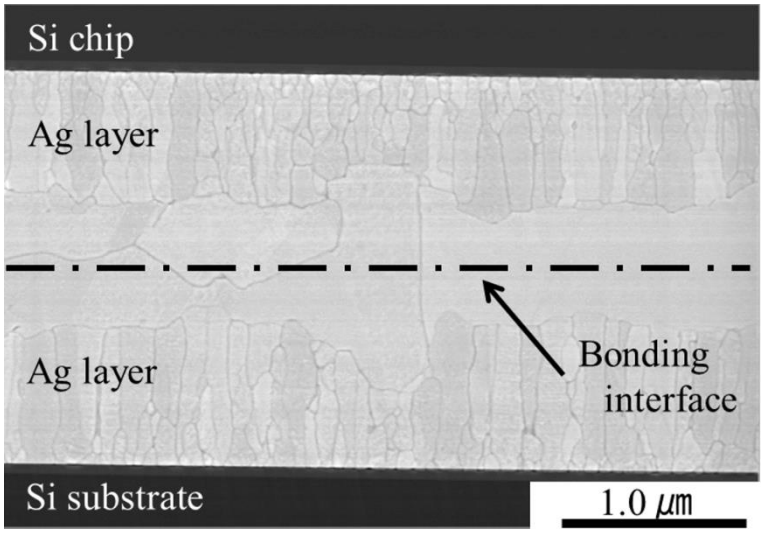

Figure 2. Cross-section SEM micrograph of Ag solid-state bonding using Ag thin films deposited at a low substrate temperature of 25 ℃.

2. 3. 2 Bonding Strengths with Various Substrate Temperatures

The die-shear strength of the bonded specimens decreases with increasing substrate temperature upon Ag film sputtering (see Fig. 3). The highest bonding strength was obtained for the specimens deposited at the lowest substrate temperature (25 °C) and Si wafer fracture was occurred during the shear tests due to the perfect bonding interface by abnormal grain growth at bonding interface as seen in Fig. 4(a). The fracture mode of the Ag grains in this case is ductile as shown in Fig. 5(a). This exhibited sound interface bonding, which was stronger than the fracture toughness of the Si wafer. Such a high strength bonding interface, which is comparable to other Si wafer bonding technologies, is a remarkable advantage particularly because of the considerably lower bonding temperature used without applied pressure compared with other wafer bonding processes [13].

As shown in Fig. 3, the die-shear strength depends on the substrate temperature of sputtering. When the substrate temperature is higher than 70 °C, the fracture occurs at the bonding interface between Si chip and Si substrate due to poor bonding interface formation (see Fig. 4(b) and (c)). The ductile fracture and film peeling can be observed particularly on the Ag films, as shown in Fig. 5(b). At a substrate temperature of 100 °C upon Ag film sputtering, the fracture mode of the bonded Si wafers changed to a bonding interface fracture between the chip and the substrate. At higher than 150 °C bonding hardly took place (see Fig. 3). The obvious dependence of the bond strength on the substrate temperature during the sputtering process implies that the bonding mechanism depends on the inherent properties of the as-deposited Ag films.

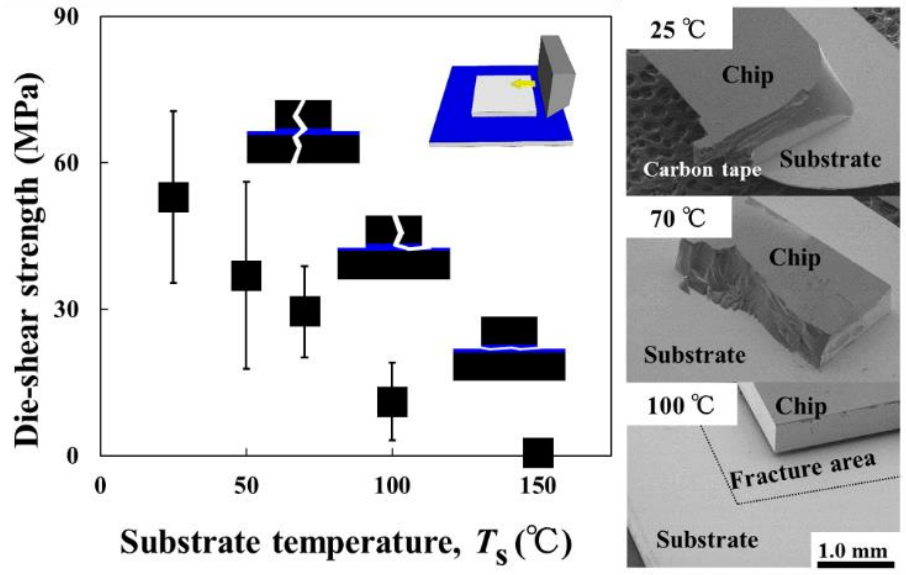

Figure 3. Shear strength of bonded sample with Ag films deposited at various substrate temperatures after heating at 250 °C for 1h.

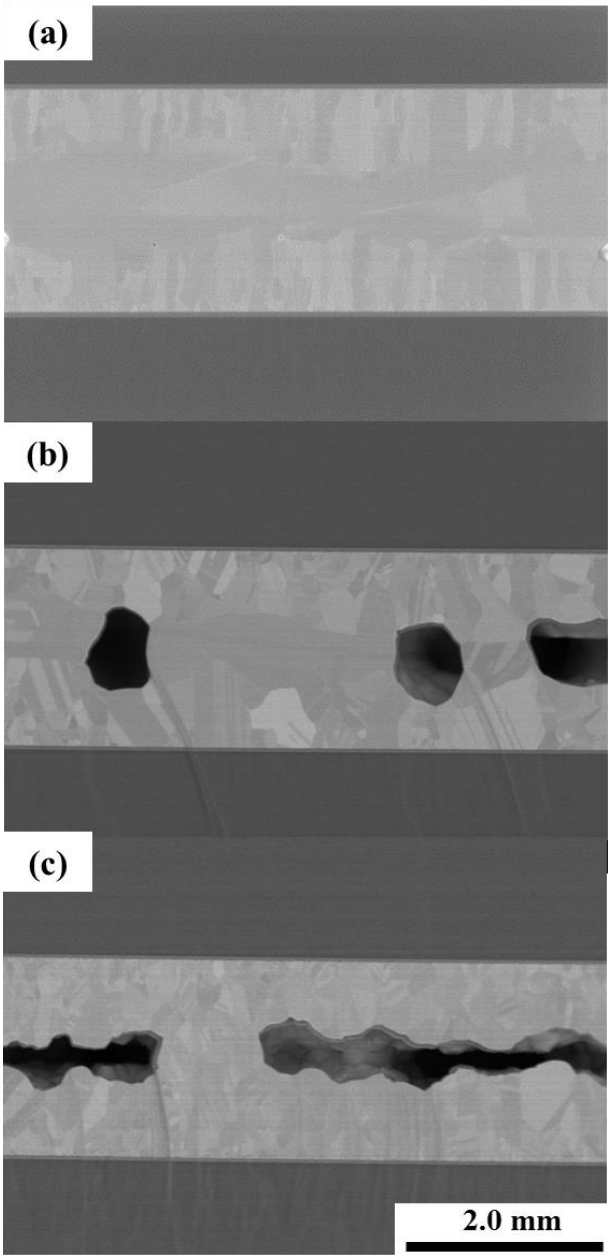

Figure 4. Cross-sectional SEM micrographs of the bonding interface after heating at 250 °C for 1h; (a) 25 °C of substrate temperature at deposition, (b) 70 °C of substrate temperature at deposition, and (b) 100 °C of substrate temperature at deposition

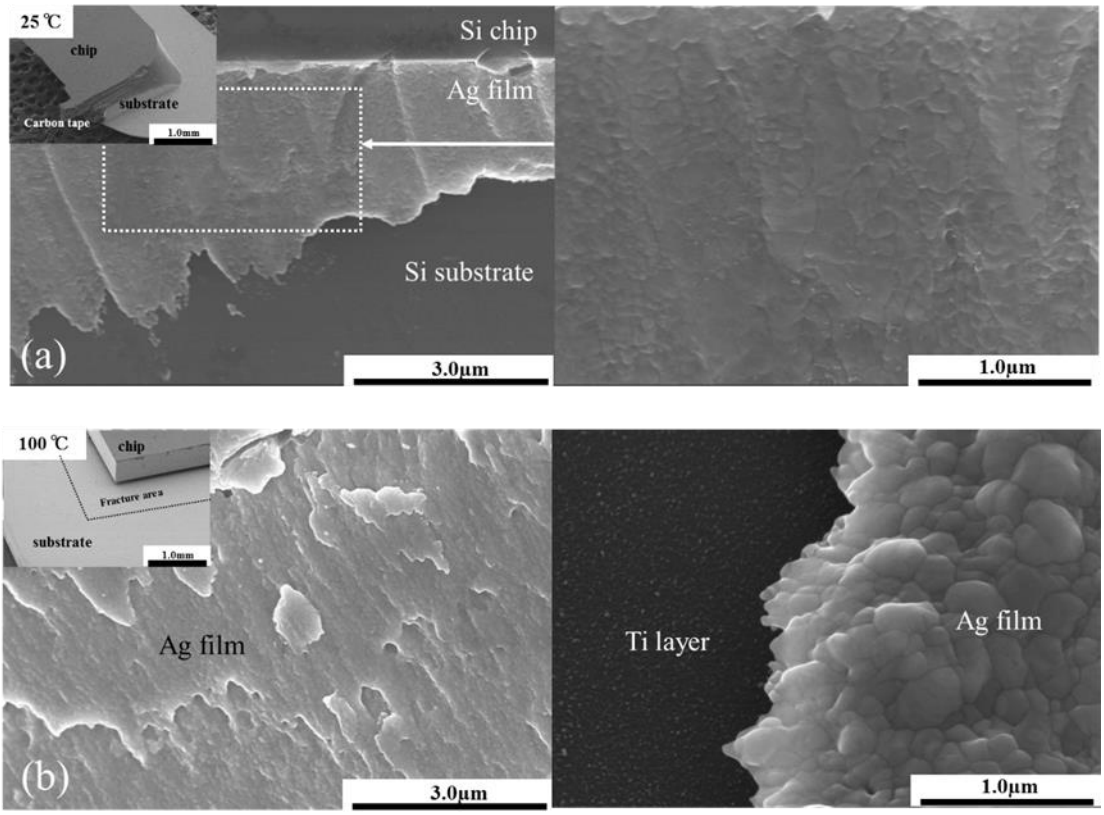

Figure 5. SEM micrographs of the Ag film fracture surface after the die-shear tests; (a) low substrate temperature (25 ℃) at Ag film deposition, and (b) high substrate temperature (100 ℃).

2. 3. 3 Microstructural Evolutions Between As-deposited and After Heating

The microstructures of the as-deposited Ag films on the Si wafer are shown in Fig 6(a). At a low substrate temperature, fine-grained silver was observed in the sputtered films, and the grain size was uniform. With an increase in the substrate temperature during the sputtering process, the size of the Ag grains increased and had a large distribution. In the early stage of the Ag film sputtering process, the nucleation of deposited materials was occurred by forming an island type grain. When island grains is connected to form continuous film, the grain boundary is generated. As the films thicken during deposition process, grain growth was occurred simultaneously by grain boundary diffusion and surface diffusion to reduce the interfacial energy associated with the grain boundary [14]. Thus, grain growth during film deposition depends on the substrate temperature because the grain growth is limited by thermally-activated diffusion. This variation in grain size that is determined by the substrate temperature has been reported for other thin films such as Cu. Ti [15].

After heat treatment during the bonding process, the microstructures in the Ag sputtered films drastically change, as shown in Fig. 6(b); many hillocks grow on the film surface. For the lowest substrate temperature, the size of generated hillocks is abnormal and larger than the grain sizes of the deposited films shown in Fig. 6(a). With an increase in the substrate temperature of film deposition, the hillock size grown by heating decreases, resulting in poor bonding interface as shown in Fig. 4. Such hillock growth on sputtered films has been reported in the literature and it results from the relaxation of compressive stress in the films and it is sensitive to the grain size [16]. The hillocks form preferentially on the triple points of the grain boundaries, and are thus affected by the

grain size in the as-deposited films [16, 17]. Therefore, the growth of hillocks can be controlled by the substrate temperature, which determines the grain size. Hillock growth is related to the bonding strength because the bonding interface is formed by hillock growth as shown in Fig. 4.

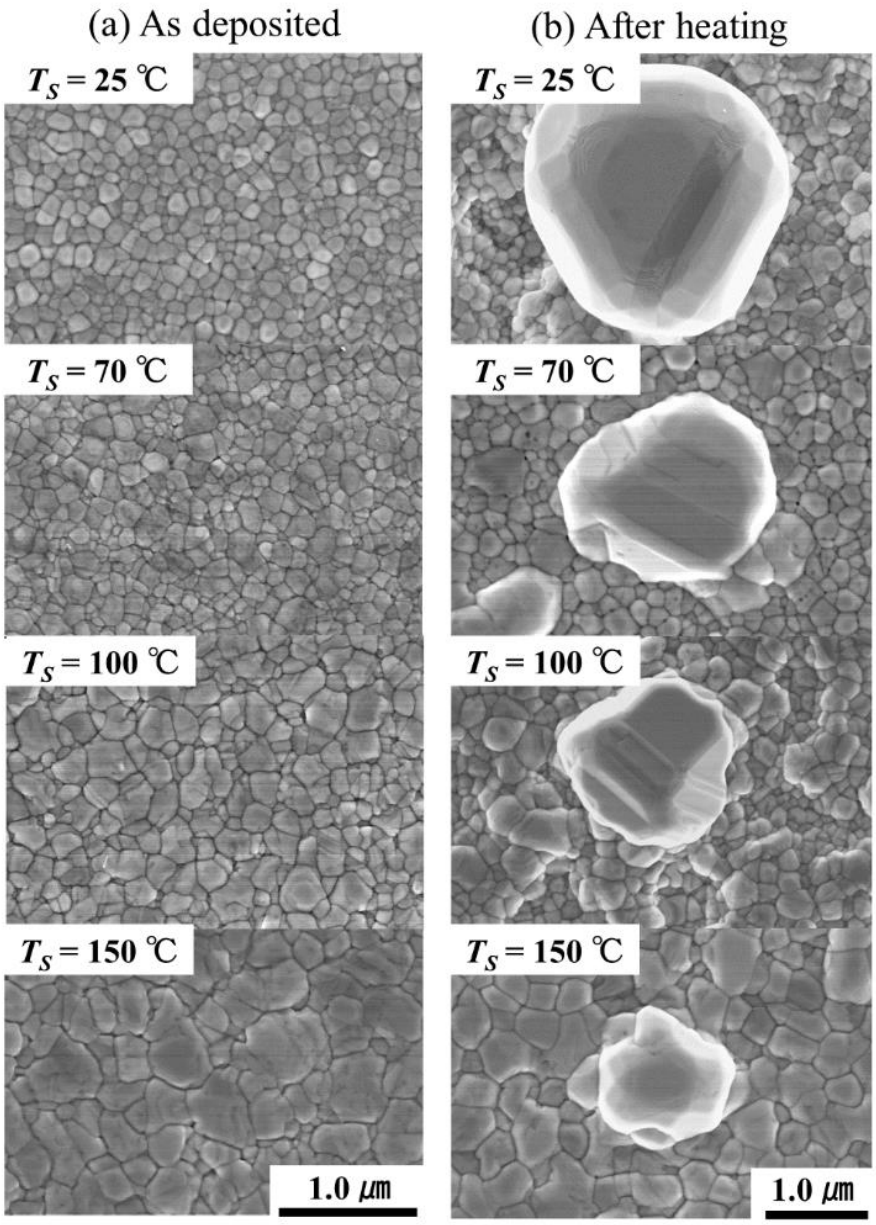

Figure 6. Surface morphology of the Ag films; (a) as-deposited, and (b) after heating at 250 °C for 1h.

2. 3. 4 Change of Residual Stress Between As-deposited and After Heating

The total residual stress in a thin film, in general, consists of three parts; internal stress σ_i, external stress σ_e, and thermal stress σ_{th} [7]. The internal stress σ_i is generated by the film structure of deposition, and the external stress σ_e comes from external reactions such as phase transformation, precipitation, and chemical reactions. The thermal stress σ_{th} is caused by the temperature variation ΔT between room temperature and the deposition temperature, as follows: [7]

$$\sigma_{th} = \frac{E_f}{1-\nu_f}(\alpha_s - \alpha_f)\,\Delta T, \quad (2)$$

where E_f and ν_f are the Young's modulus and Poisson's ratio of the film, respectively, and α_s and α_f are the coefficient of thermal expansion (CTE) of the substrate and the film, respectively. Since σ_e is negligible in the experiments, the initial stress $\sigma_{initial}$ in the Ag films before bonding is equal to the internal stress σ_i of the films deposited at room temperature. When Ag films are deposited on heated substrates, $\sigma_{initial}$ is moderated to $\sigma_i + \sigma_{th}$ since ΔT is negative upon cooling after deposition. Fig. 7(a) shows that the initial residual stress $\sigma_{initial}$ for a low substrate temperature is compressive whereas for a higher substrate temperature of more than 150 °C it becomes tensile because of thermal stress.

Regardless of the substrate temperature, however, the final residual stress σ_{final} after heat treatment becomes tensile, as shown in Fig. 7(a). At the bonding process, the film stress increases to $\sigma_{bond} = \sigma_{initial} + \sigma_{heat}$ because of rapidly increased temperature to T_{bond} = 250 °C. Upon bonding for 1 h, the stress σ_{bond} may be relaxed to σ_{bond}' when σ_{bond} is high enough to cause a plastic deformation. The final residual stress after cooling can be

written as $\sigma_{final} = \sigma_{bond}' + \sigma_{cool}$, and the total stress relaxation as $\Delta\sigma = \sigma_{final} - \sigma_{initial}$. The compressive stress relaxation can be estimated by the total stress change $\Delta\sigma$ during the whole process (see Fig. 8). This significant stress reduction $\Delta\sigma$ is accompanied by the microstructural change, i.e. hillock growth due to the stress migration, similarly to the thermal stress hysteresis reported for other metal thin films under cyclic heat treatment [18]. Therefore, the microstructural changes with hillock formation at bonding is driven by the compressive stress relaxation due to the heat treatment.

As shown in Fig. 2, the abnormal grain growth between the Ag films is relevant to achieve high bonding strength. Fig. 7(b) is a plot of the die-shear strength as a function of the stress change $\Delta\sigma$ during the bonding process. This plot confirms an approximately linear relationship between die-shear strength and stress relaxation. It is obvious that larger stress relaxation results in higher strength. This suggests that the bonding mechanism of abnormal grain growth is driven by thermomechanical stress as confirmed by the hillock growth shown in Fig. 6(b). Since such atomic migrations are accelerated by heating, the mechanism may depend on the bonding temperature in addition to the compressive stress in the films. Since It was used a constant bonding temperature of 250 °C, the bonding strength was determined by the initial residual stress in as-deposited Ag films, and hence by the total stress relaxation $\Delta\sigma$ under compression (see Fig. 7(b)). Therefore, increasing the substrate temperature upon deposition results in a lower bond strength, as shown in Fig. 3. The bonding mechanisms for stress migration that were revealed by this study allow to optimize the process for a desired bond strength. By maximizing hillock growth, it was obtained high strength bonding with sufficient abnormal grain growth. This mechanism also indicates that a lower bonding temperature may be possible once the compressive stress relaxation is optimized.

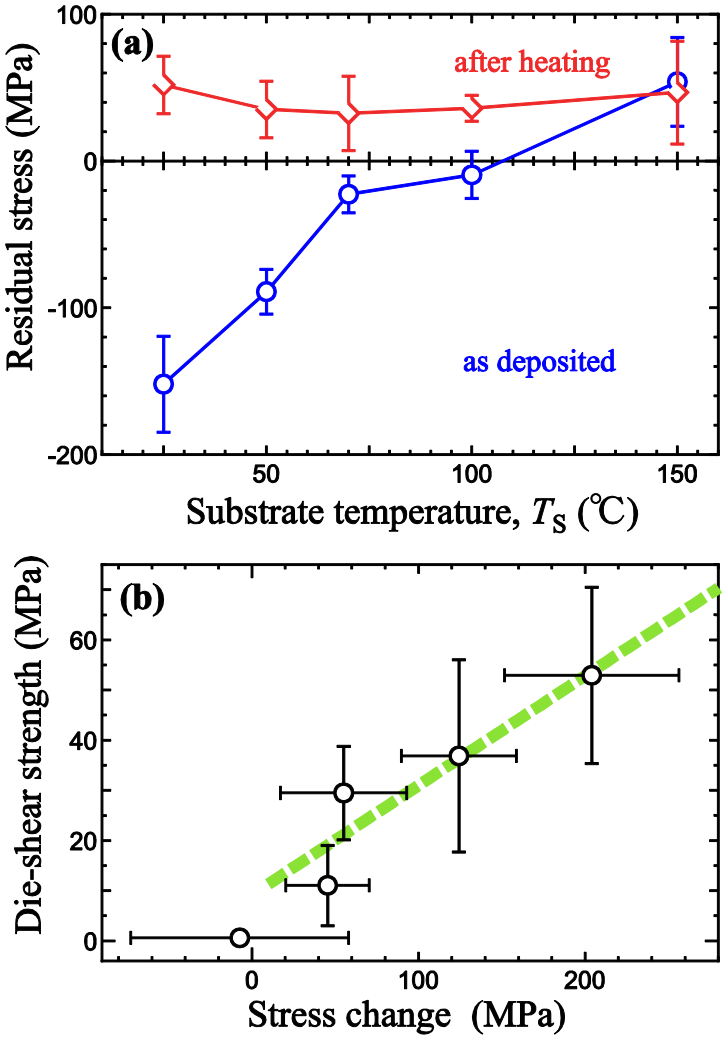

Figure 7. Compressive residual stress in the Ag films before and after heating at 250 ℃ for 1h (a). The correlation between bonding strength and stress changes between as-deposited film and heated film (b).

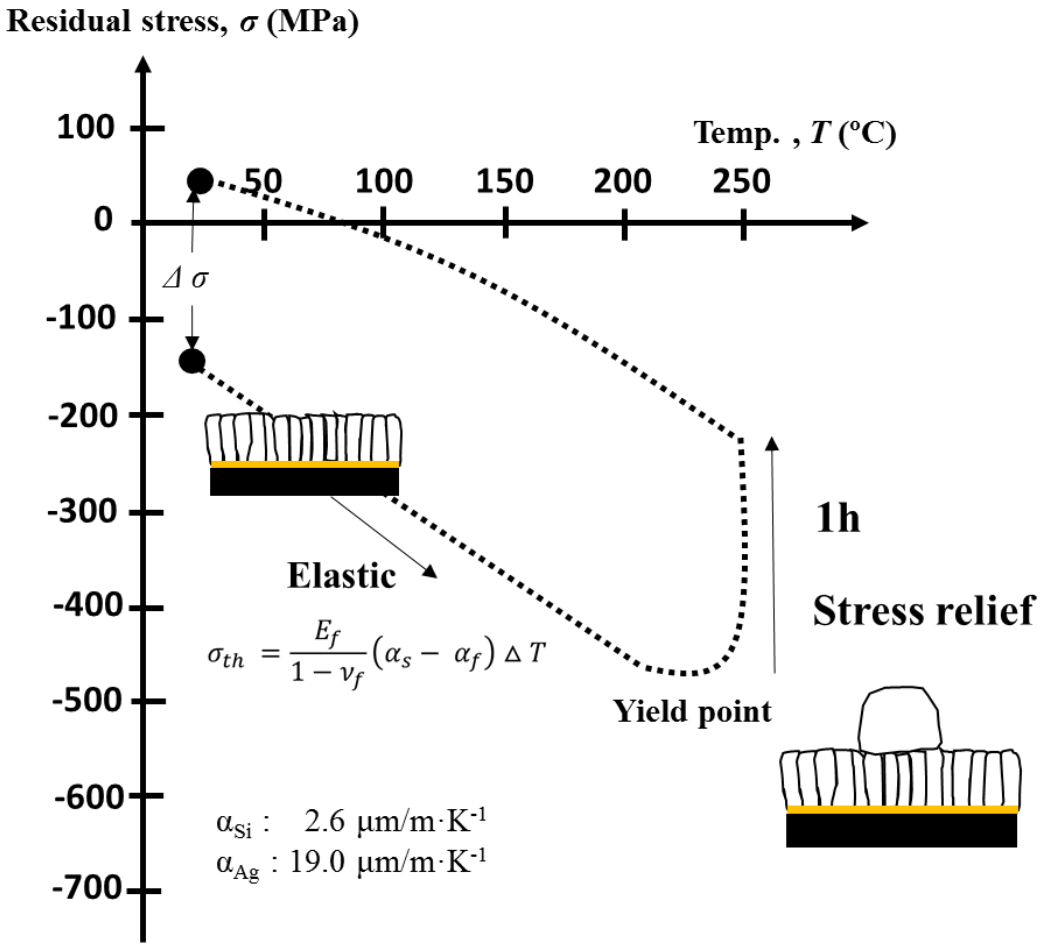

Figure 8. The behavior of stress in Ag film during heating at 250 °C for 1h and cooling at room temperature.

2.4 Conclusion

In summary, a method of Ag solid-state bonding is demonstrated using abnormal grain growth driven by stress migration in Ag thin films. The bonding mechanism is verified by hillock growth variation under controlled thermomechanical stress during the bonding process. This method presents an opportunity to tune the bond strength for individual applications by optimizing the process parameters of temperature and stress. Since the highest shear strength is much higher than the fracture strength of Si, Ag solid-state bonding is usable in a wide range of Si based device technologies.

References

[1] C. R. M. Grovenor, H. T. G. Hentzell and D. A. Smith, “The Development of Grain Structure during Growth of Metallic Films”, Acta. Metall. 32, 773 (1984).

[2] C. V. Thompson and R. Carel, “Stress and Grain Growth in Thin Films”, J. Mech. Phys. Solids 44, 657 (1996).

[3] F. A. Doljack and R. W. Hoffman, “The origins of stress in thin nickel films”, Thin Solid Films 12, 71 (1972).

[4] W. D. Nix and B. M. Clemens, “Crystallite Coalescence: A Mechanism for Intrinsic Tensile Stresses in Thin Films”, J. Mater. Res. 14, 3467 (1999).

[5] G. C. A. M, “Stress and strain in polycrystalline thin films”, Thin Solid Films 515, 6654 (2007).

[6] B.D. Cullity, Elements of X-ray diffraction (Addison-Wesley, California, 1978), p.456.

[7] R. Daniel, D. Holec, M. Bartosik, J. Keckes, C. Mitterer, “Size Effect of Thermal Expansion and Thermalintrinsic Stresses in Nanostructured Thin Films”, Acta Mater. 59, 6631 (2011).

[8] Y.A. Chang and L. Himmel, “Temperature Dependence of the Elastic Constants of Cu, Ag, and Au above Room Temperature”, J. Appl. Phys. 37, 3567 (1966).

[9] K.N. Chen, C.S. Tan, A. Fan, and R. Reif, “Morphology and Bond Strength of Copper Wafer Bonding”, Electrochem. Solid-State Lett. 7(1), G14 (2004).

[10] K.M. Zwilsky, ASM Handbook Vol.2 – Properties and Selection: Nonferrous Alloys and Special Purpose Materials (ASM International 10th ED, 2011), p. 2969.

[11] Chr. Herzig and S. V. Divinski, “Grain Boundary Diffusion in Metals- Recent Developments”, Mater. Trans. 44, 14 (2003).

[12] D. R. Gaskell, Introduction to the Thermodynamics of Materials 3rd Edition (Taylor & Francis, Washington, 1995), p.370.

[13] V. Dragoi, E. Pabo, “Wafer Bonding Process Selection”, ECS Trans. 33, 509 (2010).

[14] F.Spaepen, “Interfaces and Stresses in Thin Films”, Acta Mater. 48, 31 (2000).

[15] H. Savaloni, A. Taherizadeh, A. Zendehnam, “Residual Stress and Structural Characteristics in Ti and Cu Sputtered Films on Glass Substrates at Different Substrate Temperatures and Film Thickness”, Physica B 349, 44 (2004).

[16] D.K. Kim, W.D. Nix, R.P. Vinci, M.D. Deal, and J. D. Plumer, “Study of the Effect of Grain Boundary Migration on Hillock Formation”, J. Appl. Phys. 90, 781 (2001).

[17] T. Hanabusa, K. Kusaka, O. Sakata, “Residual Stress and Thermal Stress Observation in Thin Copper Films”, Thin Solid Films 459, 245 (2004).

[18] W. D. Nix, “Mechanical Properties of Thin Films”, Metall. Trans. A 20A, 2217 (1989).

Chapter 3

Microstructural Evolutions

in Ag Stress Migration Bonding Process

3.1 Introduction

Recently, hillock growth in metal thin films can be used for positive applications as explained in chapter 1. In previous chapter, hillock growth is intentionally introduced, in contrast to most previous research which has sought to prevent it. Solid-state bonding by stress migration in sputtered Ag films uses hillock formation to develop abnormal grain growth accompanied by stress relaxation. Hillock growth in thin films can be controlled by changing the compressive stress introduced during sputtering [1]. However, the evolution of the microstructure in Ag thin films can play one of key roles in bonding process as well, but its details have not been revealed yet.

By heating in bonding process, the diffusion process is occurred in thin film, resulting in grain growths associated with residual stress relief. In thin film, the diffusion is dependent on the film's microstructure formed in deposition, dividing into three types; A, B, C as shown in Fig. 1 [2, 3]. In Fig.1, The vertical lines shows the grain boundary and the curves are the iso-concentration contours. The diffusion source corresponds with the top horizontal lines in Fig. 1 [3].

At constant temperature, when $\sqrt{D_L t}$ is larger than L (a half of grain size), the lattice diffusion is governed in thin film as shown in Fig. 1(a). On the contrast, the grain boundary diffusion is dominant when $10\sqrt{D_L t}$ is less than $\delta/2$. According to the each regime, the evolution of microstructure in thin film is determined by predominant diffusion mechanism.

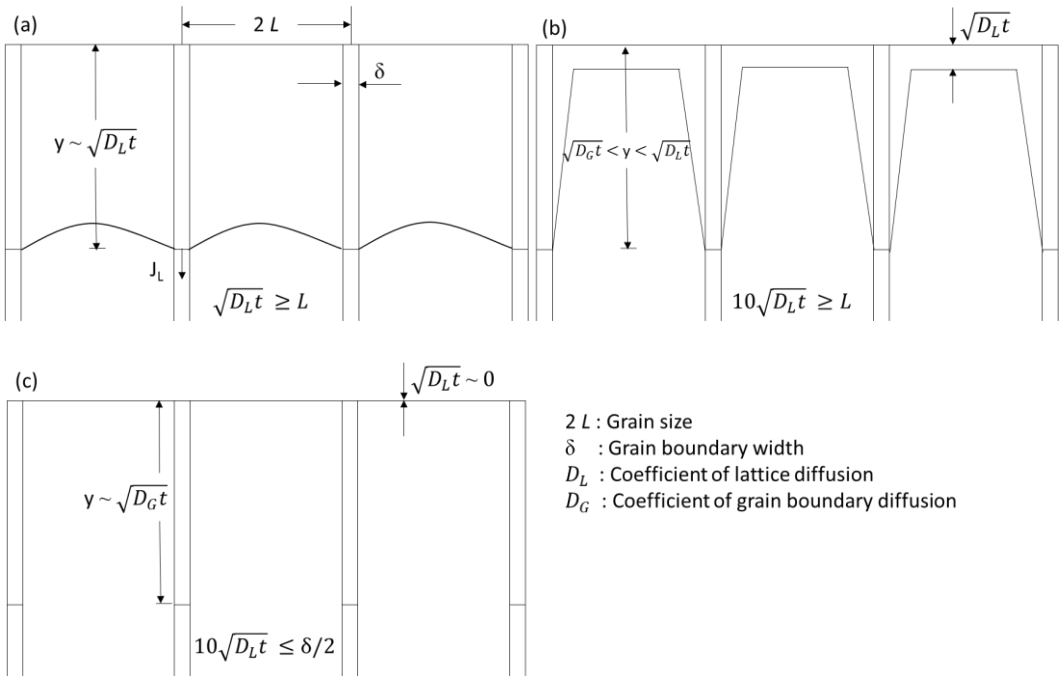

Figure 1. Schematic illustrations of (a) A-type, (b) B-type and (c) C-type kinetics in thin films [3].

In this chapter, It was investigated the development of the Ag film microstructure under various bonding conditions with diffusion dynamics. It was studied how the bond strength of Ag stress migration bonds varied with the microstructure at the bonding interface, investigating how the morphology changed with temperature and time.

3.2 Experimental procedures

The sample preparation and deposition process were carried out with the same experimental procedures in previous chapter. During deposition, the substrate temperature was kept at room temperature by a cooling system in the sputtering equipment.

After mounting a chip on substrate as followed by same experimental procedures in previous chapter, the specimens were placed in an oven in air without an applied load. To find the lowest bonding temperature that produced a sound bond, bonding temperature was increased in steps of 10°C up to 230°C, keeping a constant time of 1 h at each temperature steps. After finding the initial bonding temperature, the bonding temperature was increased in steps of 50°C from 250°C up to 400°C to evaluate the bonding properties at various process temperatures. To investigate the effect of process time, the bonding time is changed from 10 min to 120 min at bonding temperature of 250°C. The condition of die-shear test shear is same with the previous chapter. For each bonding condition, five bonded specimens was measured by the die-shear test.

Scanning electron microscopy (SEM) was used to observe how the surface and cross-sectional morphologies of the Ag film changed with the bonding process parameters. The number and size of the hillocks were measured using 20 μm × 25 μm areas from SEM micrographs. X-ray diffraction (XRD) was used to measure the texture of the sputtered Ag films. These XRD results were also used to calculate the residual stress of the sputtered Ag film at room temperature, using the $\sin^2 \psi$ method in previous chapter. Five specimens were measured to determine the residual stress for each bonding condition.

The bonding interface in Ag solid-state bonding was observed by Transmission

Electron Microscope (TEM), as well as the crystalline orientation of abnormal grain growth. For TEM observations, bonded samples were prepared by mechanical polishing with specified fixture along with water to remove the damage by heat generated during sample preparation.

3.3 Results and discussion

3. 3. 1 Microstructure of As-Deposited Ag Films

Figure 2(a) shows the presence of fine (~ 100 nm) grains on the surface of the sputtered Ag film. The grain size distribution was homogeneous across the surface of each Si chip and substrate. Figure 2(b) shows typical cross-sectional SEM images of the Ag grain structure. Many grains appear columnar, although some equiaxed grains appeared near the Ti layer. The quality of the columnar structure in deposited Ag films may depend on the film thickness [4].

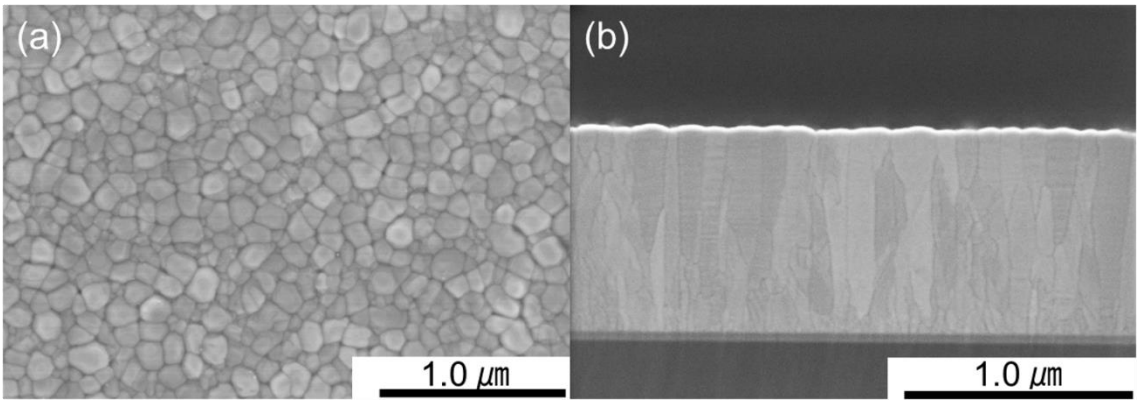

Figure 2. Fine-grained microstructure of as-deposited Ag films: (a) SEM micrograph of typical film surface and (b) cross-sectional columnar structure.

Figure 3(a) shows a typical XRD profile of as-deposited Ag films, matching the diffraction pattern of the face-centered cubic (fcc) Ag crystal structure. The 2θ profile clearly indicates the polycrystalline nature of the deposited film, but the (111) diffraction peak was remarkably higher than the others. It was confirmed the preferential <111>

orientation of the sputtered Ag films by plotting the integrated intensity of the (222) and (004) peaks as a function of $\sin^2\psi$, as shown in Fig. 3(b). The differing behavior of the two peaks indicates a preferential <111> axis normal to the film surface. Moreover, the integrated (222) intensity was higher than that of (004) over the whole $\sin^2\psi$ range available for Cu Kα X-rays, even though the calculated integrated intensities were similar for the fcc Ag crystal structure factors. This preference comes from the (111) plane having the lowest surface energy in the fcc structure because of thermodynamics. The strong <111> orientation also supports the internal stress analysis by $\sin^2\psi$ measurements, using only (333) diffraction and neglecting the overlapping (115) peak.

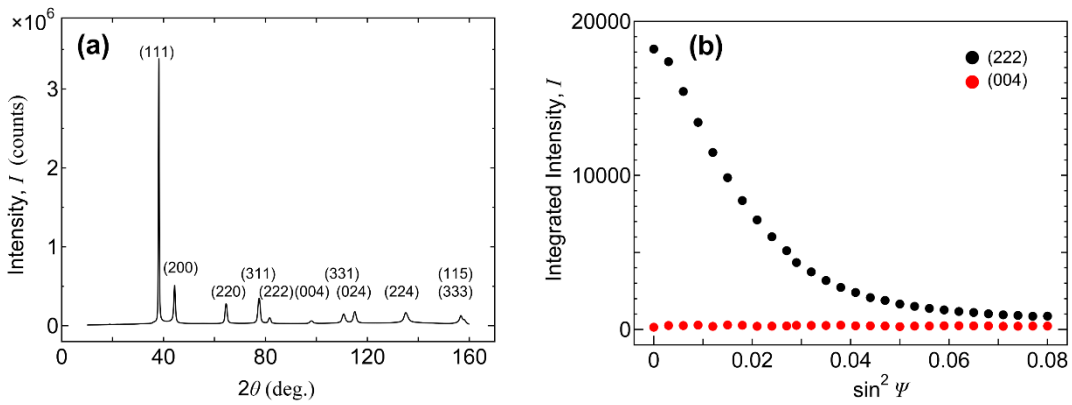

Figure 3. (a) XRD profile obtained for as-deposited Ag films; (b) integrated intensity of the (222) and (004) peaks..

During heating at 250 °C for 1h, if the hillocks which are grown vertically are faced each other as seen in Fig. 4(a), it's observed that the perfect interface without any voids is formed between hillocks as shown in Fig. 4(b) and Fig. 4(c). In Fig. 4(c) and Fig. 4(d), the fringe spacing with 0.24nm suggests that the hillocks in Ag thin film are grown with (111) crystalline orientation of Ag, matching well with the XRD results of as-deposited

films.

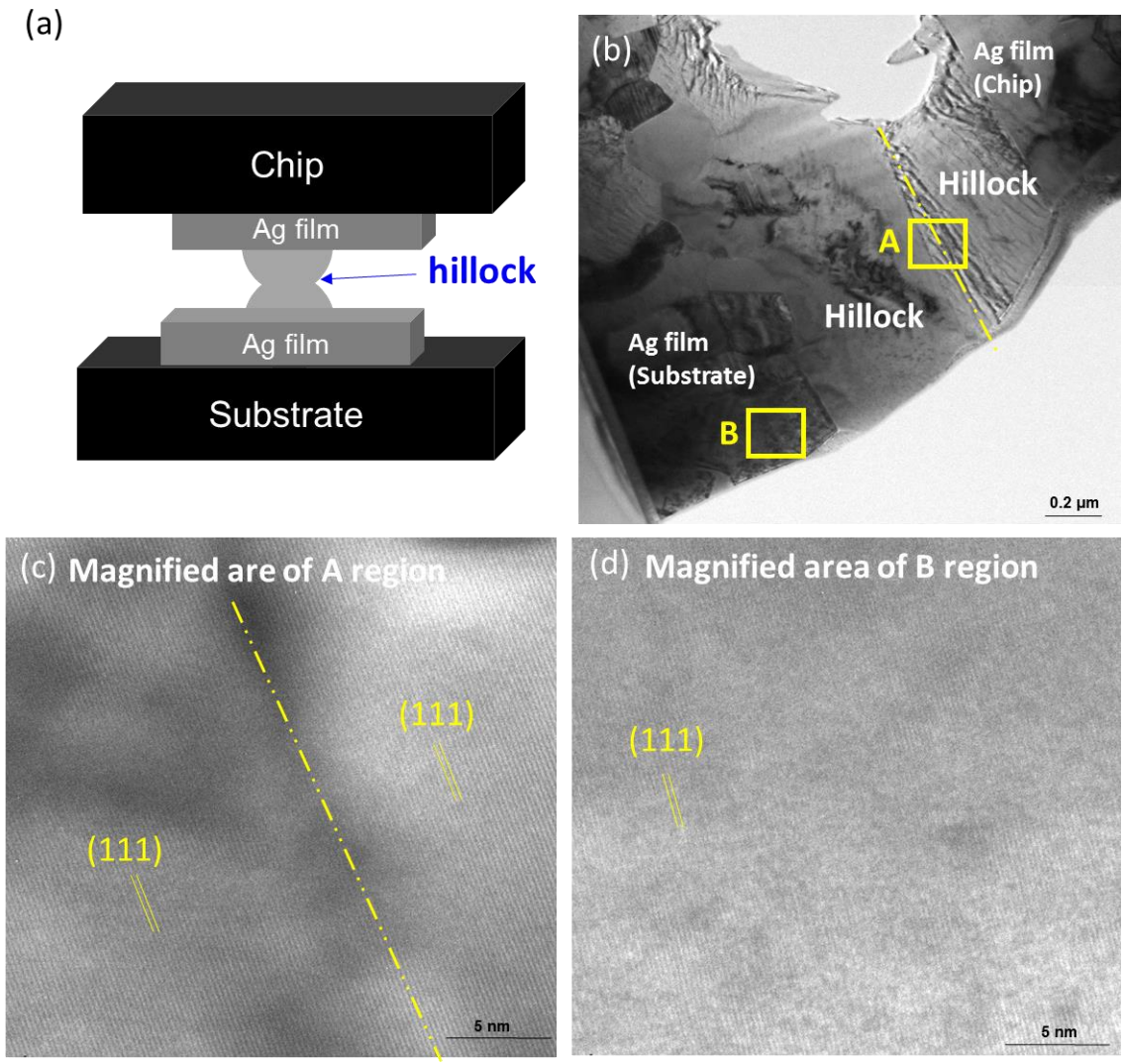

Figure 4. (a) Schematic illustrations of Ag solid-state bonding by hillock growth during heating at 250 °C for 1h; (b) Cross-sectional TEM micrograph at the interface of bonded sample at 250 °C for 1h with magnified area of interface (c) and sputtered film (d).

2. 3. 2 Changes in Microstructural Evolution and Bonding Properties with Bonding Temperature

Figure 5 shows how the microstructure of the as-deposited Ag films changed after heat treatment for 1 h at various temperatures. In films heated at 250 °C, the optimum bonding temperature, massive hillock growth was observed. At elevated temperatures during bonding, stress in the sputtered Ag film accumulates because of a large mismatch in the coefficient of thermal expansion (CTE) between the film and substrate. The compressive stress induced during heating causes stress migration of Ag atoms, driving hillock formation as the stress relaxes. Metal hillocks can nucleate at triplet junctions of grain boundaries, indicating pronounced grain-boundary diffusion [5]. Hillocks form much more easily on Ag films than Cu films because the grain boundary self-diffusivity of Ag is ten times faster than that of Cu [6] at 250 °C. Increasing the bonding temperature decreased the number of hillocks, although the hillock size sometimes increased, as shown in Fig. 5. At 400 °C, little hillock growth in the Ag film was observed, as shown in Fig. 5. Instead, the Ag grains grew and voids formed uniformly on the Ag film surface.

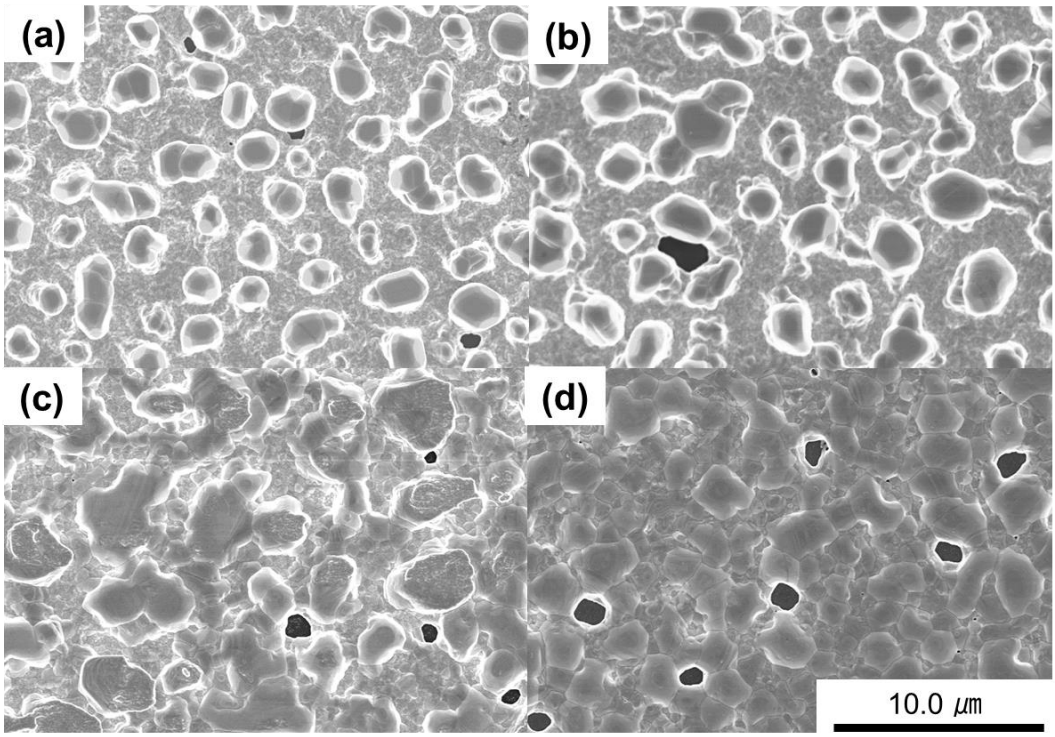

Figure 5. SEM micrographs of the microstructural evolution of Ag films at various bonding temperatures under a constant bonding time (1 h): (a) 250 °C, (b) 300 °C, (c) 350 °C, and (d) 400 °C.

At bonding temperatures of 230 °C and above, solid-state bonding is occurred by stress migration in Ag film, as shown in Fig. 6(a), indicating that the hillock growth becomes effective by increasing the activation energy necessary for growth diffusion in the experiment system. The error bar is calculated from the standard deviation of five specimens, possibly contributed from non-uniform contact due to thermal warpage of a chip. Over 230 °C, the hillock size increases significantly enough to develop abnormal grains completely at bonding interface. The highest bonding strength, >50 MPa, is obtained at 250 °C. The results is much better than values produced by other bonding technologies [7]. Above 250 °C, the die-shear strength decreases. The bond area grow by

abnormal grain growth and the original columnar structure disappears, as shown in Fig. 6(b). More over 350 °C, large non-bonded regions appear at the bonding interface due to smaller number of hillock growth, while relatively small voids appear along grain boundary near the bottom of the Ag film due to sufficient much diffusion over 350 °C from the interface between film and substrate to the surface of film by stress gradient in film. These non-bonded regions in the bonding interface are present where hillock growth doesn't occur, causing the lower bonding strength. At 400 °C, large Ag grains develop at the bonding interface and the columnar structures in the Ag film disappear completely.

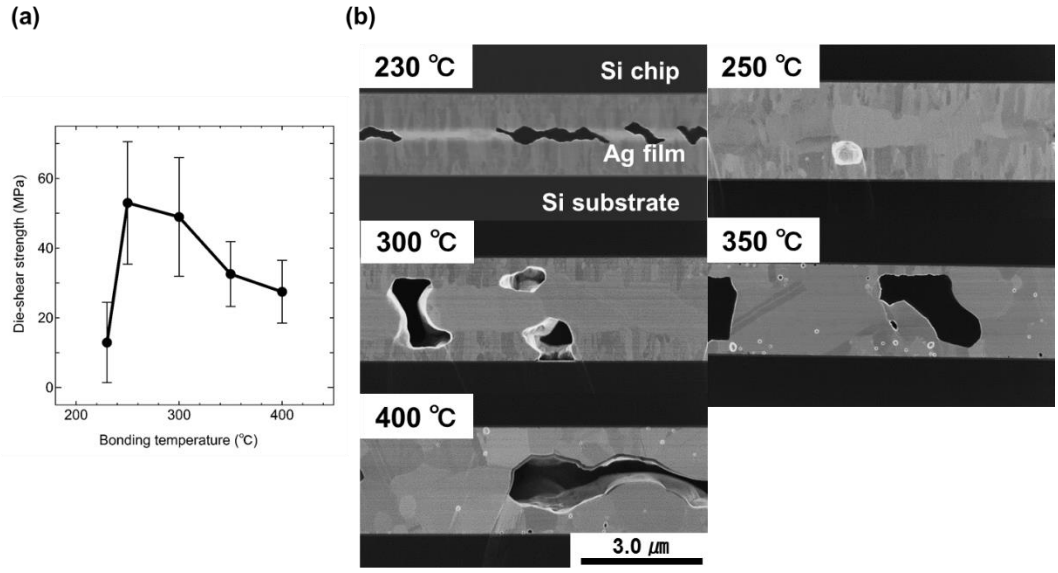

Figure 6. (a) Die-shear strength of samples and (b) cross-sectional SEM micrographs of the bonding interface at various bonding temperatures under constant bonding time (1 h).

Fig. 7(a) shows cross-sectional SEM images of the Ag microstructure across various heating temperatures. At 250 °C, large Ag hillocks appear on the columnar structure of the Ag sputtered film. However, as the bonding temperature increases, the Ag hillocks

grow laterally and downward, consuming the as-sputtered structure and generating large, disc-like cross-sectional hillocks, as shown in Fig. 7(b). The decrease of hillock height makes it vulnerable to bond directly each other; this result corresponds with the appearance of non-bonded areas in the bonding interface at high bonding temperatures, as shown in Fig. 6. As shown in Fig. 7(a), at higher bonding temperatures, the voids precipitate along the grain boundary of the sputtered Ag grain, further implying that hillock growth is dominated by grain boundary diffusion. At 400 °C, however, the Ag grains grow on all areas of the sputtered film with larger voids in the grain boundaries of the Ag film.

Assuming that the Ag film remains under in-plane, equally biaxial stress condition ($\sigma_{xx} = \sigma_{yy}$), stress ($\sigma$) – strain ($\varepsilon$) relationship under elastic region is simply given by

$$\sigma = \frac{E}{1-\nu}\varepsilon \tag{1}$$

where E and ν are Young's modulus and Poisson's ratio for thin film, respectively. When the film is under stress (σ) condition, the volume (V_σ) of the film is

$$V_\sigma = (1+\varepsilon)^2(1-\nu)V_0 \tag{2}$$

where V_0 is the volume of the film under stress free ($\sigma = 0$) condition. Considering the concentration of Ag film under stress condition, the concentration (C_σ) of the film is

$$C_\sigma = \frac{n}{V_\sigma} = \frac{n}{V_0}\frac{1}{(1+\varepsilon)^2(1-\nu)} = \frac{C_0}{(1+\varepsilon)^2(1-\nu)} \tag{3}$$

where n is the number of atoms in unit volume and C_0 is the concentration of the film

under stress free ($\sigma = 0$) condition. If the ε is very small, the equation of concentration variation with strain can be derived from eq. (3).

$$\frac{\partial c}{\partial \varepsilon} = \frac{-2c_0}{(1+\varepsilon)^3(1-\nu)} \sim \frac{-2c_0}{(1-\nu)} \tag{4}$$

From, eq. (1), the equation of concentration variation with stress can be derived

$$\frac{\partial c}{\partial \sigma} \sim \frac{-2c_0}{E} \quad (\varepsilon << 1) \tag{5}$$

Therefore, the diffusion flux can be expressed by stress distribution of Ag film with film thickness as follows,

$$J_{TOTAL} = -D\frac{\partial c}{\partial z} = -D\frac{\partial c}{\partial \sigma}\frac{\partial \sigma}{\partial z} \sim D\frac{2c_0}{E}\frac{\partial \sigma}{\partial z} \tag{6}$$

Assuming that stress gradients in the lattice and along grain boundary of Ag film are the same, the total diffusion flux J_{TOTAL} through the lattice J_{L} and boundary J_{GB} is

$$J_{TOTAL} = \frac{J_{GB}\delta + J_L d}{d} = \left(\frac{D_{GB}\delta + D_L d}{d}\right)\frac{2c_0}{E}\frac{\partial \sigma}{\partial z} \tag{7}$$

where δ, d are the grain boundary width, grain size, respectively. In this study, the gradient of compressive stress is parallel to the z-axis. The effective width of the grain boundary is assumed as $\delta \approx 0.5$ nm from the literature [8], while the measured grain size $d \approx 100$ nm in this study. In this case, the effective diffusion coefficient D_{Eff} is

$$\frac{D_{EFF}}{D_L} = 1 + \frac{D_{GB}\delta}{D_L d} \quad (8)$$

where D_L and D_{GB} are the lattice and grain boundary diffusivities, respectively. If $D_{GB}\delta$ is larger than $D_L d$, then grain boundary diffusion dominates the total diffusion flux. Taking $D_L = 5.58\times10^{-24}$ m^2/s and $D_{GB} = 1.09\times10^{-14}$ m^2/s at 250 °C from the lattice and grain boundary diffusivities in the literature [8], the ratio $D_{GB}\delta/D_L d$ from Eq. (8) to be ≈ 9.73×10^6 is calculated. Thus, at 250 °C, the total diffusion flux is governed by grain boundary diffusion, as shown in Fig. 7(c). Following the classification of the diffusion types by Horrison [2], type-C kinetics in which diffusion flux is limited only to the grain boundary is exhibited in the case of 250 °C. When the temperature exceeds 300 °C, type-B kinetics occurs where the grain boundary diffusion leaks into grain body. The ratio $D_{GB}\delta/D_L d$ at 400 °C decreases two orders of magnitude lower, ≈ 3.88×10^4, as shown in Fig. 7(d). Though the lattice diffusion thus increases the contribution to the stress relaxation at 400 °C, the grain boundary diffusion continues to dominate. However, the ratio $D_{GB}\delta/D_L d$ may decrease much less than the plot in Fig. 7(d) at 400 °C because of the enlarged grain size d as calculated from Eq. (8). For the measured grain size d ≈ 2.0 μm after 60 min at 400 °C (see Fig. 5(a)), the ratio becomes lower in three orders of magnitude: $D_{GB}\delta/D_L d \approx 1.94\times10^3$. At 400 °C, therefore, the lattice diffusion contributes more to the total diffusion flux, causing lateral grain growth rather than vertical hillock growth. The change of hillock growth morphology with temperature drives the changes in the bonding interface, affecting bond strength and reliability.

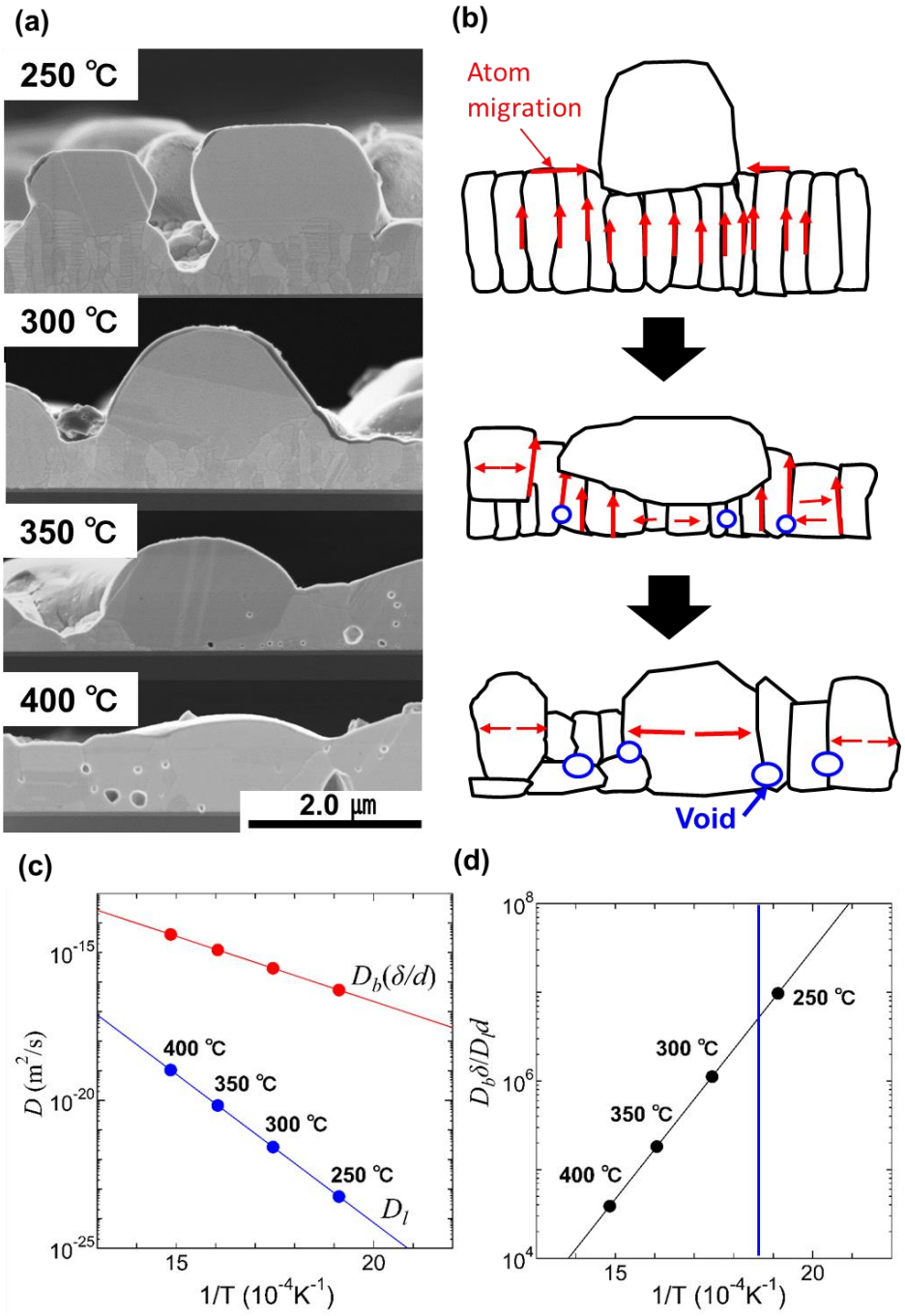

Figure 7. (a) Cross-sectional SEM micrograph and (b) schematic of hillock growth at various heating temperatures under constant bonding time (1 h). (c) Plotting the diffusivities of the grain boundary and lattice and (d) the ratio $D_{GB}\delta/D_Ld$ with temperature.

The number and size of the hillocks grown on the Ag films heat treated at various bonding temperatures for 1 h were measured; Fig. 8 shows these as functions of the bonding temperature. The average hillock diameter increased with bonding temperature, while the number decreased. The shear strength depended on the bonding temperature, with the highest bond strength being achieved at 250 °C, the intersection of increasing hillock size and decreasing hillock number. Note that the dependence of bond strength on the process temperature was closely related to the microstructure changes caused by the heat treatment, as shown in Fig. 5 and 6.

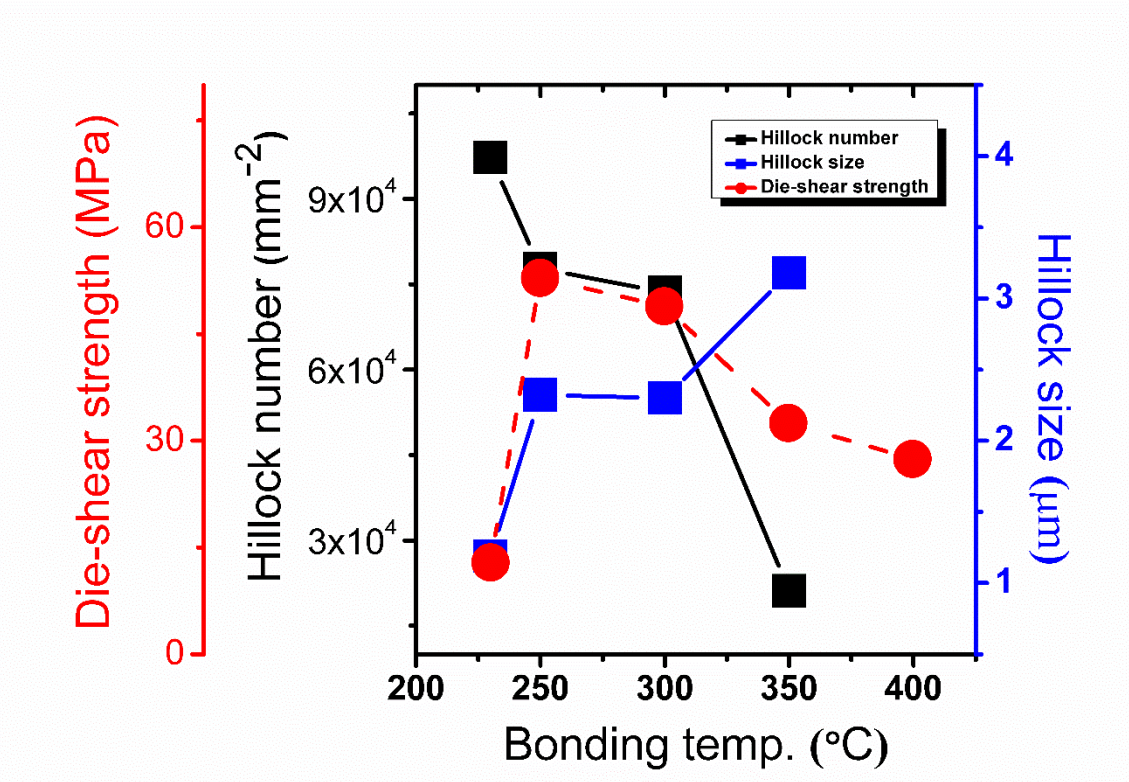

Figure 8. Correlation of the size and number of hillocks with the measured die-shear strength of bonded samples.

2. 3. 3 Changes in Microstructural Evolution and Bonding Properties with Bonding Time

Adopting an optimized process temperature of 250 ℃, it was investigated how varying the bonding time affected the microstructural evolution of Ag films, as shown in Fig. 9. The hillock number and size increased with bonding time. However, after 60 min, many more voids formed in the Ag film with little increase in the hillock size. At times longer than 120 min, the hillock size remained constant and the grains surrounding the hillocks grew slightly. Hillock growth appears to have saturated at bonding times exceeding 60 min.

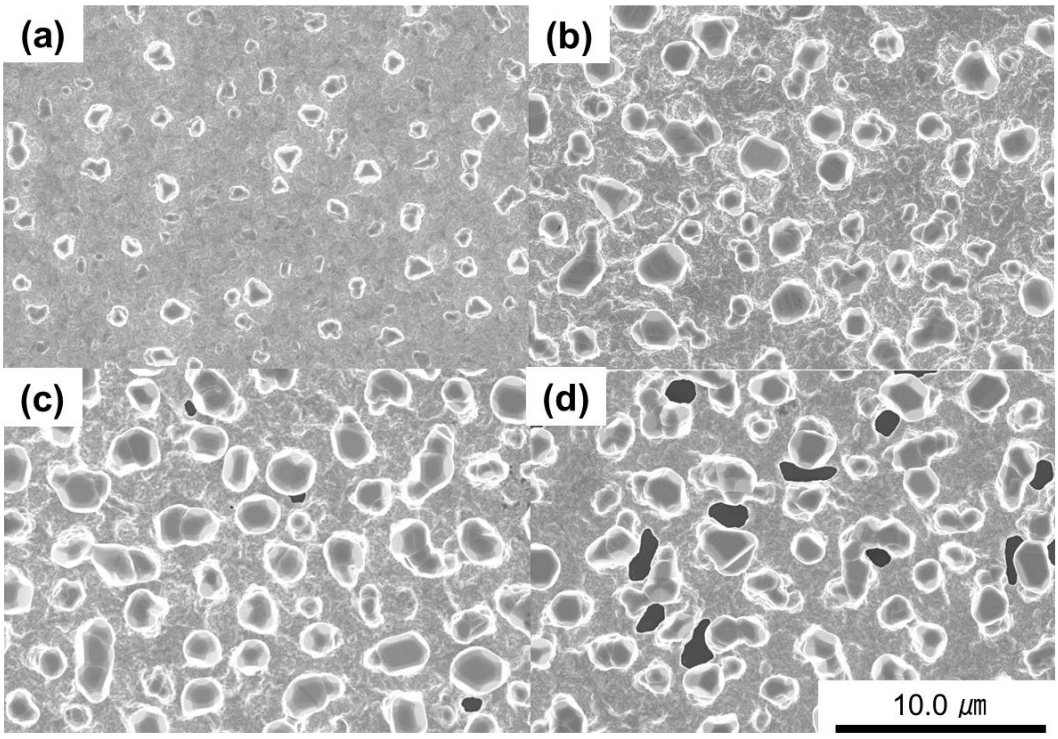

Figure 9. SEM micrographs of microstructural evolution at various bonding times under constant bonding temperature (250 °C): (a) 10 min, (b) 30 min, (c) 60 min, and (d) 120 min.

Fig. 10(a) shows the bonding strength of samples at a bonding temperature of 250 °C. The die-shear strength increases with bonding time. This result agrees well with the changes in cross-sectional microstructure with bonding time, as shown in Fig. 10(b). Abnormal Ag grain growth due to hillock growth occurs at the bonding interface area, enlarging the bond interfacial area with bonding time up to 60 min, forming a sound bonding interface while maintaining the original columnar structure in the Ag film.

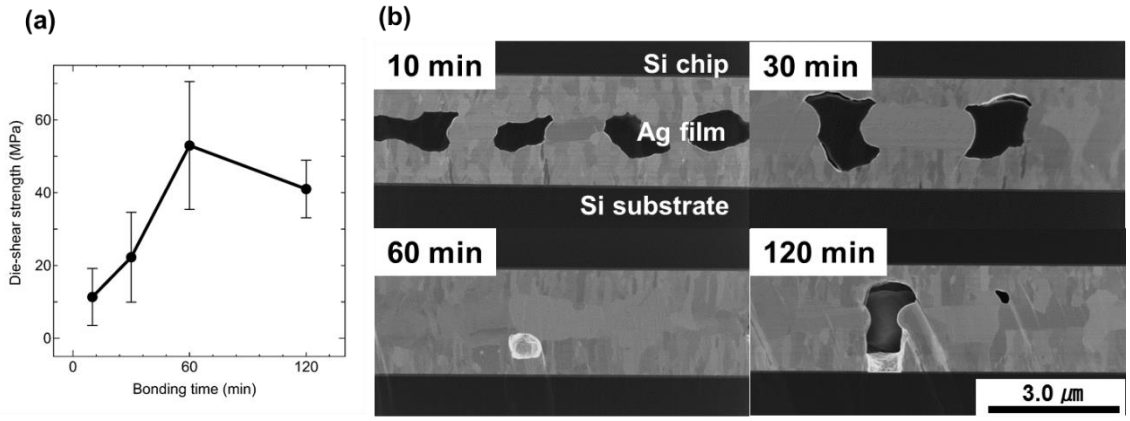

Figure 10. (a) Die-shear strength of samples and (b) cross-sectional SEM micrographs of the bonding interface at various bonding times under constant bonding temperature (250 °C).

The hillock growth in the Ag film was observed until 60 min, as shown in Fig. 11(a). It takes much time to become large hillock growth for bonding. Provided the sufficient bonding temperature and time for the atomic migration, the hillock growth continues until the compressive stress is relaxed. After bonding for 120 min, however, an area of large void appears in the Ag film and the film thickness became much thinner, as shown in Fig. 11(a). These large voids are created from aggregated atomic vacancies left behind sufficient diffusion for longer time. In Fig. 11(b), the variation of the Ag film thickness increases with increasing heating time due to increased instability in thin films. The void near the bond interface may impair abnormal grain growth. To ensure sound bonding, it is essential to optimize the heat treatment time to maximize hillock growth (i.e., abnormal grain growth) while also suppressing the formation of large voids at the bonding interface.

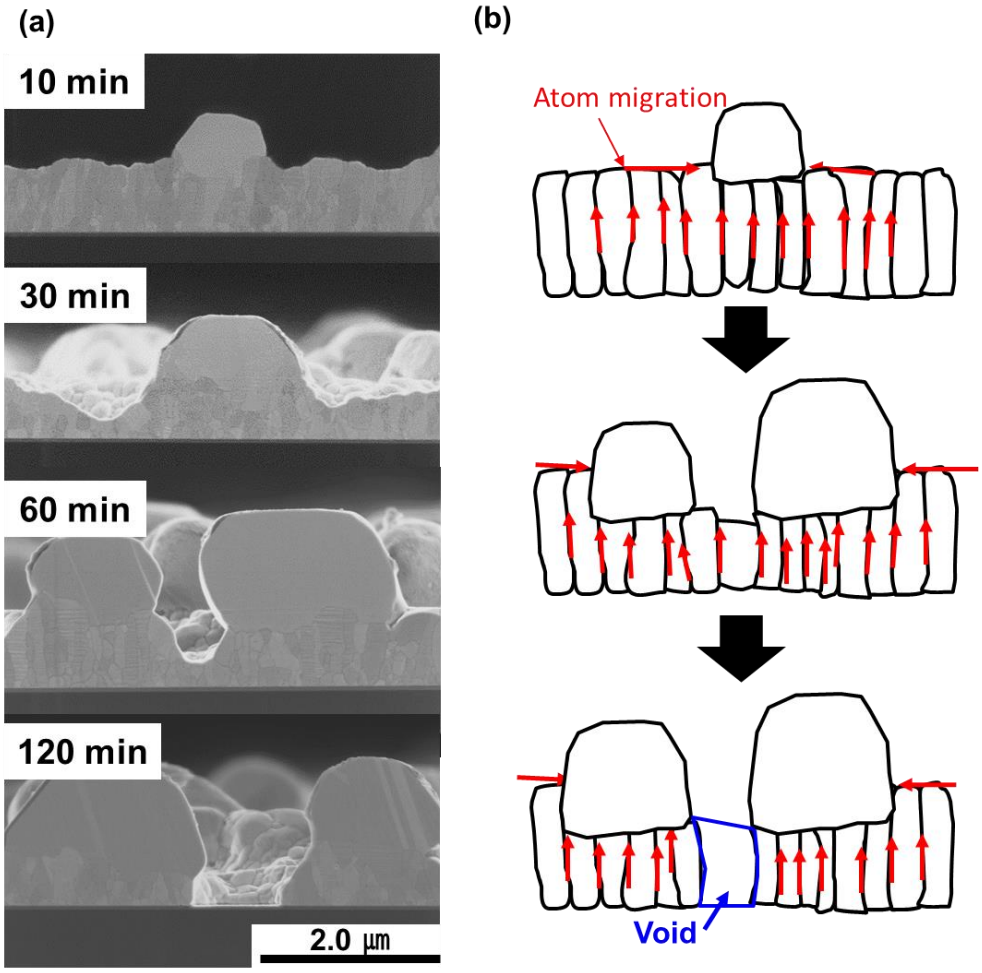

Figure 11. Cross-sectional SEM micrograph (a) and schematic (b) of hillock growth at various bonding times under constant bonding temperature (250 °C).

The hillock growth process has been scrutinized by means of the heat treatment time. Figure 12 shows the hillock number and size on the Ag films at 250 °C as a function of the process time, with the bond strength superimposed. The bond strength increased greatly with process time up to 60 min, then decreased slightly. This behavior agrees well with the hillock size and number on the film surface. The large areas of voids appearing after 60 min may have affected the bond strength, because a less dense structure formed, lacking obvious abnormal grain growth at the bonding interface.

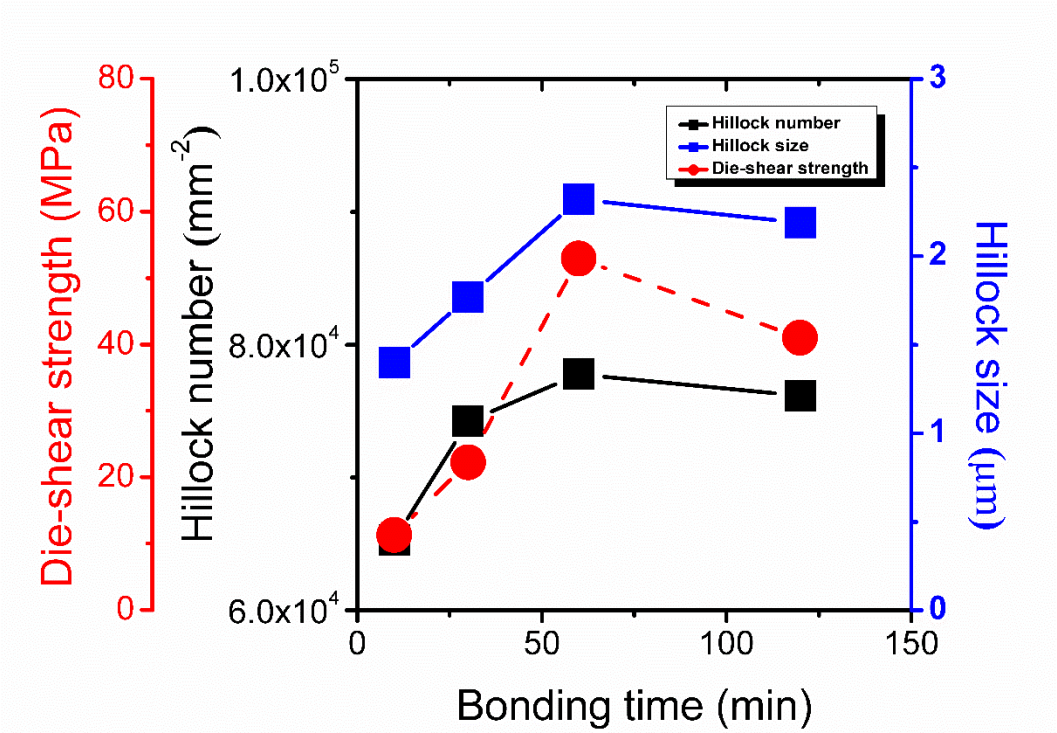

Figure 12. Correlation among the size and number of hillocks and the die-shear strength of bonded samples at various bonding times under constant bonding temperature (250 °C).

2. 3. 4 Changes in Residual Stress with Bonding Conditions

After the bonding heat treatment, the original compressive stress turned into tensile stress, as shown in Fig. 13. Stress relaxation in thin metal films during such heat treatment is usually caused by microstructural changes—in this case, hillock generation and grain growth—induced by thermal diffusion and accelerated by compressive stress [9]. The stress in the Ag films changed considerably after heat treatment (Fig. 13), and the stress after heat treatment was about constant over all bonding conditions in this study, except at the shortest bonding time of 10 min. This indicates that the stress relaxation was almost constant in the range of experiment conditions tested because the sputtering condition is same in the experiment for investigating the bonding process. However, the formation of bonding interface is governed by time-dependent diffusion process although it is the constant compressive stress relaxation. Thus, the microstructural changes in the Ag films during heat treatment depended on the temperature and process time, as shown in Figs. 5 and 9. The microstructural changes essential for bonding were mainly caused by thermally activated atomic diffusion, which was strongly driven by the compressive stress accumulated during both film deposition and heating.

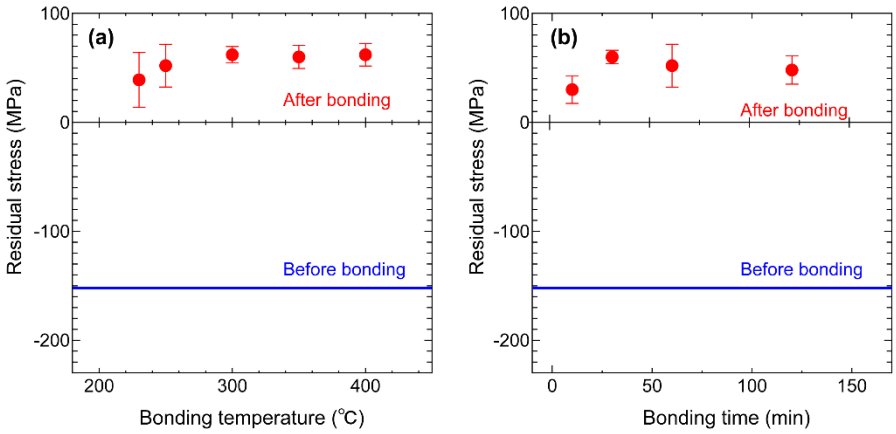

Figure 13. Residual stress in Ag films before and after heat treatment at various (a) bonding temperatures under constant bonding time (1 h) and (b) bonding times under constant bonding temperature (250 °C).

3.4 Conclusion

It is studied solid-state bonding, realized by abnormal grain growth on the surfaces of deposited Ag films. Fine columnar grains with (111) preferential crystalline orientation developed on the Si wafer. After heat treatment, it is observed how the Ag film microstructure evolved (including hillock growth), how it varied over various bonding conditions, and how it related to the bond strength. The changes in the Ag film microstructure were driven by significant stress relaxation from compressive to tensile at the elevated temperatures. By studying the hillock growth and grain growth over various bonding conditions, it can explain how the bond strength varied. The highest bond strength was achieved when many large hillocks grew while maintaining the columnar structure inside the remaining film. Stress migration bonding occurs more readily when grain boundary diffusion dominates. These hillocks transformed into abnormally grown, large Ag grains, forming a sound bonding interface with extremely high shear strength. It is believed that this bonding method will cause little damage to semiconductor chips when used for die bonding in electronics packaging.

References

[1] S. Ri, M. Saka, “Diffusion–fatigue interaction effect on hillock formation in aluminum thin films under thermal cycle testing”, Mater Lett 79, 139 (2012).

[2] L. G. Harrison, “Influence of dislocations on diffusions on diffusion kinetics in solids with particular reference to the alkali halides”, Trans. Faraday Soc. 57, 1191 (1961).

[3] D. Gupta and P. S. Ho, “Diffusion Processes in Thin Films”, Thin Solid Films 72, 399 (1980).

[4] J. Greiser, P. Müllner and E. arzt, “Abnormal growth of giant grains in silver thin film”, Acta mater. 49, 1041 (2001)

[5] D.K. Kim, W.D. Nix, R.P. Vinci, M.D. Deal, and J. D. Plumer, “Study of the effect of grain boundary migration on hillock formation”, J. Appl. Phys. 90, 781 (2001)

[6] Chr. Herzig and S. V. Divinski, “grain Boundary Diffusion in Metals- Recent Developments”, Mater. Trans. 44, 14 (2003)

[7] J. Yan, G. Zou, A-P Wu, J. Ren, J. Yan, A. Huc and Y. Zhou, “Pressureless bonding process using Ag nanoparticle paste for flexible electronics packaging”, Scripta mater. 66, 582 (2012)

[8] R. E. Hoffman, D. Turnbull, “Lattice and Grain Boundary Self Diffusion in Silver”, J. Appl. Phys. 22, 634 (1951).

[9] W. D. Nix, “mechanical properties of thin films”, Metall. Trans. A 20A, 2217 (1989)

Chapter 4

Effect of Substrate Materials on Ag Stress Migration Bonding

4.1 Introduction

In chapter 2, the effect of deposition process was investigated. The grain size was determined by substrate temperature at deposition process, leading to different bonding strengths. The bonding strengths were correlated well with the residual stress differences between as-deposited film and heat-treated film. Controlling the initial residual stress in thin film at deposition process is one of key factors in the Ag solid-state bonding.

In chapter 3, the effect of bonding process was also investigated on the Ag solid-state bonding. Boning temperature and bonding time changes the microstructure of Ag film, affecting in the bonding properties. The highest bonding strength was obtained in the condition that many large hillock grew. Therefore, the evolution of microstructure in Ag film is important factor for the Ag solid-state bonding.

However, in previous chapters, it was studied how the bonding properties vary with external conditions such as deposition and bonding, in condition that only Si materials was used in the experiments. In addition, Si materials has large thermal mismatch with Ag materials, occurring the hillock growth easily. Therefore, it is necessary to review the effect of inherent properties such as coefficient thermal expansion of materials.

Here, different substrate materials were examined to control the thermal stress fundamentally in Ag films, to understand the inherent mechanism of Ag solid-state bonding. Together with the results in previous chapters, these results provide an opportunity to adapt bonding to future high-temperature power devices.

4.2 Experimental procedure

The experimental procedure of the simple Ag solid-state bonding process is presented schematically in Fig. 1. First, various substrates of SiC, Mo, and Ti were prepared to provide different thermal stresses in the sputtered Ag films during the bonding process. Second, Ag films were deposited on the dummy chips and substrates by sputtering. Third, the samples were heated in an oven for an hour at each bonding temperature.

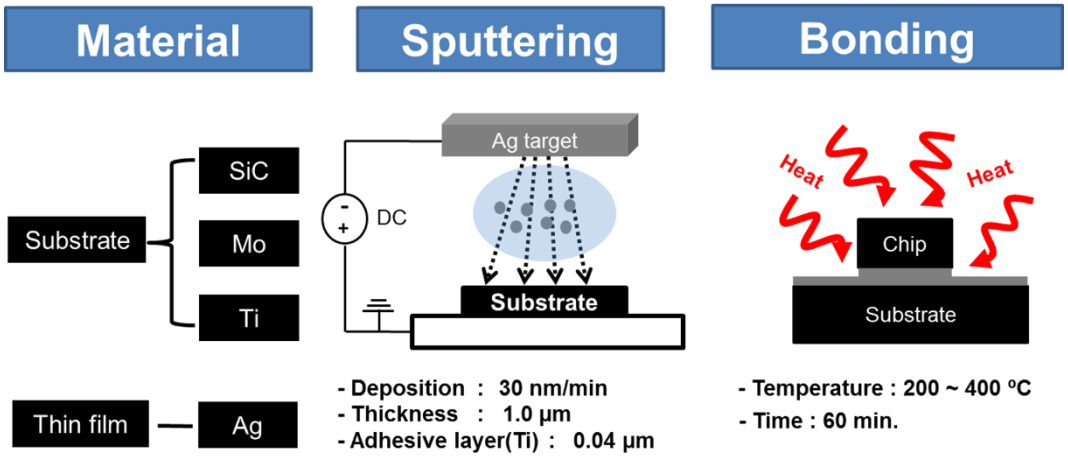

Figure 1. Schematic of the experimental procedure of the Ag solid-state bonding process.

In the SiC samples, 4H-SiC substrates with a thickness of 0.35 mm were selected because they are widely used in power electronics. The Mo and Ti samples had the larger thickness of 0.5 mm to give higher thermal stresses in the deposited Ag thin films. The dummy chips and substrates were prepared with the dimensions 3 mm × 3 mm and 6 mm × 6 mm. For all samples, the cleaning process, sputtering process, and mounting process

were carried out with the same experimental procedures in previous chapters.

The samples were then inserted into an oven in air and heated at a constant temperature for 1 h without applying any bonding pressure. The bonding temperature was varied from 200 °C to 400 °C in 50 °C steps, while the bonding time is kept as 1h. However, for the SiC samples, the bonding temperature was increased at an interval of 10 °C before the initial bonding temperature was obtained.

The die shear strengths of the five bonded samples were measured for each condition and evaluated as a function of the bonding temperature for each material. The condition in die shear test was same with previous chapters. The cross-sectional microstructures of the bonding interfaces as well as the morphological changes in the Ag film surfaces after the heat treatment were observed by scanning electron microscopy (SEM).

4.3 Results and discussion

4. 3. 1 The Microstructures of the Ag Film Surfaces on SiC Substrates

The evolution of the microstructures of the Ag film surfaces on SiC substrates were investigated by comparing as-deposited films and after heat treatment at the bonding temperature (see Fig. 2). The grain sizes in the Ag films were uniform regardless of the substrate material because the sputtering conditions were kept constant for all experiments. After the heat treatment for bonding, it was confirmed that grain growth and hillock formations appeared on all of the Ag film surfaces, as shown in Fig. 2(b).

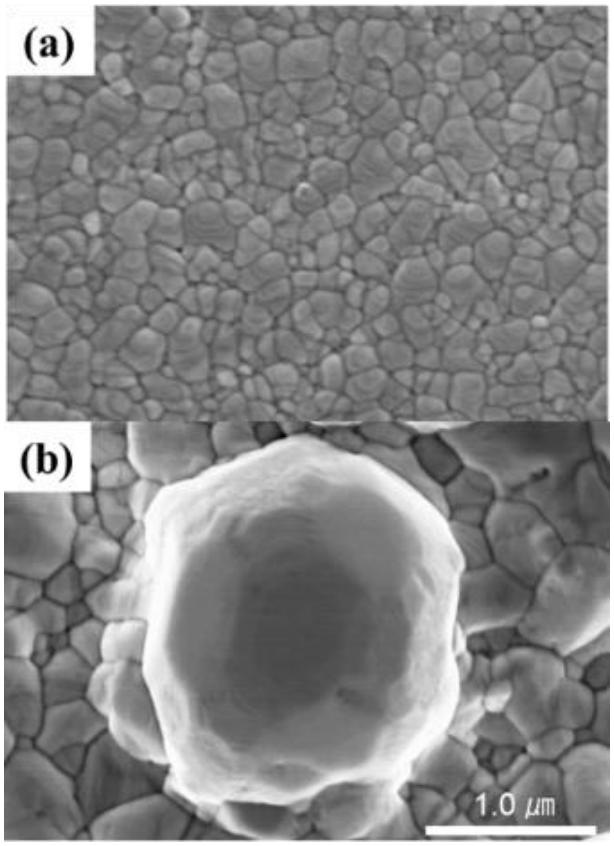

Figure 2. SEM micrographs of the microstructures of Ag films for an (a) as-deposited film and (b) after heating at 250 °C under constant bonding time (1 h).

4. 3. 2 Bonding Strengths with Various Substrates and Bonding Temperatures

Figure 3 shows the die-shear strengths of the bonded samples with various bonding temperatures and materials. The error bars were obtained from the standard deviation of five samples. The statistical errors are possibly responsible for the non-uniform contacts, caused by both the chips and substrates becoming thermally warped. Ag solid-state bonding of the SiC chips and substrates was successfully achieved at the low bonding temperature of 230 °C, resulting in 16 MPa of die-shear strength. With an increasing bonding temperature, the shear strength of the bonding increased to 43 MPa at 250 °C and then decreased until it became 16 MPa at 400 °C. The decreased bonding interface at higher bonding temperatures are caused by large voids at the interface between the Ag film and the substrate material because lateral grain growth in the Ag film was more dominant than hillock growth. The decreased contact interface area of the Ag film and substrate, thus moderates the die-shear strength. However, compared with Si materials as represented in Fig 6(a) in chapter 3, the bonding strength of SiC samples is lower under all the bonding temperatures (see Fig. 3). For the Mo chips and substrates, Ag solid-state bonding was occurred only above a bonding temperature of 300 °C resulting in 34 MPa of shear strength, while Ag solid-state bonding is failed under 300 °C. The shear strength of the Ag solid-state bonding also decreased with the bonding temperature. For the Ti samples, the Ag solid-state bonding was required a bonding temperature of at least 350 °C, resulting in 21 MPa of shear strength.

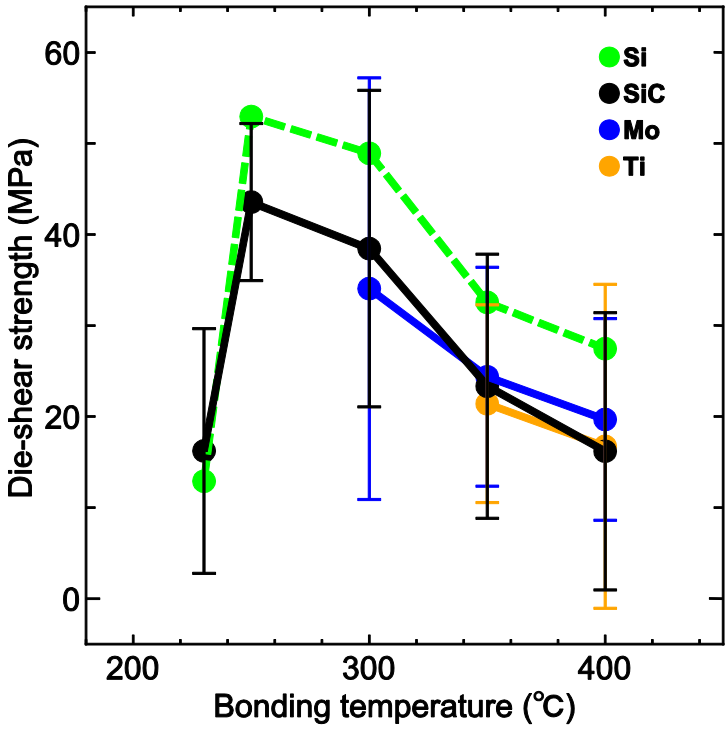

Figure 3. Die-shear strengths of the bonded samples for each material at various bonding temperatures under constant bonding time (1 h).

4. 3. 3 Microstructural Evolutions with Various Temperatures

To clarify the die-shear strength for each material, the hillock growth on the Ag film surfaces was observed on various substrates, as shown in Figs. 4 and 5. At a bonding temperature of 250 °C under constant bonding time (1 h), large amounts of hillock growths were observed on the SiC substrates, as shown in Fig. 4(a). When large and dense hillock growths occurs on both of the SiC chips and substrates (see Fig. 4(a)), the hillock growths turn into the abnormal grain growth at the contact interface of the chips and substrates, forming the bonding interface. However, the hillock growths on the Mo and Ti substrates were too small to create a bonding interface, while the sizes of the hillock growths on the Mo substrates were larger than those on the Ti substrates, as shown in Fig. 4.

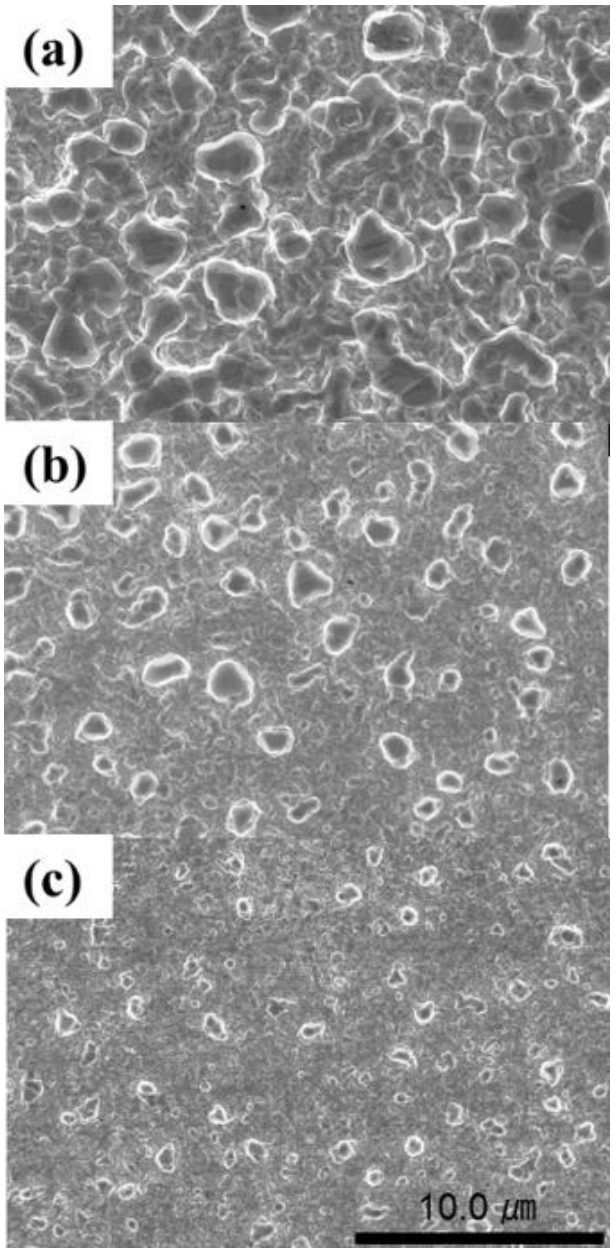

Figure 4. SEM micrographs of the microstructures in the Ag films after heating at 250 °C under constant bonding time (1 h) on (a) SiC, (b) Mo, and (c) Ti substrates.

At a bonding temperature of 350 °C under constant bonding time (1 h), the size of the hillock growths became significantly large, leading to successful Ag solid-state bonding for the all samples. However, lateral grain growth, together with hillock growth was mainly observed, as shown in Fig. 5. In addition, for the SiC substrates, the number of hillock growths decreased at a bonding temperature of 350 °C, as shown in Figs. 5(a). This behavior is compatible with the results of Si materials as explained by the contribution of Ag atomic diffusion in chapter 3.

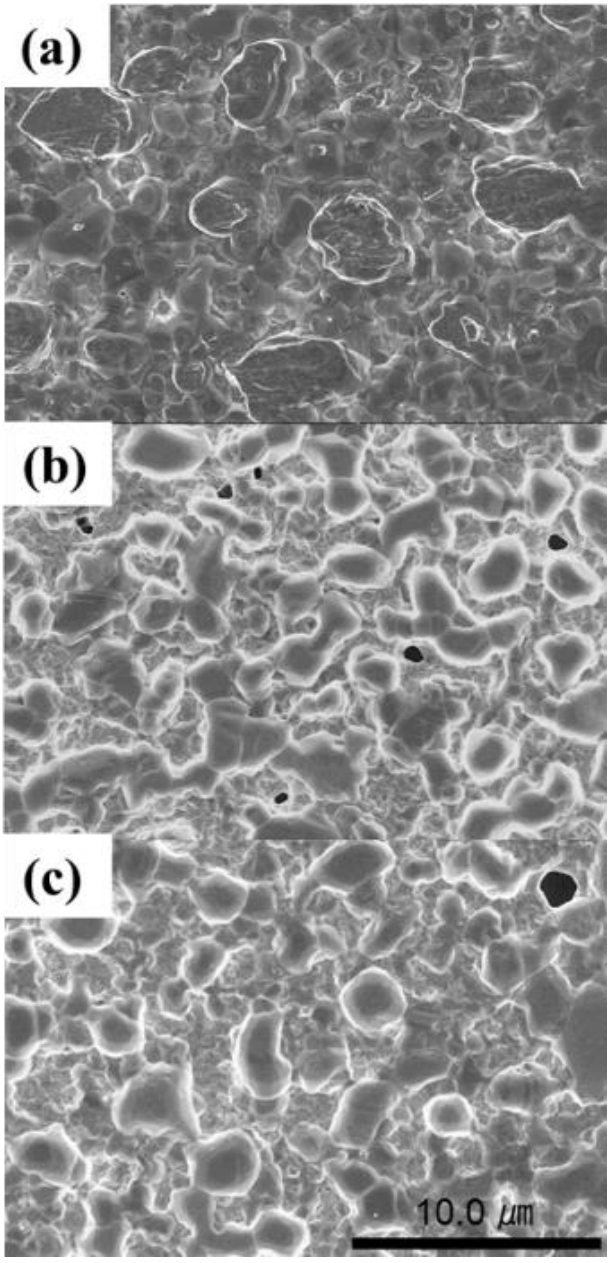

Figure 5. SEM micrographs of the microstructures in the Ag films after heating at 350 °C under constant bonding time (1 h) on (a) SiC, (b) Mo, and (c) Ti substrates.

Figure 6 presents typical cross-sectional microsctructure of the bond interfaces giving highest die-shear strength for each substrate material. The large grain growths in the films were confirmed at the bonding interfaces between the chips and substrates in all the cases. Abnormal grain growth occurred during the bonding process, because of the significant stress migration sufficient for the hillock formation on the film surfaces. However, the abnormal grain growth at the bonding interface was different for each substrate material. For SiC, the bonding interface was well formed with large grain growth. On the contrast, for Mo and Ti, the non-bonded area at the bonding interface remained. These results agree well with the maximum die-shear strengths for each substrate.

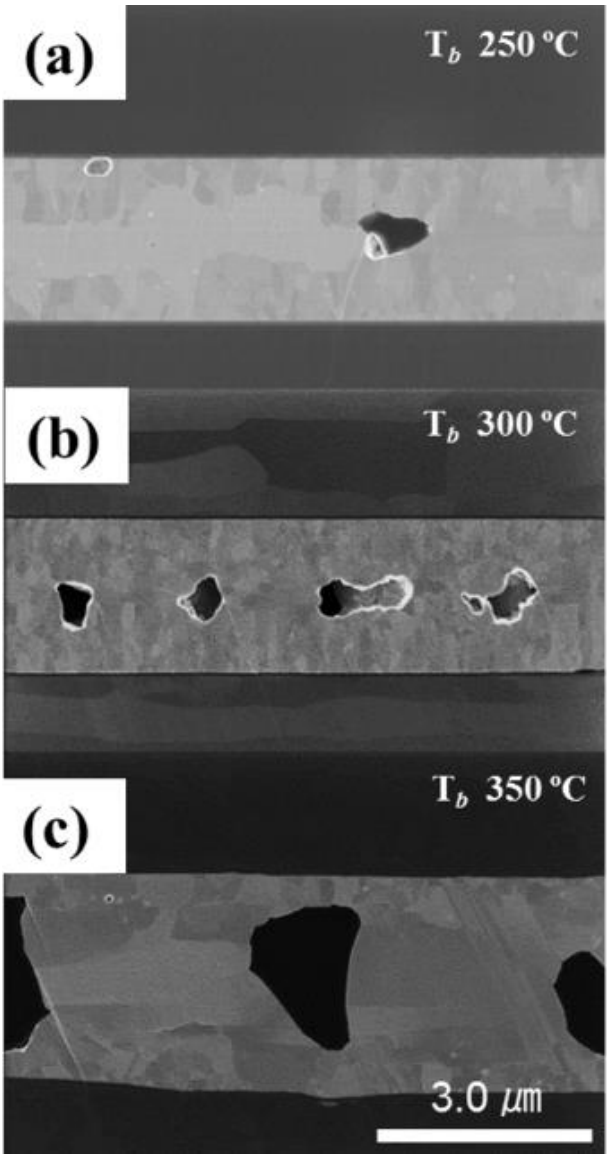

Figure 6. Cross-sectional SEM micrographs of the bonding interfaces where the highest strengths are shown for the (a) SiC, (b) Mo, and (c) Ti substrates.

4. 3. 4 Correlation between the Bonding Strength and the Bonding Temperature for Each Substrates

By using the $\sin^2\psi$ method introduced from chapter 2, the internal stress generated during film deposition were compressive and similar for all the materials. From Eq. (2) in chapter 2, the compressive stress of the Ag film increases with an increasing bonding temperature, as well as with an increasing CTE mismatch between the film and the substrate. Table 1 summaries the mechanical properties for the materials used in the experiments. For a constant ΔT, the thermal stresses of the Ag films deposited on SiC are higher than those of the Ag films deposited on other materials, such as Mo or Ti. However, the thermal stress of the Ag films deposited on SiC is lower than that of the Ag films deposited on Si.

Table 1. Mechanical properties of the materials used in the experiments [1-9].

	CTE (μm/m· K^{-1}) (298 K)	Young's modulus (GPa)	Poisson's ratio
Si	2.6	185	0.28
4H-SiC	4.3	221	0.21
Mo	5.1	325	0.29
Ti	8.6	115	0.31
Ag	19.0	71	0.37

Figure 7 plots the highest bonding strength and the corresponding bond-process temperature as a function of CTE difference between the Ag films and the substrate materials. The high thermal stress due to the large CTE mismatch in the case of SiC and Si materials causes numerous hillock growths, achieving the highest die-shear strengths

at the bonding temperatures of 250 °C, although the strength of Si materials is higher than that of SiC materials due to higher thermal stress. It also confirms that the effective solid-state bonding is shown above 230 °C in both SiC and Si materials by ensuring the activation energy necessary for growth diffusion in the experiment system. The process temperature for the strong bonding needs to be increased with decreasing CTE mismatch for the cases of Mo and Ti, to generate the sufficient compressive stress in Ag film required for hillock growth. Thus the achievable die-shear strength of Mo and Ti were lower than that for SiC due to the lower thermal stress derived by Eq. (2) in chapter 2. The tendency of the CTE mismatch between Ag and the substrate material is consistent with that of the highest bonding strength available for each substrate material. The results confirm that the thermomechanical compressive stress in Ag films is the key driving force for Ag solid-state bonding.

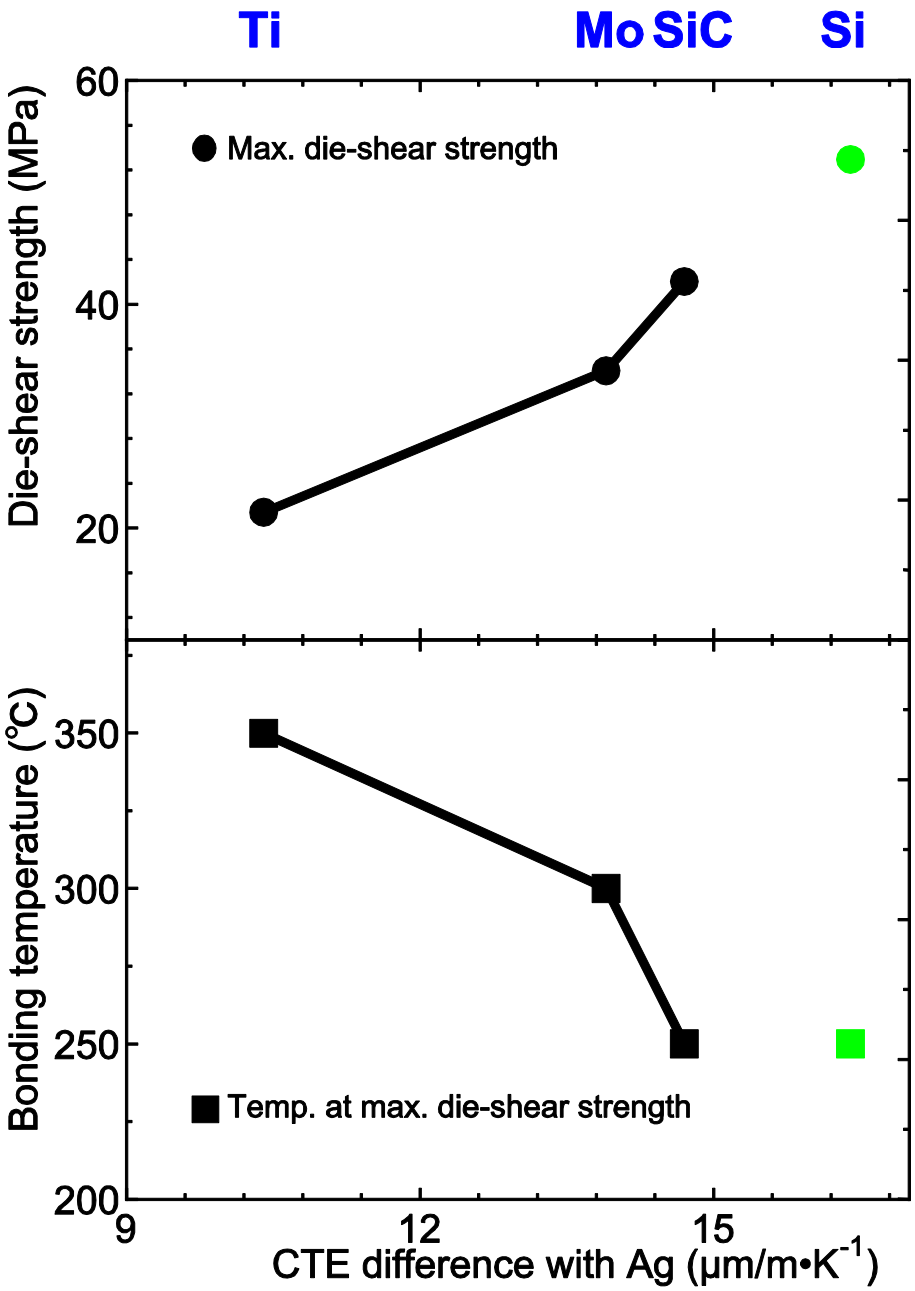

Figure 7. Correlation between the highest bonding strength and the corresponding bond-process temperature for each substrate material.

4.4 Conclusion

In this study, it has been revealed that the large stress migration sufficient for hillock formation is the driving force for achieving Ag solid-state bonding. The thermalmechanical stress induced during heat treatment could be controlled by the CTE mismatch between the Ag film and substrate. When sufficiently high compressive stress is generated in the Ag film, a large stress migration, enough to form hillocks, causing abnormal grain growth at the bonding interface. Therefore, Ag solid-state bonding could be achieved at low bonding temperatures, as long as the bonding thermal conditions had a sufficient compressive stress for hillock formation on the Ag film surfaces.

References

[1] Z. Li, R. C. Bradt, “Thermal Expansion of the Hexagonal (4H) Polytype of SiC”, J. Appl. Phys. 60, 612 (1986).

[2] G.K. White, T.F. Smith and R.H. Carr, “Thermal Expansion of Cr, Mo and W at Low Temperatures”, Gryogenics 18, 301 (1978).

[3] J. A. Cowan, A. T. Pawlowicz, and G. K. White, “Thermal Expansion of Polycrystalline Titanium and Zirconium”, Gryogenics 8, 155 (1968).

[4] K. M. Zwilsky, ASM Handbook Vol.2 – Properties and Selection: Nonferrous Alloys and Special Purpose Materials, 10th edn. (ASM International, the United States of America 2011), p. 2969.

[5] P. Villain, P.-O. Renault, Ph. Goudeau, K.F. Badawi, “X-Ray diffraction measurement of the Poisson’s ratio in Mo sublayers of Ni/Mo multilayers”, Thin Solid Films 406, 185 (2002).

[6] M. Chinmulgund, R.B. Inturi, J.A. Barnard, “Effect of Ar Gas Pressure on Growth, Structure, and Mechanical Properties of Sputtered Ti, Al, TiAl, and Ti_3Al films”, Thin Solid Films 270, 260 (1995).

[7] K. Kamitani, M. Grimsditch, J. C. Nipko, C.-K. Loong, M. Okada, and I. Kimura, “The Elastic Constants of Silicon Carbide A Brillouin-Scattering Study of 4H and 6H SiC Single Crystals”, J. Appl. Phys. 82, 3152 (1997).

[8] S. Karmann, R. Helbig, and R. A. Stein, “Piezoelectric properties and elastic constants of 4H and 6H SiC”, J. Appl. Phys. 66, 3922 (1989).

[9] J. J. Wortman, R. A. Evans, “Young’s modulus, shear modulus and poisons ration in silicon and germanium”, J. Appl. Phys. 36, 153 (1965).

Chapter 5

Flip Chip Bonding

Using Ag Stress Migration Bonding

5.1 Introduction

In the previous chapters, variations in the process and material parameters at Ag stress migration bonding have been investigated in terms of die bonding as well as for deeper understanding of the inherent bonding mechanism. We have found that thermomechanical stress control with substrate materials is essential, to manage the microstructure evolution during the bonding process. On the basis of the obtained knowledge of our Ag stress migration bonding method, we here explore another interconnect application, namely, flip-chip bonding.

In recent days, flip-chip package, which replaces traditional wiring between chip electrodes and lead frames with bump-to-bump direct soldering, has widely been adopted in smart electronics to achieve higher density device integration for performance oriented applications. As the process-rule becomes finer in IC devices, the interconnection technology of solder bump in the popular flip-chip bonding nowadays is facing the technical limitations in pitch-size due to bump bridging at processing, or lesser long-term reliability [1]. Therefore, alternative interconnection technologies such as Cu-Cu direct bonding have been developed to replace the solder bonding in the flip chip packaging.

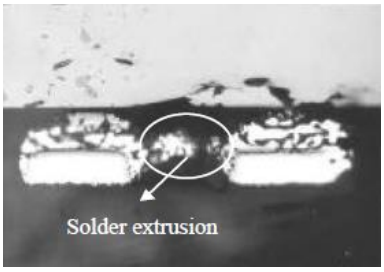

Figure 1. The defect of solder extrusion between solder bumps, i.e. bump-bridging, in a flip-chip packaging process [1].

In this chapter, the Ag stress migration bonding process is applied to flip-chip bonding to explore the further opportunity in fine-pitch and high-density smart electronic devices (see Fig. 2.) As we discussed before, Ag stress migration bonding has many advantages to Cu-Cu direct bonding, and typical Pb-free soldering. In particular, Ag stress migration bonding is free from bump-bridging defects in Fig. 1 because the method is solid-solid bonding without any liquid phases. To realize Ag stress migration bonding flip-chip bonding, Ag thin films must be deposited on Cu bumps, and the chip placed on substrate the in precise positioning within the bump pitch before heat treatment. The design of Cu bumps has been reviewed to obtain the best quality of the bonding. The results clarify the detailed requirements for successful Ag solid-state bonding to be adopted as a novel flip-chip interconnection technology for fine pitch smart electronic devices.

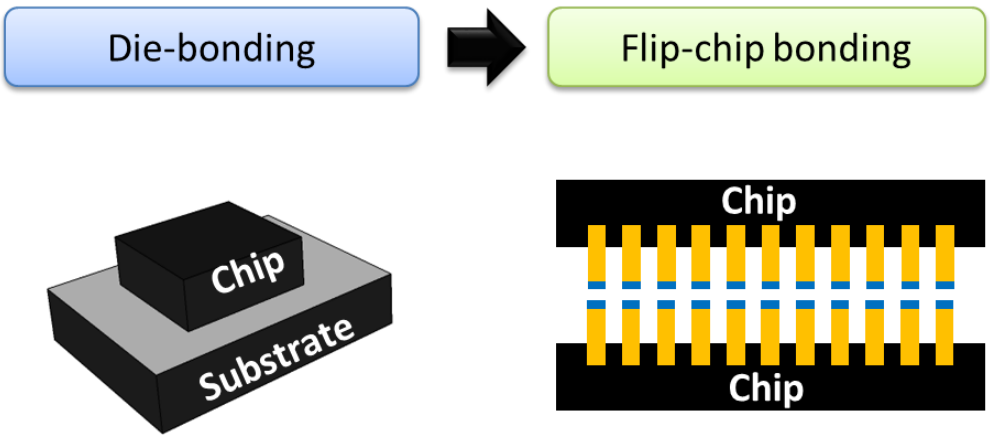

Figure 2. The expansion of application field for Ag stress migration stress bonding.

5.2 Experimental procedures

The experimental flow of the flip-chip bonding process is schematically presented in Fig. 3. The procedure basically follow the typical flip-chip bonding while the solder bump is replaced with Ag film on a Cu electrode. As shown in Fig.3, active photo resist (PR) process is utilized to make dummy Cu bump pattern on a mirror-polished Si wafer chip, followed by Ag film deposition by sputtering before stripping the resist pattern. The Si chips substrates with patterned Cu/Ag bumps are bonded by stress migration bonding under the optimal conditions as described before.

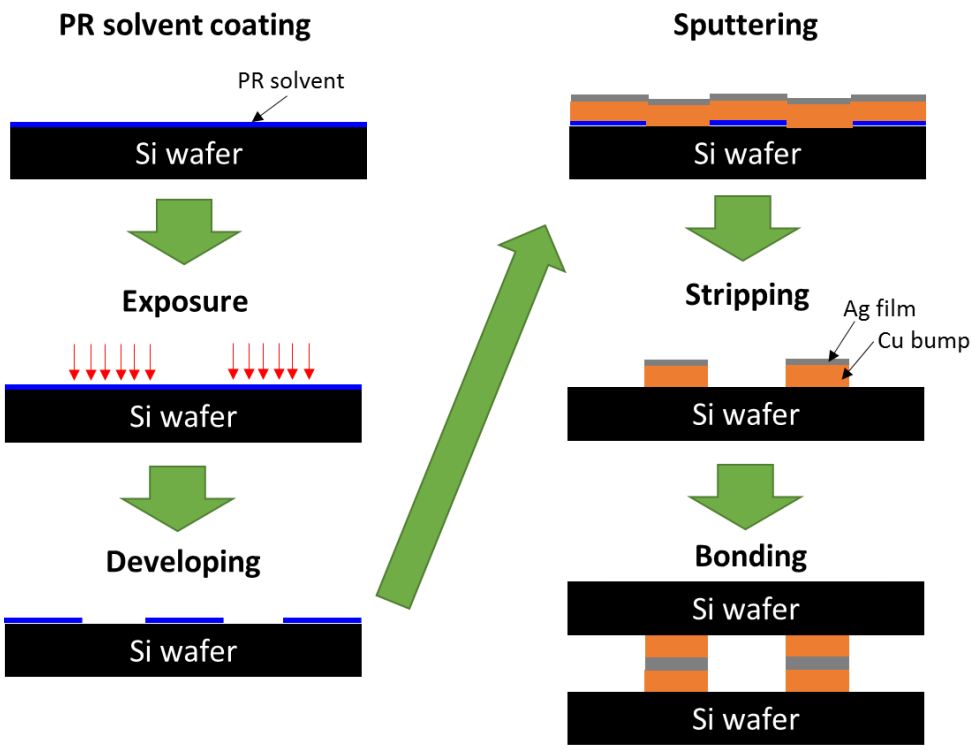

Figure 3. Schematic of the experimental procedure of the flip chip bonding using Ag stress migration bonding.

The dummy chips and substrates were prepared with the dimensions 5 mm × 5 mm and 10 mm × 10 mm respectively, to meet the fixture requirement of the photo exposure equipment (DL-1000, Nanosystem solutions). The photo-resist material is spin-coated on the Si surface, and heated at 90 ℃ for 1 min. Then, the samples were exposed to the light of 405 nm wavelength in the mask-less photo-exposure equipment for the Cu bump patterning. After the exposure process, the samples were inserted in the solvent for developing the photo resist pattern. The developed Cu bump pattern is shown in Fig. 4, where the pitch and spacing is 250 μm and 50 μm, respectively.

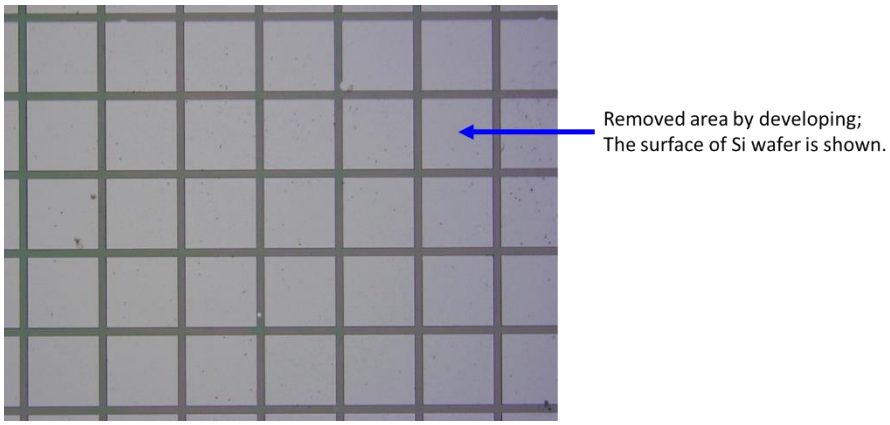

Figure 4. The optical image of bump pattern after developing process.

After finishing the developing process, Cu bumps were fabricated by sputtering process, followed by Ag film deposition. The thickness of Cu bumps were changed to investigate the effect of Cu thickness as shown in Fig. 5, while the thickness of Ag film was kept constant to 1.0 μm following to the optimal conditions determined in Chapter 3. Ti adhesion layers with 0.04 μm thick were inserted at each surface between Ag, Cu and Si.

(a)

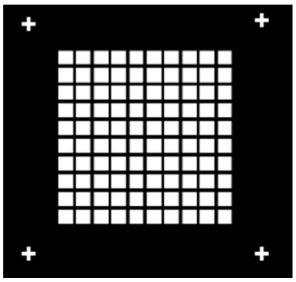

(b)

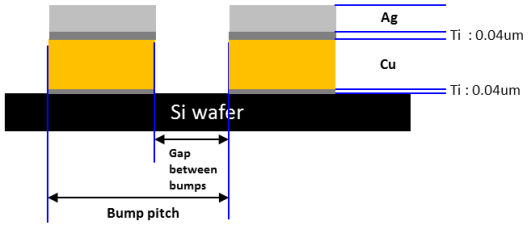

(c)

(um)

Sample		1	2
Bump	Ag thickness	1.0	1.0
	Cu thickness	1.0	0.4
Bump pitch		250	250
Gap between bumps		50	50

Figure 5. The design of Cu bumps used in the experiments; (a) Bump pattern, (b) Cross-sectional schematic illustration of bump structure, and (c) detailed dimensions of bump structure.

After the deposition processes, the samples were immersed in acetone solvent for 1 h to remove the residual photo resist deposited on the gap between bumps. The samples are cleaning by ultrasonic in acetone, and the mounting process was precisely carried out by custom-made flip-chip bonder where the alignment accuracy is less than 10 um as shown in Fig. 6. The mounted samples were then inserted into an oven and heated at 250 °C for 1 h in air without applying any pressure. The optimal bonding conditions same to those obtained from the previous results were adopted for sound bonding interface. The cross-sectional microstructures of the bond interfaces were observed by SEM, as well as the morphological changes on the Ag film surfaces after the similar heat treatment.

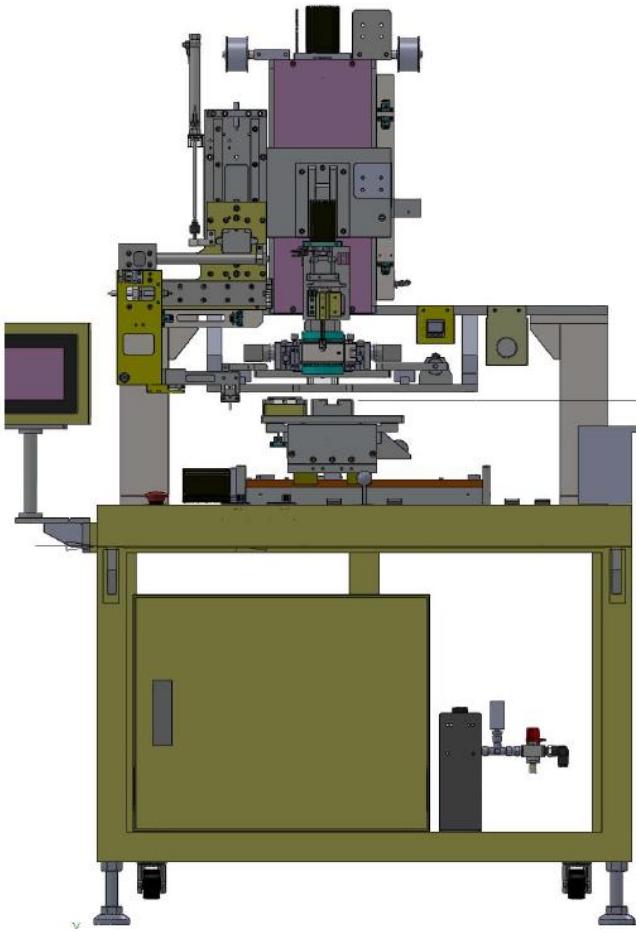

Figure 6. The Schematic illustration of flip-chip bonder.

5.3 Results and discussion

5. 3. 1 Ag Film Microstructures on Cu Bumps

The dimensions of fabricated Cu/Ag bump pattern are measured as shown in Fig. 7(a), and confirmed identical to the intended gap-pitch design. No defects in the fabrication process such as bump misalignment, or contaminations of photo resist solvent was observed on any surfaces of the tested samples.

After the heat treatment is heated at 250 °C of bonding temperature for 1 h, a lot of hillock were homogenously grown on each bump as seen in Fig. 7(b) where the Cu bumps height is 0.4 μm. The observed change of the surface morphology agrees well with the results in the previous chapters.

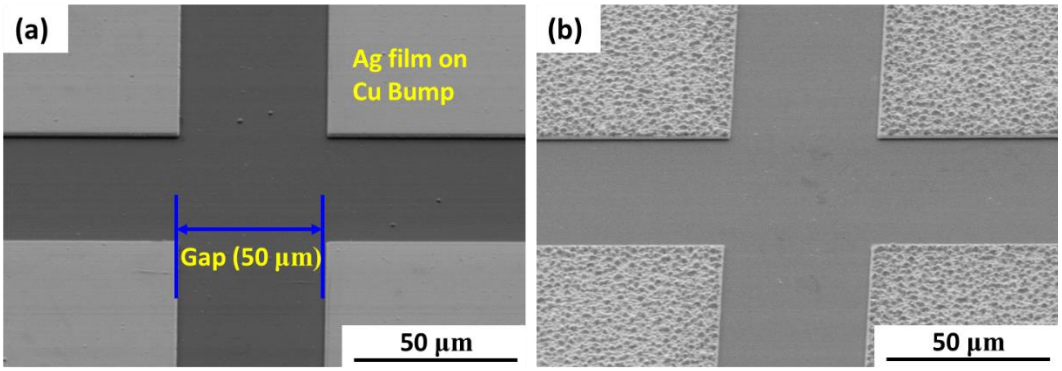

Figure 7. SEM micrographs of the microstructures of Ag films on Cu bumps; (a) after fabrications of Cu bumps, and (b) after heating at 250 °C for 1 h.

5. 3. 2 Microstructure Variations with Different Thicknesses of Cu Bumps

To investigate the thickness effect of Cu bumps on Ag stress migration bonding, two different dimensions of Cu bumps were examined; the one was 1.0 μm height and the other was 0.4 μm. After heat treatment at 250 °C for 1 h, the evolution of surface microstructure in each sample was observed as shown in Fig. 8. A small number of hillocks appeared on the Ag film surface on the 1.0 μm Cu bumps, while a lot of hillocks were emerged from the Ag film surface on 0.4 μm Cu bumps. However, the hillock size was similar in both of case. This indicates that the thickness of Cu has a significant effect on the number of hillocks grown on Ag film. In addition, the grain growths were confimed in Ag film along with the hillock growth, particularly on the 0.4 μm bumps as seen in Fig. 8(b).

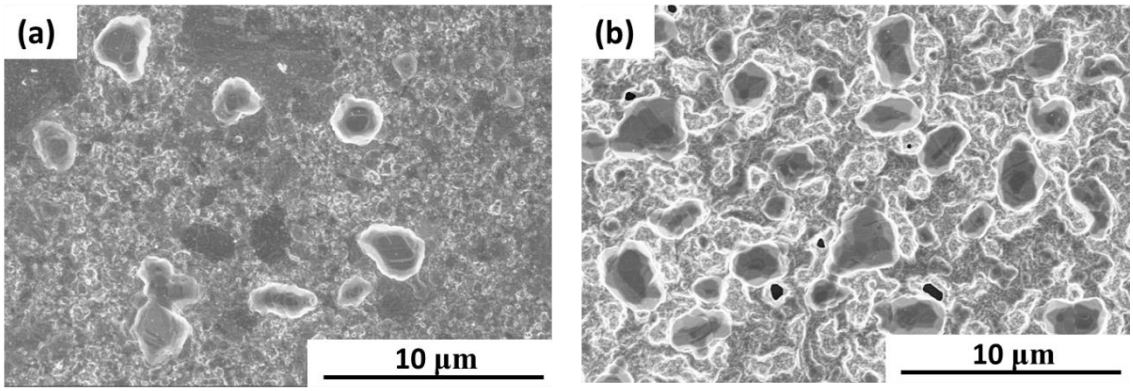

Figure 8. SEM micrographs of the microstructures in the Ag films after heating at 250 °C for 1h on (a) Cu bumps of 1.0 μm thickness, and (b) Cu bumps of 0.4 μm thickness.

Fig. 9 shows typical cross-section microstructure of the bonding interface on a sample heated at 250 ℃ for 1 h. In the Cu bumps with 1.0 μm thickness, the bonding interface has a large gap indicating that the abnormal grain growth was not sufficient. This is consistent with the poor hillock growths on the open surface after the heat treatment as shown Fig. 8(a). When numerous hillock growths occurs as shown in Fig. 8(b), on the other hand, abnormal grain growths turned from the abnormal grain growths occurs enough to fill the gap at the interface, resulting in the sound interface formation as shown in Fig. 9(b). These observations confirm that the bond interface formation by hillock growth is related to the thickness of Cu bump.

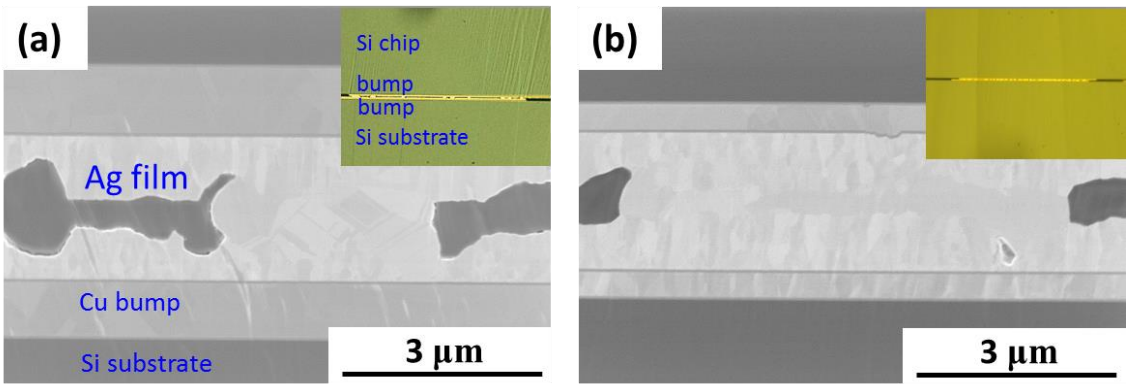

Figure 9. Cross-sectional SEM micrographs of the bonding interface between Cu bumps after heating at 250 ℃ for 1h for (a) Cu bumps of 1.0 μm thickness and (b) Cu bumps of 0.4 μm thickness.

Since the Ag coated Cu bumps actually consist of two metal thin-films on Si substrate, the thermomechanical stress in Ag films at an elevated temperature $T + \Delta T$ is obtained from multilayer model as follows [2]:

$$\sigma_{\mathrm{i}} = \frac{E_{\mathrm{i}}}{1-\nu_{\mathrm{i}}}\left[(\alpha_{\mathrm{s}} - \alpha_{\mathrm{i}}) + 4\frac{1-\nu_{\mathrm{S}}}{E_{\mathrm{S}}t_{\mathrm{S}}}\sum_{j=1}^{n}\frac{E_{\mathrm{j}}}{1-\nu_{\mathrm{j}}}t_j\left(\alpha_{\mathrm{j}} - \alpha_{\mathrm{s}}\right)\right]\Delta T\,, \qquad (1)$$

where E_{i}, ν_{i}, α_{i} are the Young's modulus, Poisson's ratio and coefficient of thermal expansion (CTE) of layer i, respectively, while E_{S}, ν_{S}, α_{S} are those corresponding to the substrate (see Fig. 10). In our case of flip-chip bonding, the change of temperature ΔT is constant, representing the difference between the room temperature and the bonding temperature of 250 °C.

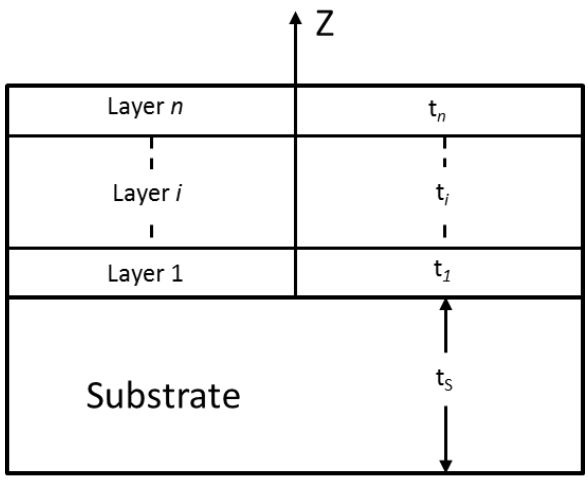

Figure 10. Schematics showing a multilayer structure and the coordinate system [2].

Table 1 summaries the mechanical properties for the materials used in the experiments. In the elastic region, From Eq. (1), the compressive residual stress of the Ag films in 0.4

μm Cu bump is 2.5 times larger than that of the Ag films in 1.0 μm Cu bump Therefore, Ag hillock growth on 0.4 μm Cu bump appears more significantly than that on 1.0μm, resulting in a better interface quality of the bonding.

Table 1. Mechanical properties of the materials used in the experiments [3-4].

	CTE (μm/m· K^{-1}) (298 K)	**Young's modulus (GPa)**	**Poisson's ratio**
Si	2.6	185	0.28
Cu	16.5	128	0.31
Ag	19.0	71	0.37

The decrease of Cu bump height may be limited by the electric current required for device. In a typical flip-chip packaging nowadays, underfill process is carried out sequentially after flip-chip bonding, by filling polymer material into the gap between the bumps to protect the device and bumps from the surrounding environment. When the thickness of Cu bump is reduced, the gap between the bumps is too narrow to fill the underfill materials. Even the Ag stress migration bonding structure is tougher than usual solder interconnections, flip-chip bonding with the Ag stress migration bonding would require further review of the sealing method of the bonded structure, as well as Cu bump height.

5.4 Conclusion

In this chapter, we have demonstrated flip-chip interconnections by using Ag stress migration bonding. When Cu bumps coated by Ag is heated at 250 °C for 1 h, certain Ag hillock growth on bump surface is confirmed. It is found that the amount of hillock growth depends on the thickness of Cu bumps, and that t compressive residual stress at the heat treatment increases with decreasing Cu thickness. Thus the stress induced hillock growth leads to abnormal grain growth to form the sound bond interface. Our experimental results of Ag solid-state bonding opens a feasibility for various applications such as flip-chip bonding in future three-dimensional high integration packaging technology.

References

[1] T. Wang, T. H. Chew, and L. Foo, “Reliability Studies of Flip Chip Package with Reflowable Underfill”, Proceeding of Pan Pacific Microeletronics Symposium, 65 (2001).

[2] C.-H. Hsueh, “Modeling of elastic deformation of multilayers due to residual stresses and external bending”, J. Appl. Phys. 91, 9652 (2002).

[3] K. M. Zwilsky, ASM Handbook Vol.2 – Properties and Selection: Nonferrous Alloys and Special Purpose Materials, 10th edn. (ASM International, the United States of America 2011), p. 2969.

[4] J. J. Wortman, R. A. Evans, “Young’s modulus, shear modulus and poisson’s ratio in silicon and germanium”, J. Appl. Phys. 36, 153 (1965).

Chapter 6

Conclusions

The bonding method using Ag thin film has been introduced in the electronic industry as a new interconnection technology. In this dissertation, this bonding method has been developed through three different ways to understand the inherent bonding mechanism; sputtering process, bonding process, and substrate materials. The formation of microstructure in Ag thin film is dependent on the sputtering process, determining the bonding properties. The bonding conditions such as temperature and time can control the growth of Ag thin film and the different substrate materials changes the thermo-mechanical stress between substrate and Ag thin film, affecting the bonding properties. Finally, the bonding method using the Ag thin film has been realized through the findings in three approaches to apply in advanced electronic packages such as 3D integration and wide band gap power device.

Chapter 1 described the current bonding technologies with electronic package and the issues of bonding technology along with the development of electronic packages. The electronic package has been developed into applicative and advanced packaging with higher performance and smaller size, driving the difficulties to bonding technologies to meet their severe requirements. Although the soldering, sintering, and direct bonding which are used widely, have been reviewed with their bonding mechanism, development, application, and technical limits, the present bonding methods aren't satisfactory with all the needs of advanced devices. In the thesis, the new bonding technology, called the Ag stress migration boding, has been proposed as an alternative bonding technology in advanced devices. In order to build the Ag stress migration bonding, three key factors have been demonstrated in the following chapters.

In Chapter 2, the effect of substrate temperature at sputtering process has been reviewed. By changing substrate temperature at sputtering, the microstructure evolution was investigated between as-deposited and after bonding. The residual stresses for each substrate temperature were evaluated to find the correlation of the microstructure variation with the bonding property. These results explain how substrate temperature at sputtering process affects the bonding properties with hillock growth in thin film. The strong bonding strength is exhibited by the large difference between initial compressive stress and tensile associated with stress relaxation by abnormal grain growth at specific substrate temperature during sputtering.

Chapter 3 discussed the bonding behavior according to various bonding temperatures and times at the bonding process. The change of microstructure at each temperature and time was observed by Scanning Electron Microscope (SEM), and explained with the Ag self-diffusion for grain boundary and lattice. The residual stress for each condition was measured to reveal the stress relaxation effect with bonding properties. The bonding strength for each condition was evaluated to show how the micro-structural evolution is dependent on the bonding temperature and time. Sound bonds with high die strength can be achieved only when the large hillocks grew while maintaining the original columnar structure of the deposited Ag film at the optimum bonding temperature and time.

Chapter 4 addresses the effect on the substrate materials for the Ag stress migration bonding. Three substrate materials were evaluated to modify thermomechanical stress by generating between the substrate and Ag film. The different hillock growth in Ag film was observed with increasing bonding temperature, finding the minimum bonding temperature for each substrate. In addition, the bonding strengths for each substrate were evaluated with the bonding temperature. These results verify that stronger bonding at a lower bonding temperature can be obtained by larger thermal stress generated between the substrate and Ag thin film during bonding.

Chapter 5 describes the possibility of flip chip bonding using Ag stress migration bonding. By introducing positive photo resist method, the flip chip bonding has been realized with Ag stress migration bonding. Depending the thickness of Cu bump, the microstructure of Ag film is varied, affecting the formation of bonding interface at flip chip bump interconnection. From our results, the flip chip bonding with Ag solid-state bonding shows the opportunity for ultra-fine pitch flip chip bonding.

In conclusion, Ag stress migration bonding has been characterized by investigating the sputtering process, bonding process, and substrate materials. Based on the results, the key factors for Ag solid-state bonding have been clarified in both the driving force and the dynamic growth. It however had better reduce the bonding temperature and time to apply it for practical application by ensuring satisfactory bonding reliability. Finally, it is expected that Ag stress migration bonding can be accepted as a

potential alternative interconnection technology for advanced devices like 3D integration and wide band gap power device.

List of Publication

A. Papers

1. **Pressureless wafer bonding by turning hillocks into abnormal grain growths in Ag films**

   Chulmin Oh, Shijo Nagao, Teppei Kunimune, and Katsuaki Suganuma

   Applied Physics Letters 104, 161603 (2014)

2. **Pressureless bonding using sputtered Ag thin films**

   Chulmin Oh, Shijo Nagao, and Katsuaki Suganuma

   Journal of Electronic Materials 43, 4406 (2014)

3. **Hillock growth dynamics for Ag stress migration bonding**

   Chulmin Oh, Shijo Nagao, Tohru Sugahara, and Katsuaki Suganuma

   Materials Letters, 137, 170 (2014)

4. **Silver stress migration bonding driven by thermomechanical stress with various substrates**

   Chulmin Oh, Shijo Nagao, and Katsuaki Suganuma

   Journal of Materials Science: Materials in Electronics, (minor revision).

B. Proceeding and Presentation

1. **Effect of Ag film deposition temperature on Ag direct bonding**

   Chulmin Oh, Shijo Nagao, Teppei Kunimune, Masafumi Kuramoto, and Katsuaki Suganuma

   8th Handai Nanoscience and Nanotechnology International Symposium, Osaka University, Japan, 2012.12.10.

2. **Thermo-mechanical Stress-driven Ag Direct Bonding**

   Chulmin Oh, Shijo Nagao, and Katsuaki Suganuma

   8th PRICM8 (Pacific Rim International Congress on Advanced Materials and Processing), Hawaii, America, 2013. 8.

3. **銀ダイレクトドンディングにおける接合条件の最適化**

   呉　哲昊, 長尾 至成, 菅原 徹, 菅沼 克昭

   第23回マイクロエレクトロニクスシンポジウムMES2013, 大阪大学, 2013.9.13.

4. **Pressre-less Si wafer bonding using sputtered Ag thin films**

   Chulmin Oh, Shijo Nagao, and Katsuaki Suganuma

   TMS 2014 143rd Annual Meeting & Exhibitions, San Diego, America, 2014. 2. 17.

5. **Flip chip interconnection using Ag solid-state bonding**

   Chulmin Oh, Shijo Nagao, and Katsuaki Suganuma

   IUMRS-ICEM 2014 (The International Union of Materials Research Societies – International Conference on Electronic Materials), Taipei, Taiwan, 2014. 6. 13.

6. **Pressureless Ag thin-film die-attach for SiC devices**

   Chulmin Oh, Shijo Nagao, Tohru Sugahara, and Katsuaki Suganuma

   ECSCRM 2014 (European Conference on Silicon Carbide & Related Materials), Grenoble, France, 2014.9.21

7. **Zero stress die-attach" for wide band gap semiconductor power devices**

   Katsuaki Suganuma, Jingting. Jiu, Shunsuke Koga, Tohru Sugahara, Seongwon Park, Semin Park, *Chulmin Oh*, and Shijo Nagao

   IMAPS (International Microelectronics Assembly and Packaging Society) 2014, San Diego, America, 2014. 10. 16.

8. **Silver Sinter Joining and New Thin Film bonding for WBG die-attach**

   Katsuaki Suganuma, Shijo Nagao, Tohru Sugahara, *Chulmin Oh*, Hao Zhang, Shunsuke Koga, and Semin Park,

   International Conference on Nanojoining and Microjoining 2014, Emmetten, Switzerland, 2014.12.7

9. Ag stress migration bonding

Chulmin Oh, Shijo Nagao, Tohru Sugahara, and Katsuaki Suganuma

TMS 2015 144rd Annual Meeting & Exhibitions, Orlando, America, 2015. 3. 15.

10. Diffusional hillock growth in Ag stress migration bonding for power device interconnections

Chulmin Oh, Shijo Nagao, Tohru Sugahara, and Katsuaki Suganuma

Electronic Components and Technology Conference (ECTC) 2015, San Diego, America, 2015. 5. 26.

C. Patent

1. ストレスマイグレーション接合法

菅沼 克昭，長尾 至成，*呉　哲皓*

Acknowledgements

I would like to express my truthful thank to Prof. Katsuaki Suganuma at the Institute of Scientific and Industrial Research (ISIR) in Osaka University for his insightful advices and guidance. In addition, I would like to thank to Prof. Shijo Nagao sincerely. With his professional advice and recommendations, I was able to solve various issues in my research. His reasonable method for answering a problem helps me to think out of the box at all times.

I am deeply indebted to Won Sik Hong at Korea Electronics Technology Institute for giving an opportunity to study in Osaka University. His thoughtful encouragement and support give me a courage to overcome difficulties during my stay in Japan.

I am also thankful to my colleagues, Dr. Jung-Lae Jo, Dr. Chang-Jae Kim, Dr. Sung-Won Park, and Dr. Young-Suk Kim for their useful discussion and kind supports for living in Japan.

Lastly, I would like to express my thanks to my families for their devoted encouragement. Their dedicated supports drives me to finish my research. I'm particularly grateful so much to my parents, my daughters, and my wife, Eunjoo Kim.

Osaka, Japan, 2014

Chulmin Oh